Princetonlaan 6
3584 CB Utrecht
Postbus 80015
3508 TA Utrecht

www.tno.nl

T +31 88 866 42 56

Retouradres: Postbus 80015, 3508 TA Utrecht

Ministerie van Economische Zaken en Klimaat
Directie Klimaat en Energie
Warmte en Ondergrond
T.a.v. Ing. B.H. Bussemaker
20401 Postbus
2500 EK DEN HAAG

Datum
23 juli 2021

Onze referentie
AGE 21-10.055

Contactpersoon
W.W. van Driel

E-mail
wiebe.vandriel@tno.nl

Bijlage(n)
3

Onderwerp Aanvraag “permanent opslaan van CO_2 in het voorkomen P18-2”

Geachte heer Bussemaker,

In reactie op uw adviesverzoek over de aanvraag “Permanent opslaan van CO_2 in het voorkomen P18-2” van 12-2-2021 door de aanvragers TAQA Offshore B.V. en EBN CCS B.V. (hierna: de aanvragers) vindt u hierbij ons antwoord.

Op 12 februari jl. hebben wij de aanvraag en het begeleidende document met technische rapportages ontvangen. In maart zijn verschillende additionele rapporten van de aanvrager toegestuurd. Op 22 juli jl. heeft u ons een versie 2.0 van de aanvraag met begeleidende documenten doen toekomen.
Deze versie 2.0 heeft ons te laat bereikt om nog de volledige technische analyses op de aangepaste modellen uit te voeren.

U vraagt specifiek om advies op een aantal onderwerpen. In bijlage 1 ‘Beantwoording adviesvraag’ worden de door u aangegeven onderwerpen behandeld. De kaart van het aangevraagd gebied wordt in Bijlage 2 gegeven. De onderliggende technische analyse is bijgevoegd als Bijlage 3 “Technische rapportage evaluatie opslagvergunning P18-2”. Onze evaluatie heeft op hoofdlijnen geresulteerd in de volgende bevindingen:

Kwaliteit van de aanvraag
TNO-AGE beoordeelt de kwaliteit en inhoud van de aanvraag en de aanvullend aangeleverde informatie als adequaat. Echter, enkele punten zullen voor injectie nog verder uitgewerkt moeten worden alvorens alle vragen, zoals door u gesteld, goed gefundeerd beantwoord kunnen worden.

Geschiktheid opslagreservoir
TNO-AGE is van mening dat het beoogde opslagreservoir P18-2 geschikt is voor CO_2-opslag. De aanvrager heeft dit voldoende aangetoond met haar geotechnische onderbouwing die is gebaseerd op een uitgebreide dataset en de jarenlange ervaring opgedaan tijdens de gasproductie. Ook het bestaan van een analoog natuurlijk gasvoorkomen met een zeer hoog CO_2 gehalte (Werkendam-Diep) sterkt TNO-AGE in die mening.

Operationele aspecten
TNO-AGE is van mening dat de tot dusver uitgevoerde studies aangeven dat een veilige opslag in beginsel mogelijk is, maar dat de operationele kant van het CO_2 injectie- en opslagproces nog niet voldoende is uitgewerkt. De vier plannen, die samen de praktische uitvoering moeten beschrijven, hebben nog niet hun definitieve vorm: de aanvragers geven een reeks van nog lopende of uit te voeren (deel)onderzoeken aan.

TNO-AGE zal alleen dan een uiteindelijk oordeel kunnen vellen wanneer de definitieve plannen bij de minister zijn ingediend, ruim voor de feitelijke start van de injectie. TNO-AGE is van mening dat de vier plannen een coherent onderdeel moeten zijn van een effectief en doelmatig risicobeheerssysteem. Meer specifiek moeten onverwachte en ongewenste gebeurtenissen tijdig te detecteren zijn, om vervolgens effectieve corrigerende maatregelen te kunnen nemen (‘closed loop’ monitoring). Cruciaal is dat de modelvoorspellingen worden voorzien van een onzekerheids-bandbreedte en er een maat wordt gesteld, die aangeeft wanneer er sprake zou zijn van een ‘significante afwijking’ waarop ingegrepen kan en moet worden.

Monitoring
De door de aanvragers voorgestelde ondergrondse monitoring omvat niet veel meer dan in de reguliere gasproductie gebruikelijk is (het meten van debieten en drukken in de putten). De enige aanvulling is het meten van temperatuur.
TNO-AGE meent, dat de aanvragers onvoldoende motiveren, hoe met een dergelijk beperkt monitoringsysteem adequaat risicobeheersing kan worden uitgevoerd bij CO_2 opslag.

Door noviteit van het project (eerste in de wereld op deze schaal) en daaruit voortkomende relatieve onbekende processen adviseert TNO-AGE om de aanvragers op te dragen ruim voor de start van de injectie het monitoringsysteem meer effectief en doelgericht op te zetten (en weer te geven in een actualisatie van het Monitoringplan). Aandachtspunten daarbij zijn:

- Definiëring van onzekerheidsbandbreedte teneinde significante afwijkingen te kunnen bepalen.
- Waarnemingen van (micro-)seismiciteit (om eventuele thermische frack-ontwikkeling of breukactivatie te monitoren)
- Verspreiding van het CO_2 binnen het opslagreservoir, resp. detectie van significante afwijkingen van de prognoses
- Migratie danwel lekkage van CO_2 naar buiten het opslagreservoir danwel -complex.

Afsluiting en overdracht van de opslag
Het plan voor Afsluiting voorziet ook in overdracht aan de overheid van de verantwoordelijkheid van het opslagcomplex en bijbehorende opgeslagen massa CO2. TNO-AGE adviseert om aan dat belangrijke aspect meer aandacht te besteden in een te actualiseren Afsluitingsplan. In feite zou ‘overdracht naar de overheid’ een eigen plan rechtvaardigen, waarin de criteria voor overdracht helder zijn verwoord. Dit onder het besef, dat ‘overdracht aan de overheid’ in feite al begint met de vergunningverlening en de daaraan te stellen voorwaarden.

Graag geven wij desgewenst een toelichting op ons advies,

Met vriendelijke groet,

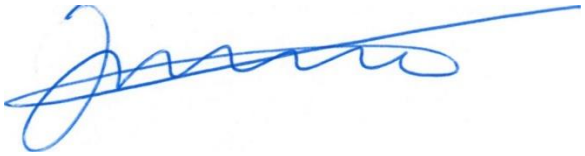

Drs. J.A.J. Zegwaard
Hoofd Adviesgroep Economische Zaken

Bijlage 1 – Beantwoording adviesvragen
Bijlage 2 – Kaart van het gebied
Bijlage 3 – Technische rapportage evaluatie opslagvergunning P18-2

Datum
23 juli 2021

Onze referentie
AGE 21-10.XXX

Blad
1/12

Bijlage 1 Beantwoording van de adviesvraag

Introductie

TNO-AGE heeft de vergunningaanvraag primair beoordeeld aan de hand van de volgende specifiek door EZK genoemde onderwerpen (per email van 12-02-2021):

1. De manier waarop de aanvrager voornemens is de activiteiten met betrekking tot het permanent opslaan van CO_2 te verrichten, waaronder de bij de activiteiten te gebruiken technieken, hulpmiddelen, of stoffen in het licht van de huidige kennis en technieken, de hoeveelheid CO_2, in relatie tot de duur van de vergunning en de omvang van het vergunning gebied;
2. De geotechnische onderbouwing van de aanvraag, waaronder een beoordeling van de gegevens met betrekking tot de hydraulische eenheid;
3. Beoordeling van de veiligheid van de opslag c.q. of er bij opslag onder de voorgestelde exploitatievoorwaarden een significant risico van lekkage bestaat, of significante milieu- of gezondheidsrisico's bestaan;
4. De grenswaarden van de druk van de opgeslagen CO_2 en de maximum toelaatbare snelheid en druk bij injectie van CO_2 en de maximale toelaatbare druk van het opgeslagen CO_2;
5. Plannen:
    - Risicobeheerplan overeenkomstig artikel 29c Mbb;
    - Plan voor corrigerende maatregelen overeenkomstig artikel 29d Mbb;
    - Plan voor monitoring overeenkomstig artikel 29f Mbb jo artikel 1.3.4a, vierde lid, Mbr;
    - Plan voor afsluiting overeenkomstig artikel 29g Mbb;
6. Bodembeweging overeenkomstig artikel 29h Mbb.

Daarnaast laat de adviesvraag ruimte voor het behandelen van eventuele andere risico's die TNO-AGE relevant acht voor de vergunningaanvraag. Voor zover deze niet onder vragen 1 t/m 6 worden behandeld komen deze separaat in onderdeel 7 terug.

TNO-AGE heeft zich beperkt tot technische risico's en beleidsmatige aspecten in het licht van de nieuwheid van dit project. Beoordeling van veiligheidsrisico's is primair de taak van SodM, zeker ook waar het gaat om het bepalen van grenswaarden. Commerciële risico's zijn buiten beschouwing gelaten, hoewel technische en veiligheidsrisico's daar uiteraard wel op van invloed kunnen zijn.

Inhoudelijk heeft TNO-AGE de focus gelegd op de kennis van het opslagreservoir, de kwaliteit van de voorspellende modellen in de CO_2-injectiefase, en de samenhang tussen modellen en monitoring. Dit alles met als onderliggende vraag, of ongewenste effecten in verband met technische risico's tijdig kunnen worden onderkend en daarop ook tijdig en effectief mitigerende en corrigerende maatregelen kunnen worden getroffen.

Onderwerp 1; De manier waarop de aanvrager voornemens is de activiteiten met betrekking tot het permanent opslaan van CO_2 te verrichten, waaronder de bij de activiteiten te gebruiken technieken, hulpmiddelen, of stoffen in het licht van de huidige kennis en technieken, de hoeveelheid CO_2, in relatie tot de duur van de vergunning en de omvang van het vergunning gebied;

Technieken, hulpmiddelen of stoffen
Er bestaat op dit moment alleen praktijkervaring met het injecteren van CO_2 in aquifers (m.n. Noorwegen) en voor Enhanced Oil Recovery (o.a. de VS). Praktijkervaring met het grootschalig injecteren van CO_2 in een leeggeproduceerd gasveld met het oogmerk om dat veld weer geheel te vullen met CO_2 bestaat wereldwijd nog niet. In dat licht is het evident, dat alle prognoses en ook de planning van het Porthos project steunen op modellen, die in het beste geval zijn ontleend aan kennis vanuit de gasproductiefase.
De aanvraag maakt gebruik van informatie uit de gasproductie-fase, zij het dat daarbij slechts één base case model als uitgangspunt wordt genomen.

Advies

TNO adviseert om in de operationele plannen beter zichtbaar te maken, welke onzekerheden bestaan met betrekking tot het reservoirgedrag onder CO_2-injectie en hoe die via monitoring en model-updates verkleind kunnen worden.

Duur van de vergunning in relatie tot hoeveelheid CO_2
De aanvrager heeft (in de tweede versie van de aanvraag) een looptijd aangevraagd voor de opslagvergunning voor de periode van 2024 tot 2041 (17 jaar). In die planning lijkt door de aanvrager geen uitlooptijd bij onvoorziene omstandigheden te zijn opgenomen.
De aanvrager geeft aan, dat de injectieduur 15 tot 20 jaar zal zijn gebaseerd op de operationele en commerciële plannen en onzekerheden daarin. Eventuele effecten op de integriteit van de afsluitende laag of op de stabiliteit van breuken treden waarschijnlijk pas op aan het einde van de injectie-periode.

Advies

De beoogde duur van injectie in relatie tot de hoeveelheid CO_2 is redelijk, TNO-AGE geeft ter overweging mee deze duur op minimaal 20 jaar te houden startend op moment van injectie.

Duur van de vergunning in relatie tot overdracht naar de overheid
De aangevraagde duur houdt ook onvoldoende rekening met de – nog nader te bepalen – voorwaarden voor overdracht van de opslag aan de overheid.
De aanvrager voorziet een relatief korte periode (circa 1 jaar) van post-injectie monitoring onder haar verantwoordelijkheid voor de opslagvergunning. TNO-AGE heeft ernstige twijfels of die termijn voldoende zal zijn om de insluiting en stabiliteit van de opslag aan te tonen (zie ook ‘Sluitingsplan’). Realistischer is een scenario waarin de aanvrager tijdens de injectie- en monitoringfase - de kwaliteit en voorspellende kracht van hun modellen op reservoirgedrag en bijbehorende

effecten zal demonstreren, evenals de effectiviteit van het monitoringsysteem (zie hieronder 'monitoringsplan').

Advies

TNO-AGE adviseert om de duur van de opslagvergunning te relateren aan het operationele onderdeel van de plannen (zie duur van injectie in advies boven) en de doorlooptijd behorend bij de de voorwaarden voor overdracht aan de overheid. Uitgangspunt moet zijn, dat de vergunninghouder verantwoordelijk blijft voor de opslag, totdat een correcte overdracht naar de overheid heeft plaatsgevonden.

Omvang van het vergunningsgebied

TNO-AGE heeft een pre-advies (zie bijlage 2) uitgebracht over de vergunning afbakening[1]. Dat advies betreft een kwaliteitscontrole op de door de aanvrager aangeleverde coördinaten van de grenzen.

Op basis van de modellen gepresenteerd in de aanvraag en onderliggende rapportages zal de opgeslagen CO_2 onder normale omstandigheden, d.w.z.. zonder lekkage naar buiten het opslagcomplex, binnen de vergunning grenzen blijven zoals in de aanvraag aangegeven. Dit geldt ook als CO_2 tijdelijk in de aquifer naast het opslagreservoir terecht zou komen.

Hoewel het niet volledig kan worden uitgesloten dat de CO_2 in geval van lekkage en vervolgens laterale migratie buiten de aangevraagde vergunningsgrenzen zal treden, acht TNO-AGE het nu niet nodig om op voorhand ruimere grenzen te stellen die deze gebeurtenissen zouden dekken. In dit verband merken wij ook op, dat de aanvraag geen diepte-begrenzing kent.

Samenhang met P18-4

TNO-AGE merkt op dat de beoogde vergunning grenzen niet aansluiten aan bestaande P18-4 begrenzing. Aangezien de aanvrager niet kan uitsluiten dat er tussen het P18-4 en P18-2 opslagvoorkomen enige drukcommunicatie zal plaatsvinden zou het te overwegen zijn om deze vergunningengebieden te combineren dan wel de vergunning grenzen direct te laten aansluiten.

Advies

TNO-AGE adviseert de vergunningsafbakening aan te houden zoals voorgesteld door de aanvrager. De samenhang met de ‘P18-4’ vergunningaanvraag moet worden meegenomen.

[1] E-mail van TNO-AGE aan EZK “Gebiedsbeschrijving aangevraagde opslagvergunning "P18-2" “, 24-2-2021

Onderwerp 2; De geotechnische onderbouwing van de aanvraag, waaronder een beoordeling van de gegevens met betrekking tot de hydraulische eenheid; Aantonen geschiktheid reservoir voor CO_2-opslag

TNO-AGE interpreteert hier onder 'geschiktheid' effectiviteit van insluiting, niet alleen het opslagvolume en de injectiviteit.

TNO-AGE acht dat het voorgestelde opslagvoorkomen op basis van de aanvraag voldoet aan de eisen voor geschiktheid voor CO_2-opslag indien effectieve operationele limieten worden vastgesteld (o.a. druk). Uit versie 2.0 van de aanvraag blijkt de operationele rapportage significant gewijzigd te zijn ten opzichte van de originele aanvraag en nog niet definitief zijn, daarom kan TNO-AGE hier verder geen oordeel over vormen. TNO-AGE verwacht op basis van de huidige rapportages dat de aanvrager goed in staat is deze gegevens in de finale plannen, technisch onderbouwd, kan leveren

Advies

TNO-AGE ziet in de algemene geotechnische onderbouwing geen reden negatief te adviseren met betrekking tot de geschiktheid van het reservoir voor CO_2-opslag.

Onderwerp 3; Beoordeling van de veiligheid van de opslag c.q. of er bij opslag onder de voorgestelde exploitatievoorwaarden een significant risico van lekkage bestaat, of significante milieu- of gezondheidsrisico's bestaan;

TNO-AGE beperkt dit advies tot het modelleren en monitoren van de injectie en insluiting van de CO_2 door de aanvrager. Op basis van de modeluitkomsten en het monitor-plan is beoordeeld of het voorgestelde systeem in staat is om significante afwijkingen van het 'ideale' gesloten tankgedrag te kunnen detecteren, en de mogelijke duiding daarvan.

In hoeverre deze afwijkingen een risico voor milieu en/of gezondheid kunnen zijn, valt buiten dit advies. TNO-AGE heeft lekkage langs de put niet meegenomen in haar beschouwing, dit is met EZK afgestemd aangezien dit afdoende in het advies van SodM wordt meegenomen.

Verticale lekkage door de afsluitende lagen.
De afsluitende lagen hebben onder geologische tijdschalen (~miljoenen jaar) afdoende gefunctioneerd om aardgas in te sluiten. In het geval dat er alsnog lekkage optreedt door de afsluitende lagen naar buiten het opslagcomplex is de kans minimaal dat het opgeslagen CO_2 binnen voor het klimaatbeleid relevante tijdschaal (~1000 jaar) in de atmosfeer komt.

Lekkage langs breuken
De aanvrager heeft elk mogelijk lekpad uit het model of theorie modelmatig beschreven. Hieruit blijkt dat er op enkele locaties een kleine kans op laterale lekkage zou bestaan op basis van juxtapositie. In het scenario geschetst door de aanvrager heeft zij voldoende aannemelijk kunnen maken dat er lateraal geen lekkage zal optreden op basis van gegevens uit de gasproductiefase. Echter TNO-AGE heeft op de opzet en gebrek aan verschillende versies van het statisch model wel kritiek (verdere details zijn opgenomen in het technisch rapport). Door alternatieve interpretaties kunnen significante verschillen in potentiële lekpaden ontstaan.
De sensitiviteitsanalyse van het statisch model dienen in de actualisatie of de definitieve versie van het plan dat voorafgaande aan de start van de injectie ter goedkeuring moet worden overlegd aan de minister te worden meegenomen om adequaat een inschatting te kunnen maken van laterale lekkage.

Seismiciteit
Zie bodembeweging (hieronder)

Advies

TNO-AGE adviseert om in de actualisatie of de definitieve versie van het risicobeheerplan rekening te houden met onzekerheden in alle elementen, waaronder seismische interpretatie, productiegeschiedenis, reservoireigenschappen, reservoirdistributie, stromingseigenschappen etc.

Onderwerp 4; De grenswaarden van de druk van de opgeslagen CO_2 en de maximum toelaatbare snelheid en druk bij injectie van CO_2 en de maximale toelaatbare druk van het opgeslagen CO_2;

Toegestane injectie-snelheid:
De aanvrager geeft aan de CO_2-injectiesnelheden per put te beperken tot 40 kg/s. Echter, vanwege specifieke eigenschappen zal de toelaatbare snelheid per put kunnen afwijken, gezien de variërende injectiviteiten en beperkingen met betrekking tot koeling en impact op geomechanische risico's (rekening houdend met de locatie van een put in het opslagcomplex). De operationele scenario's zijn in versie 2.0 van de aanvraag significant gewijzigd ten opzichte van de originele aanvraag. De aanvrager geeft ook aan dat de operationele plannen nog niet gefinaliseerd zijn, mede daarom kan TNO-AGE hier verder geen oordeel over vormen

Advies

TNO-AGE adviseert om per put maximale injectiedrukken en injectiesnelheden toe te staan en de aanvrager deze gefaseerd te laten definiëren. Hierbij rekening houdend met de resultaten van de early stage monitoring. Deze aanpak dient onderdeel te zijn van de (te actualiseren) plannen.

Grenswaarden van de druk en maximaal toelaatbare druk
De drukbegrenzing is met name bepaald om het risico te verminderen voor:

a) Mechanische stabiliteit van de top seal (door onder de initiële reservoirdruk te blijven)
b) CO_2 lekkage langs verticale lekpaden (door een lagere druk dan de hydrostatische gradiënt aan te houden zal er vloeistof het opslagvoorkomen instromen in plaats van uitstromen)
c) Destabilisatie van breuken door o.a. temperatuureffecten.

TNO-AGE acht punt c) minder relevant aangezien dit vooral bij hogere drukken optreedt dan de maximale drukken behorend bij a) en b).

Het opleggen van een druk zal met doel b) de meest stringent zijn (laagste maximale druk) waarmee ook direct doel a) wordt behaald.
Echter dit vereist een juiste definitie van de hydrostatische gradiënt en deze wordt op basis van de aanvraag onvoldoende gedefinieerd. Daarom stelt TNO-AGE voor om deze met een afdoende onzekerheidsbandbreedte te bepalen, hiermee tenminste rekening houdend met alle bekende metingen, zoutgehaltes, verschillen in drukken na injectie en een afdoende brede onzekerheidsanalyse om een veilige grens te kunnen bepalen.

Advies

TNO-AGE adviseert om bij de start van het project de hydrostatische druk als maximaal gemiddelde reservoirdruk aan te houden. Deze dient wel afdoende onderbouwd te worden aangeleverd door de aanvrager.

Onderwerp 5; Beoordeling van de plannen

In lijn met de eisen uit de EU CCS-richtlijn zoals geïmplementeerd in de Nederlandse mijnbouwwet heeft de aanvrager (concepten van) de vier plannen ingediend:
1) Risicobeheerplan
2) Monitoringsplan integraal opslagcomplex
3) Plan van corrigerende maatregelen
4) Afsluitingsplan
Alle vier plannen behoren bij het ‘integrale P18-opslagcomplex’.

TNO-AGE is van mening dat deze plannen coherent moeten zijn om samen een risicomanagementsysteem te vormen. Meer specifiek hebben we het praktische vermogen geëvalueerd om onverwachte en ongewenste gebeurtenissen tijdig te detecteren, wat leidt tot effectieve corrigerende maatregelen. Deze ‘closed loop’ monitoring beschouwen wij als een essentieel onderdeel van een betrouwbaar risicomanagementsysteem.

Risicobeheerplan
Het risicobeheerplan omvat een veelvoud aan potentiële risico’s en heeft deze in kwalitatieve zin beoordeeld. TNO-AGE is van mening dat de kansen op risico’s kwantitatief benaderd dienen te worden om een objectieve beoordeling te kunnen maken. De specifieke elementen van het Risicobeheerplan worden in de beantwoording van Onderwerp 3 beschreven.

Monitoringsplan
TNO-AGE heeft de nadruk gelegd op de vraag in hoeverre het door aanvrager voorgestelde monitoringsysteem daadwerkelijk lekkages kan detecteren, wat uiteindelijk veiligheidsrisico's kan opleveren voor het milieu en voor de gezondheid. Dat noemen we ‘controle op de integriteit van de CO_2-opslag’.

TNO-AGE constateert dat het door de aanvrager voorgestelde monitoringsysteem in wezen berust op:

1. Bewaken van de druk en temperatuur in de operationele injectieputten;
2. Gebruik van de p/Z-curve afgeleid van de gasproductiefase om het p/Z-gedrag in de CO_2-injectiefase (en verder in de post-injectiefase) te herleiden.

Het voorgestelde 'p/Z'-monitoringsysteem is alleen gebaseerd op materiaalbalansgronden (volume) en kan als zodanig niet bepalen hoe CO_2 uit het opslagreservoir is ontsnapt. Een afwijking in de p/Z monitoring kan duiden op:
- ‘lekkage’ (CO_2 passeert de topseal en/of putten), en/of
- ‘migratie’ (CO_2 verlaat de opslagreservoirs, maar blijft onder de top seal.

Daarnaast is de p/Z monitoring niet zonder complicaties. Door het Joule-Thomson effect treden er tijdens injectie grootschalige temperatuur fluctuaties op in het reservoir. Hierdoor kan men niet uitgaan van een constante Z waarde, waardoor de p/Z niet lineair is. De Z moet daarom afdoende gekalibreerd worden aan de

temperatuurmodellen om bruikbaar te zijn voor monitoring. Dit is in de huidige aanvraag nog niet meegenomen.

De monitoringsgegevens dienen periodiek aangeleverd te worden door aanvrager. Beoordeling daarvan zou een kwaliteitscontrole van de gegevens kunnen zijn, maar die verantwoordelijkheid ligt primair bij de aanvrager.
Van veel groter belang is, dat de aanvrager in haar rapportages (periodiek en/of ad hoc) ook aangeeft, in hoeverre de monitoring aanleiding geeft tot waarneming van 'significante' afwijkingen van het op basis van modellen verwachte meetsignaal, en welke maatregelen de aanvrager daaraan verbindt in termen van modelaanpassing en/of correctieve maatregelen.
TNO-AGE meent, dat de aanvrager onvoldoende motiveert, hoe met een dergelijk beperkt monitoring systeem effectieve risicobeheersing kan worden uitgevoerd bij CO_2 opslag.

Advies

TNO-AGE meent dat de aanvrager onvoldoende motiveert hoe het voorgestelde, beperkte, monitoringsysteem adequaat risicobeheersing kan behelzen bij CO_2 opslag. Daarom stelt TNO-AGE ook voor om de monitoringsplannen ruim voor begin van injectie te laten actualiseren met een adequaat systeem. TNO-AGE adviseert om een meet en regelprotocol te laten opstellen waarin het 'closed loop' karakter van het Monitoring plan en het Risicobeheerplan voldoende tot uiting komt.

Plan van corrigerende maatregelen
Gezien de huidige lacunes in de Risicobeheerplannen en monitoringsystematiek is het niet zinvol om over dit plan te adviseren aangezien deze afgeleid is van het risicobeheer- en monitoringsplan.

Afsluitingsplan
TNO-AGE stelt voor om de tijdslimiet voor het "afsluitingsplan" uit te stellen omdat het modelleringswerk niet voldoende is gekalibreerd tot er meer informatie is over de lange termijn. Het voorgestelde tijdsbestek van 1 jaar na het stoppen van de injectie lijkt echter erg kort op basis van het dynamische modelleringswerk. Uiteindelijk zal het reservoirgedrag leidend moeten zijn en pas als de stabiliteit van het reservoir afdoende is aangetoond, met goedkeuring van de minister, kan het systeem worden afgesloten en uiteindelijke overgedragen aan de staat.

Advies

TNO-AGE stelt, gezien de nog niet uitgewerkte versies, de plannen te laten actualiseren (zie ook Onderwerp 7). De definitieve plannen behoeven dan instemming van de minister alvorens de injectie kan worden gestart.

Onderwerp 6; Bodembeweging

De aanvrager heeft een uitgebreide studie gedaan naar geomechanische effecten die zouden kunnen optreden bij de gasproductie en CO_2-injectie in het P18-veld. Deze effecten zijn breukactivatie, met bodemtrillingen tot gevolg, en ondergrondse scheurvorming door druk- en/of temperatuurverschillen. De studie is op grondige wijze uitgevoerd met redelijke aannames voor de belangrijkste parameters. Zonder monitoringsgegevens is het echter niet mogelijk om deze onderzoeksresultaten te valideren. Doordat Porthos het eerste grootschalige CO_2-opslagproject in een gedepleteerd gasveld zal zijn, is ook niet mogelijk om de onderzoeksresultaten te vergelijken met eerdere projecten. Daarnaast is er nog onvoldoende aangetoond dat de getoetste situaties werkelijk representatief zijn door het ontbreken van een geïntegreerde sensitiviteitsanalyse uitgevoerd met foutpropagatie uit een statisch en dynamisch model. Specifieke zaken worden verder in het technische rapport besproken.

In Nederland zijn verschillende ondergrondse aardgasopslagen waarbij geïnduceerde seismiciteit heeft opgetreden (Bergermeer, Norg, Grijpskerk). Tot op heden heeft gaswinning uit het P18-veld geen meetbare seismiciteit veroorzaakt. De aanvrager is daarom van mening dat het huidige KNMI-netwerk ook afdoende is om seismiciteit tijdens de injectiefase te monitoren. Hoewel TNO-AGE de kans klein acht dat er seismiciteit optreedt die veiligheidslimieten zal overschrijden, vindt TNO-AGE deze afweging onvoldoende onderbouwd. Het Porthos project is qua gasvolumes en injectiesnelheden vergelijkbaar met aardgasopslagen, maar CO_2-injectie zorgt voor afkoeling van een significant gesteentevolume. Hierdoor kunnen nabijgelegen breuken worden gedestabiliseerd waardoor de kans op seismiciteit wordt verhoogd ondanks de stabiliserende werking van de drukverhoging door injectie. Dit komt ook naar voren in de modelresultaten van de aanvrager. TNO-AGE ziet daarom liever een uitgebreider meetsysteem met een lagere detectielimiet. Hiermee zou breukstabiliteit kunnen worden gemonitord door lokalisatie van (micro)seismische events. Daarnaast zou het systeem mogelijk ook gebruikt kunnen worden om thermisch geïnduceerde scheurvorming vroegtijdig te detecteren.

Advies

TNO-AGE adviseert om een volledig geïntegreerde gevoeligheidsanalyse uit te voeren, waarbij ook onzekerheden uit de statische als dynamische modellen worden meegenomen. Dit zal voor zowel bodemtrillingen als scheurvorming, de basis moeten vormen voor de geomechanische limieten qua operationele parameters als druk, temperatuur en injectiesnelheid.
Hiernaast adviseert TNO-AGE om effectieve monitoring te implementeren boven op het voorgestelde meetsysteem. Hiermee kunnen de modellen empirisch worden gekalibreerd en kan het optreden van eventuele onverwachte of ongewenste ontwikkelingen beter worden gecontroleerd.

Onderwerp 7; Overige relevante opmerkingen

Relatie met P18-4 en P18-6
De huidige vergunningaanvraag voor P18-2 kan niet los worden gezien van de beoogde activiteiten in de P18-4 en mogelijk de P18-6 opslaglocaties. Ondanks dat deze aanvraag juridisch gescheiden is van de andere licenties kunnen ze in technische zin niet worden gescheiden. Daarom zullen alle activiteiten in het operationele venster van het opslagcomplex zoveel mogelijk op elkaar moeten worden afgestemd. Om bovenstaande redenen acht TNO-AGE het wenselijk om alle vergunningen voor de P18 opslagvoorkomens inhoudelijk en procedureel consistent te krijgen en te evalueren.

Uniek karakter van het Porthos-project
Het Porthos-project als geheel (onder de vlag van vergunningen P18-2, P18-4 en mogelijk P18-6) is vooralsnog een uniek project. Er zijn enkele kleinschalige injecties van CO_2 in gedeeltelijk lege gasvelden [het Laq veld, K12-B], maar op deze commerciële schaal is dit nog niet eerder vertoond. Dit betekent dat veel van het werk gebaseerd is op modelleringswerk op basis van theorie en niet empirisch is gekalibreerd.

Omdat CCS in lege gasvelden potentieel een zeer grote rol voor Nederland speelt bij het behalen van de doelstellingen van het Klimaatakkoord is het van belang dat dit project wordt benut als een voorbeeld en als een leer/validatieproject. We hebben hier rekening mee gehouden in onze technische evaluatie en ons advies. Natuurlijk maakt het unieke karakter van het project niet expliciet deel uit van het formele vergunningproces, maar gemiste kansen kunnen de Nederlandse doelstellingen voor het behalen van de CO_2-reductiedoelstellingen ernstig belemmeren.

TNO-AGE acht het wenselijk om in het P18 project, gezien het pionierskarakter van het project, de monitoring extra uitgebreid in te zetten. Dit dient ter lering en validatie van de modellen, aannames en operationele scenario's van de huidige aanvragers, maar werpt tevens zijn vruchten af voor toekomstige CO_2-opslagprojecten. TNO-AGE adviseert om de aanvrager te vragen om een uitgebreid monitoringsplan waarbij de mogelijkheid wordt besproken één of meerdere putten in te zetten voor (tijdelijke) waarnemingen waaronder met name micro-seismiciteit om eventuele (thermische) scheurvorming te monitoren, drukontwikkeling en CO_2-doorbraak vanuit andere injectieputten.

Procesvoorstel actualisatie plannen
Aangezien de aanvraag gebaseerd is op lopende werkzaamheden waarover nog vele vragen bestaan en er over enkele vragen daarom nog geen finaal advies gegeven kan worden adviseert TNO-AGE om de finale versie van de plannen voor risicobeheer, corrigerende maatregelen en monitoring in het licht van het operationele plan voor het integrale P18-opslagcomplex uiterlijk 1 jaar voor injectie te laten actualiseren en goedkeuren.
Het afsluitingsplan zal pas in een later stadium, na monitoring van injectie van CO_2 geactualiseerd kunnen worden. Er zijn op dit moment nog te veel onzekerheden

om dit effectief te kunnen beoordelen. De termijn hiervoor kan na 2 jaar door de minister bepaald worden of dit opportuun is.

Datum
23 juli 2021

Onze referentie
AGE 21-10.XXX

Blad
1/2

Bijlage 2 Kaart en gebiedsbeschrijving

Het gebied van de aangevraagde opslagvergunning "**P18-2**" wordt begrensd door de grootcirkels tussen de puntenparen A-B, B-C, C-D, D-E, E-F, F-G, G-H, H-I, I-J, J-K, K-L, L-M, M-N, N-O en A-O.

De punten zijn als volgt gedefinieerd:

punt	°	'	'' O.L.	°	'	'' N.B.
A	3	53	6,165	52	10	37,121
B	3	54	2,166	52	10	27,122
C	3	54	33,168	52	9	57,121
D	3	56	44,172	52	9	28,122
E	3	57	11,174	52	9	0,121
F	3	57	45,175	52	8	51,121
G	3	59	29,180	52	7	10,119
H	3	59	55,184	52	5	30,116
I	3	58	32,182	52	5	38,116
J	3	56	27,177	52	6	33,116
K	3	56	27,176	52	7	20,117
L	3	55	55,174	52	7	41,118
M	3	55	55,173	52	8	19,119
N	3	53	46,168	52	9	14,119
O	3	52	47,165	52	10	27,121

De ligging van de bovengenoemde punten is uitgedrukt in geografische coördinaten berekend volgens het ETRS89 systeem.
De oppervlakte van het gebied waarvoor de vergunning is aangevraagd bedraagt 26,51 km^2.

Datum
23 juli 2021

Onze referentie
AGE 21-10.XXX

Blad
2/2

Aanvraag opslagvergunning "P18-2"

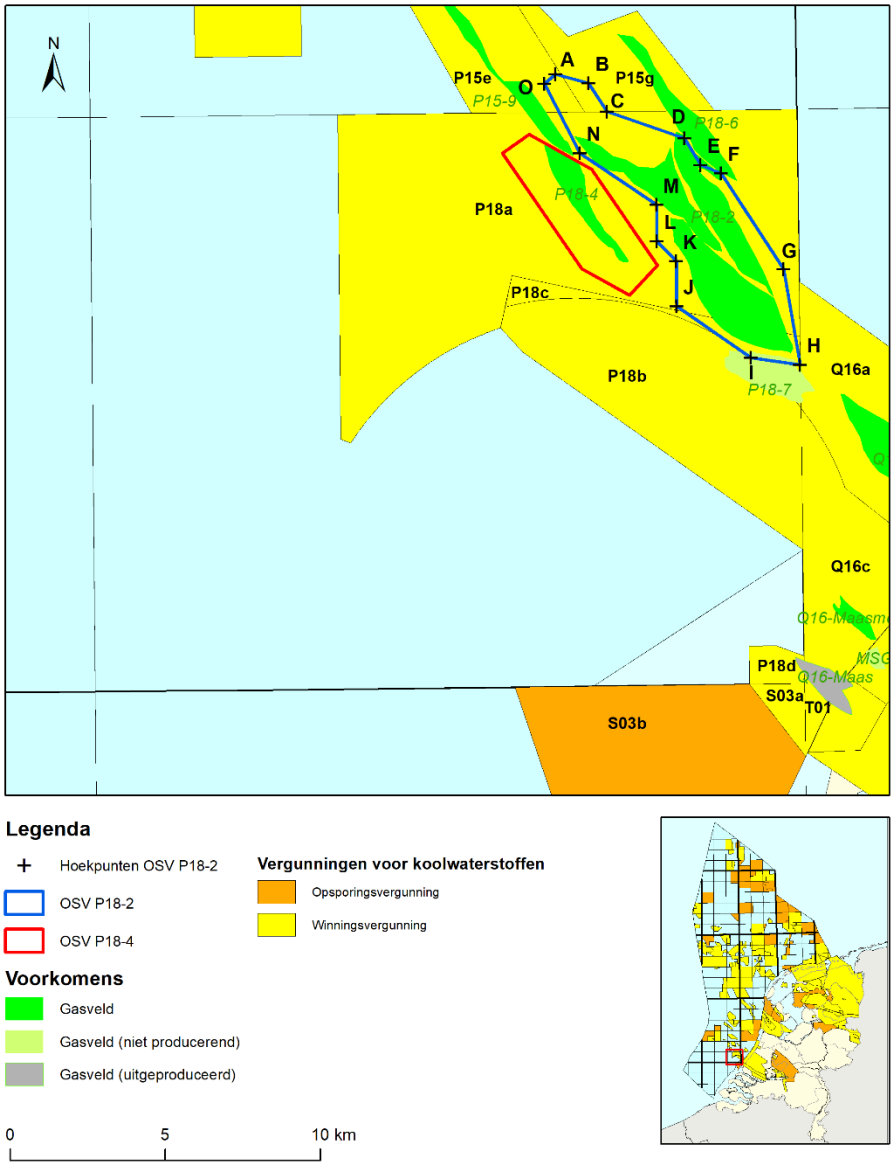

Legenda

- Hoekpunten OSV P18-2
- OSV P18-2
- OSV P18-4

Voorkomens

- Gasveld
- Gasveld (niet producerend)
- Gasveld (uitgeproduceerd)

Vergunningen voor koolwaterstoffen

- Opsporingsvergunning
- Winningsvergunning

0 5 10 km

TNO innovation for life

Princetonlaan 6
3584 CB Utrecht
P.O. Box 80015
3508 TA Utrecht
The Netherlands

www.tno.nl

T +31 88 866 42 56
F +31 88 866 44 75

TNO report

Bijlage 3 - AGE 21 - 10.055

Technical report evaluation storage license application P18-2

Date	8 October 2021
Author(s)	Rory Dalman, Jaap Breunese, Jon Limberger, Cintia Goncalves Machado, Gijs Remmelts, Bart van Kempen, Jeroen van der Molen en Wiebe van Driel
Copy no	1
No. of copies	1
Number of pages	75 (incl. appendices)
Number of appendices	2
Sponsor	
Project name	P18-2 licence application
Project number	060.47419

Samenvatting

Dit rapport bevat de resultaten van een door TNO-AGE uitgevoerde geotechnische evaluatie van het opslagcomplex P18-2. Deze evaluatie is ter onderbouwing van het door het ministerie van Economische Zaken en Klimaat (hierna: EZK) gevraagde advies [TNO-AGE 21-10.055] over de opslagvergunningaanvraag P18-2, zoals op 12 februari 2021 ingediend door TAQA en EBN.

De evaluatie omvat een toetsing van een aantal vragen door EZK betreffend operationele plannen, technische onderbouwing, veiligheid, doelmatigheid en te stellen grenswaarden. Hiervoor heeft TNO-AGE het werk van data tot model en het operationele plan geëvalueerd.

Geologische onderbouwing
De aanvrager heeft een uitgebreide studie gedaan naar de petrofysische-, seismische- en productiedata van het bestaand gasveld P18-2. Op basis hiervan is een statisch model geconstrueerd. Dit model komt grotendeels overeen met de gegevens. TNO-AGE vindt enkele keuzes van de aanvrager onvoldoende onderbouwd.

- Er zijn zeer redelijke alternatieve interpretaties mogelijk voor de seismische interpretaties van met name de breuken alsmede de top van het reservoir. Het verdient de aanbeveling deze als alternatief scenario mee te nemen.
- De toekenning van de relevante reservoir eigenschappen in het statisch model is niet overal consistent doorgevoerd. Dit betreft met name de geobserveerde afname van reservoir eigenschappen in de diepere lagen. Daarnaast ziet TNO-AGE de opschaling van de permeabiliteit en bepaling van de netto reservoirdikte als een belangrijke onzekerheid die niet meegewogen is in de verdere analyse.

Dynamisch reservoir model
Zodra de CO_2 vanuit de putmond het reservoir instroomt wordt verwacht dat er afkoelingseffecten optreden. De aanvrager heeft een adequaat model ontwikkeld om deze temperatuur effecten te evalueren. TNO-AGE heeft de volgende aanbevelingen:

- Om een effectief operationeel plan te ontwikkelen en grenswaarden voor injectiviteit en druk te bepalen is het noodzakelijk om een breed scala van verschillende modelrealisaties te berekenen.
- Er wordt door de aanvrager geen rekening gehouden met turbulente flow welke een grote invloed kan hebben in de nabijheid van de putmond.
- Door CO_2 injectie worden grootschalige temperatuurverschillen in reservoir verwacht. De effectiviteit van de beoogde monitoringsmethode door p/Z analyse zal nader aangetoond moeten worden voor deze omstandigheden.

Geomechanische evaluatie
Er is een zeer uitgebreide studie naar geomechanische effecten uitgevoerd. Dit om te bepalen of:

- er breukreactivatie en bijbehorende seismiciteit kan ontstaan;
- scheuren veroorzaakt door de temperatuurverandering kunnen leiden tot lekpaden

Hierbij zou een uitbreiding van het aantal dynamische modellen met verschillend scenario's een verbetering zijn. Alhoewel er geen grote risico's uit de modelstudies komen is er geen analoog project of empirische data voor de grootschalige opslag van CO_2 in gedepleteerde gasvelden. De keuze van de aanvrager om alleen op het KNMI netwerk te steunen om microseismiciteit te monitoren dient verder onderbouwd te worden, dit voor geïnduceerde seismiciteit alsmede thermische scheurvorming.

Conclusie
TNO-AGE acht de aanvraag van goede kwaliteit en het voorkomen geschikt voor CO_2 opslag, echter om de uiteindelijke operationele plannen te kunnen beoordelen moeten nog enkele stappen gezet worden, dit zijn met name:

- Volledige gevoeligheidsanalyse met onzekerheidspropagatie van de interpretatie van de data, naar het statisch model, dynamisch modelleerwerk tot geomechanische modellen.
- De operationele plannen dienen te worden hernieuwd en uitgebreid conform het closed-loop systeem. Met name de monitoring zoals voorgesteld is technisch beperkt door temperatuureffecten, daarnaast zijn de, bij monitoring noodzakelijke, waarden voor significante afwijkingen niet gegeven.

Content

1 Introduction

1.1 Objective

This report presents the results of the technical evaluation by TNO-AGE of the P18-2 CO_2 storage application in the P18-2 gas reservoir. The application was submitted by TAQA Offshore B.V. (subsequently TAQA is used) and EBN CCS B.V. (subsequently denoted as EBN). Colloquially the applicants are denoted as Porthos in this application document. This evaluation supports the advice (AGE 21-10.055) to the Ministry of Economic Affairs and Climate (MEAC) on 23-7-2021.

1.2 Questions for advice

Specific subjects for advice (as provided by the request from MEAC and derived from the Dutch mining law and regulation) relate to:

(1) The way in which the applicant is planning to permanently store the CO_2
(2) Duration of the license period
(3) Size of the storage complex and permit demarcation
(4) Demonstration of suitability of reservoir for CO_2 storage (containment)
(5) Geotechnical substantiation
(6) Significant risk of leakage / safety to the environment and / or health
(7) Safety limit violation due to pressure communication between multiple storage complexes
(8) Updating and assessment of monitoring data and stored CO_2 flows
(9) The limits of the pressure of the stored CO_2 and the maximum allowable speed and pressure for injection of CO_2 and the maximum allowable pressure of the stored CO_2
(10) Risk assessment plan
(11) Monitoring plan
(12) Corrective measures plan
(13) Closure/abandonment plan
(14) Ground motion

1.3 Relevant information

In this report ‘application’ pertains to all documents, models and information provided by the applicant within the framework of this licence application. A sequence of events is given in par. 2.6, including which information was requested and/ or provided when.

Completeness check
MEAC has asked for the opinion on the ‘completeness’ of the information provided in the two versions of the application document. TNO-AGE has answered by email for versions 1 [e-mail “Aanvraag P18-2 compleetheid” 12/3/2021] and for versons 2.0 [e-mail “Compleetheid aanvraag CCS P18-2 versie 2.0” 29/6/2021] . TNO has interpreted ‘completeness’ here as a measure to be able to start our evaluation, i.e. are all items mentioned in the regulation addressed at all: quality, technical depth and relevance were out of scope here yet.

Additional information provided on request from TNO-AGE
This primarily concerns delivery of the models, that underlie the application. With the help from Porthos, TNO-AGE has installed and operationalized these models. Objective was to do various quality and sensitivity tests, and have the option to run alternative scenarios. Rebuilding these models was considered out of scope. In addition to the model evaluation several reports were delivered and clarification was provided through personal communication.

Technical sessions with Porthos
Triggered by questions from both State Supervision of Mines (SSM) and TNO-AGE, technical sessions were held with Porthos aimed at clarifying the content of the application (see sequence of events).

1.4 Scoping

TNO-AGE has primarily evaluated the application on the basis of the specific questions from MEAC. Answers to the specific questions are summarized in this report and return in our advice. However, TNO-AGE has extended its remit to include storage effectiveness and efficiency and the 'fit for purpose' of the monitoring and risk management in the broad sense.

Risks
TNO-AGE considers the request for advice, and the conditions for granting the storage license, in essence to be a risk assessment. A breakdown of the various types of risks is:

1. technical risks
2. safety risks
3. policy risks
4. commercial risks

Given the available time, and specific role and expertise, TNO-AGE has focused on technical risks and policy risks. Safety risks were considered primarily the task of SSM; yet technical risks reflect themselves in the safety risk assessment, at least in the sense of monitoring and mitigation. Commercial risks were considered out of scope here, although technical risks may impact commercial risks, and thereby e.g. subsidies.

Unique nature of the Porthos project
The Porthos project as a whole (under the flag of licenses P18-2, P18-4 and possibly P18-6) is a unique project. There have been some small scale injections of CO_2 in partially depleted gas fields [e.g. the Laq field, K12-B], however the commercial scale has not been demonstrated before. This means that much of the work is based on modelling work based on theory and has not been empirically calibrated.
Additionally CCS in depleted gas fields has a potentially major role for the Netherlands in meeting its climate agreement goals. In this context the importance of this project cannot be understated. We have taken this into account in our technical evaluation and our advice.

P18 Storage complex
The current license application for P18-2 cannot be considered separate from the P18-4 and potentially the P18-6 storage sites. Despite the fact that this application is regulatorily separate from the other licenses we cannot separate them in a technical sense. Therefore it will be necessary for all licenses in the operational window of the storage complex to be aligned as much as possible.

Documentation & information
We have noted that much of the technical work presented in the license application is part of 'work in progress'. TNO-AGE had to decide to consider only the work submitted with the license application 1.0, the supporting models delivered by Porthos, and the clarifying information provided on request by Porthos.

1.5 Approach

Workflow
We have started by evaluating the submitted documents [*note: which ones in particular and why*], resulting in a series of 'first pass' observations and remarks. These were the basis for defining subsequent activities:

- questions forwarded to the applicant for clarification
- decide what subjects to focus on
- have internal experts review certain topics in depth
- quality check the models submitted by Porthos
- use these models for sensitivity analyses and test their effectiveness in the system management
- evaluate the coherence and practical feasibility of the four submitted plans

The outcome of these activities are described in this technical report. They form the basis for our advice.
.

1.6 Sequence of events

Given the fact that this application for CO_2 storage is the first under the new mining law MEAC has allowed the applicant to send a draft version of the application document and supporting reports for review. MEAC asked TNO-AGE to review this application (Table 1.1).
The actual application (Table 1.2) was submitted 12/2/2021 although an actualization was submitted on 22/6/2021.

Table 1.1 Draft version application process.

Date received	Name	Description	Direction
8/4/2020	CONCEPT_Aanvraag CO_2 opslagvergunning P18-2 6 april 2020	Word document with a draft version of the application and supporting documents	MEAC to TNO-AGE
13/5/2020	Verzoek TNO 13 mei 2020	Request for advice by MEAC on the draft application (dd 6/4/2020). Advice requested on completeness and clarity of content	MEAC to TNO-AGE
20/5/2020	Bevindingen inzake compleetheid Porthos concept vergunningsaanvragen	Content of completeness and clarity check on draft application (dd 6/4/2020)	TNO-AGE to MEAC

Table 1.2 Actual application process.

Date	Name	Description	Direction
12-02-2021	Aanvraag CO_2 opslagvergunning reservoir P18-2	Word document with a version of the application and supporting documents	MEAC to TNO-AGE
16-2-2021	Adviesverzoek TNO aanvraag vergunning permanent opslaan van CO_2 in het voorkomen P18-2	Request for advice by MEAC: on completeness, description on demarcation of license boundaries and mining law directives	MEAC to TNO-AGE

	Pre-advies OSVA P18-2 ETRS89	Description on demarcation of license boundaries	TNO-AGE to MEAC
8-3-2021	Application for a CO_2 storage permit reservoir P18-2	English translation of application documents	MEAC to TNO-AGE
12-3-2021	Aanvraag P18-2 compleetheid	Email with advice on completeness of application	TNO-AGE to MEAC
13-4-2021	Overleg tussen EBN en TNO-AGE	Clarification on choices regarding seismic interpretation and static model	Oral communication between TNO-AGE and EBN
20-4-2021	Technische werksessie TAQA/EBN/MEAC/adviseurs	Clarification on technical issues	Oral communication between SSM, EBN, TAQA and TNO-AGE and EBN
26-4-2021	Aanvulling Porthos ondersteunende documenten	Additional supporting documents missing in the original application	MEAC to TNO-AGE
22-6-2021	Aanvraag CO_2 opslagvergunning reservoir P18-2 2.0	Revised version of application document and supporting documents	MEAC to TNO-AGE

1.7 Background of the P18 complex

P18-2 Reservoir
The storage reservoir, as referred to in the application, is the current P18-2 gas field. The P18-2 field is part of a cluster of three gas fields consisting of P18-2, P18-4 and P18-6, as shown in Figure 1.1.
Prior to the CO_2 storage in the P18 cluster, the production of natural gas from the P18 fields will be stopped. This means that no more natural gas will be produced during the CO_2 injection. Six wells were drilled in the P18-2 field. There are five wells (including one well with a sidetrack), of which four producing wells and one exploration well awaiting final abandonment.

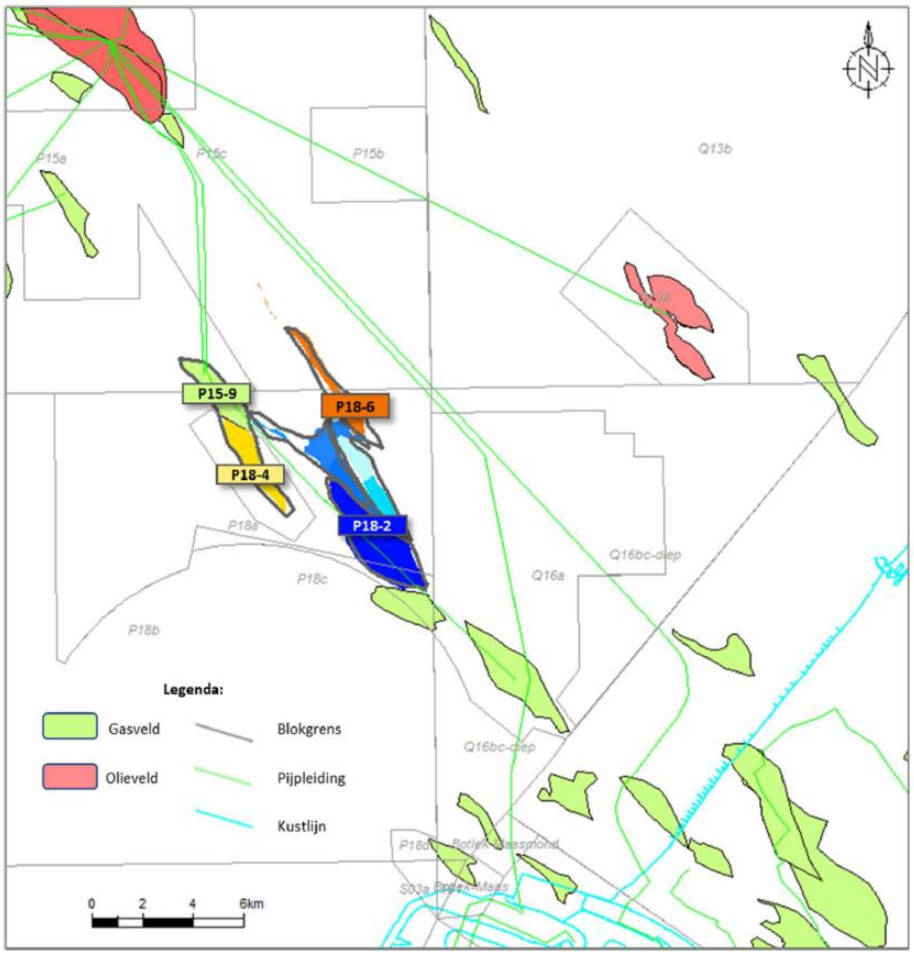

Figure 1.1 Map of block P18 and surroundings.

The applicants describe the vertical and lateral division of the reservoir on the basis of data obtained during gas production. The operating team of the gas field P18-2 has led the operations under several different owners during the entire production period of the P18 complex. As a result, there is a good understanding of the dynamics of the reservoir as a whole and the data obtained over time is largely managed by team ensuring continuity.
The storage area is made up of four vertically stacked sandstone formations of the Triassic Buntsandstein. The field consists of four blocks separated by faults to a greater or lesser extent. The field is horizontally divided into four compartments based on the pressure behaviour. The fourth compartment has not been drilled and is considered to have no connection with the adjacent compartment 3.

Structural containment hypothesis
The reservoir is bounded by faults and the reservoir layer dipping below the initial gas-water contact. The basic CO_2 containment principle is through the sealing top layer, the faults and the dipping layer, in the same way the natural gas was contained in the reservoir. The sealing potential of the faults is partly substantiated by the applicant in the form of Allen diagrams that indicate the juxtaposition of the rocks on both sides of the fault. This indicates that, for the most part, there is no direct contact between reservoirs above the gas-water contact on both sides of the fault. For those blocks there is possible reservoir-reservoir juxtaposition, the pressure development (P/Z plots showing the pressure development based on the

volume of gas produced) in those blocks during production indicates a contained reservoir within the P18-2 reservoir.

Similar reservoirs are found in the Netherlands and the P18 complex is a typical example of a Bunter field in the West Netherlands Basin. Knowledge about the geological features has been widely described in the scientific literature. Dynamic behaviour of these reservoirs are well known from the 60 years of production in the basin. This does not alter the fact that there will always be uncertainties at a detailed level about specific properties, so that the results of the simulation models also have a certain degree of uncertainty.
The knowledge about the geology and the dynamic reservoir behavior are the basis for the simulation models on which the predictions of the injection scenarios are based. These models and their technical basis are discussed in chapter 3.

Integral storage complex P18
The CO_2 storage complex is defined in the Mining Act as "storage sites for CO_2 and the surrounding geological areas that may have an impact on the overall integrity of the storage and its safety".

In principle, the storage complex applies to field P18-2, but ultimately, with CO_2 storage in the three intended fields P18-2, -4 and potentially -6, in practice the Storage complex P18-2 is part of the Integral P18 storage complex. (See Figure 2, Section 2.2.2 of Part I of the application TAQA & EBN, 2021.

Geological Delineation of Integral Storage Complex P18
The Integral Storage Complex P18 includes the following areas:
• The storage site of P18-2, P18-4 and P18-6 respectively;
• The geological capping layers above the storage reservoirs in Blocks P15 and P18, consisting of sediments belonging to the Upper Germanic Trias Group and Altena Group;
• The formations below the storage reservoir, consisting of Rogenstein and Main Claystone Formations;
• The P15-9 field with associated wells as part of the Storage Complex P18-4;
• The fault zones around the P18 fields and the side seal formations.

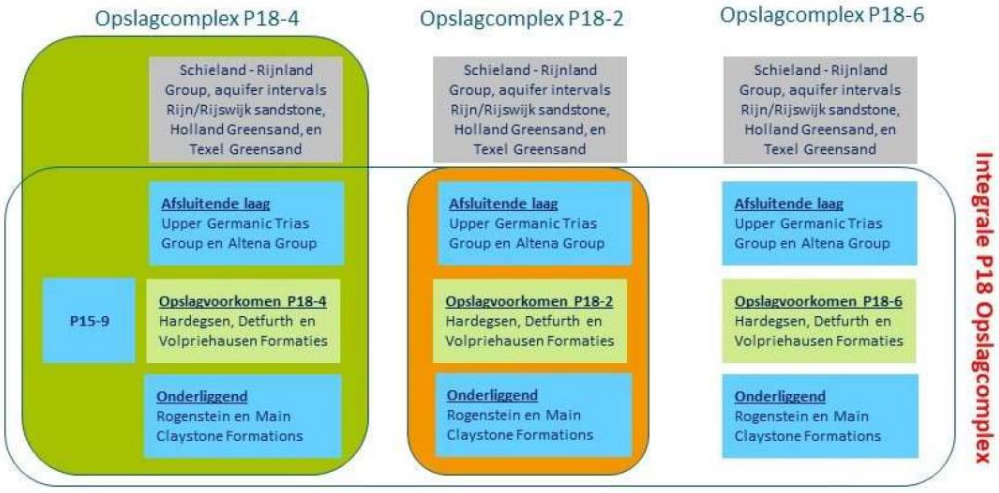

Figure 1.2 Overview of the P18 storage complex as defined by the applicant TAQA & EBN, 2021.

1.8 Location of the applied for P18-2 storage site and license boundaries

The area applied for the outlines of the storage site of P18-2 is provided in Figure 1.3.

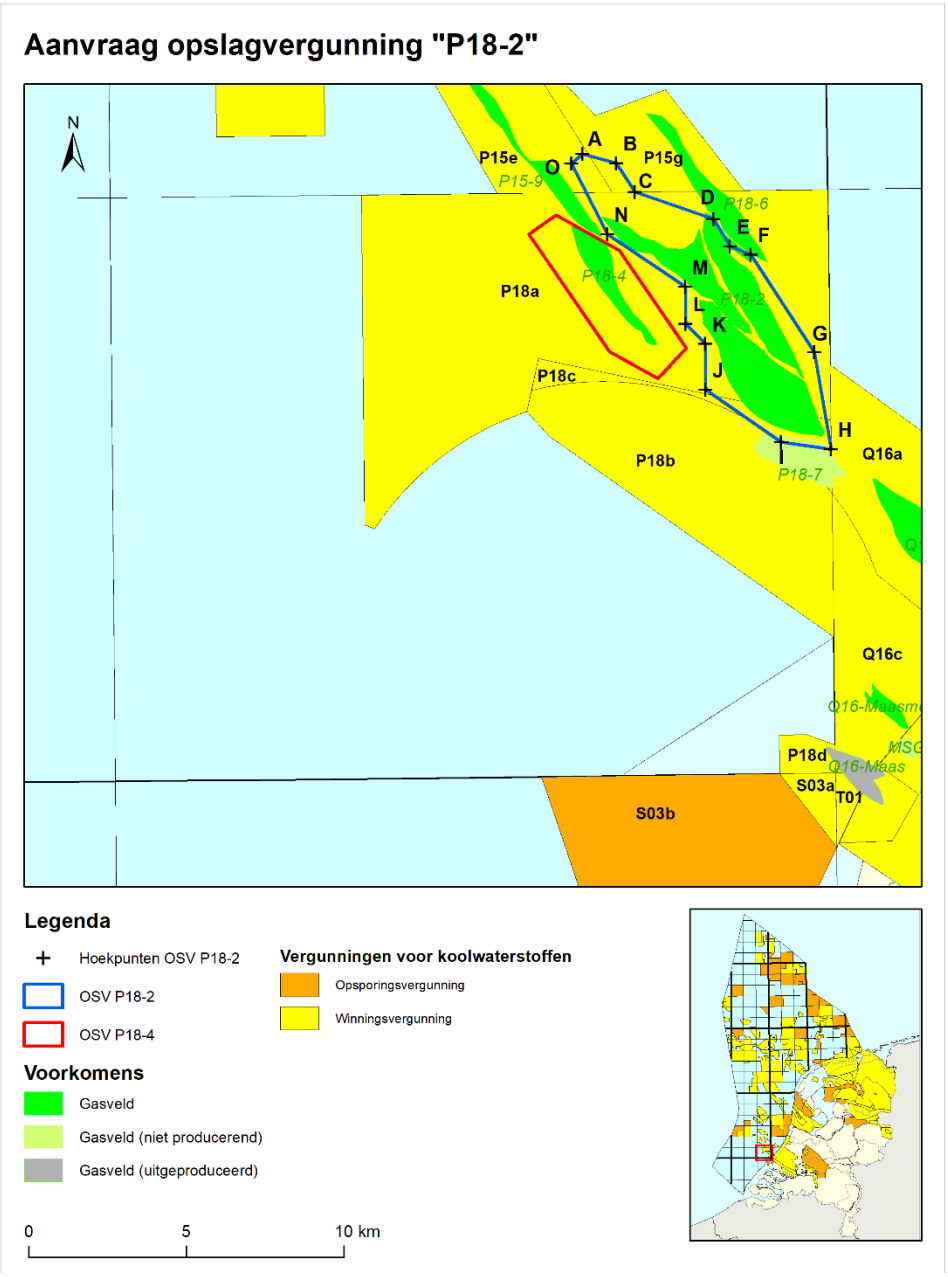

Figure 1.3 Applied for area of P18-2 (in blue) and relevant neighbouring subsurface activities. Note the existing license for CCS (P18-4) is provided in red.

2 Storage complex geological characterisation

2.1 Seismic interpretation and static modelling

2.1.1 Introduction

In order to check whether the fault interpretation and modelling of the P18-2, P18-4 and P18-6 fields were done adequately, TNO-AGE performed its own seismic interpretation of the faults. The interpretation was done using Petrel 2019.2, using the submitted Petrel model of the applicant as a basis. The submitted 3D seismic depth survey, which was also used by the applicant, was used for the interpretation, supported by a variance attribute cube. Furthermore a check was done on the quality of the interpreted and modelled top reservoir horizon and the quality of the reported juxtaposition of the reservoir rock across faults at the boundaries of the future storage reservoir. Although juxtaposed reservoir sections may prove to be sealing not all of these sections have been sufficiently proven to be sealing from production data. Thus any change in juxtaposition may result in a difference in risk assessment of potential lateral leakage. Furthermore internal faults may increase the risk of induced seismicity due to thermal effects.

2.1.2 Fault interpretation and model

As stated, TNO-AGE performed its own fault interpretation on the 3D seismic volume that was provided by the applicant. No interpreted faults were provided by the applicant, therefore the modelled fault sticks provided by the applicant are used for comparison.
Overall it can be concluded that most of the faults interpreted by TNO-AGE have also been observed by the applicant. There are some (slight) differences in the horizontal location or orientation of the modelled faults sticks from the applicant and those interpreted by TNO-AGE. This is related to the simplification of faults sticks, in this case faults sticks being completely straight, during the modelling process. TNO-AGE agrees with this applied simplification as it follows the general outline of the interpreted faults fairly well.

One major difference observed by TNO-AGE is that the interpretation done by TNO-AGE demonstrated that P18-2 Block IV (Figure 2.1) seems to continue in northwestern direction, into what the applicant calls the downthrown block P18-2 II. The eastern fault of P18-2 Block IV merges with the major boundary fault of P18-6. In this case, the juxtaposition between P18-6 and the main P18-2 structure reported by the applicant is not towards the downthrown P18-2 block II, but with what in the Petrel model is called Downdip 4. This potential alternative interpretation should be presented as such in the risk assessment.
TNO-AGE interpreted some minor internal faults in the P18-4 field and in all blocks of the P18-2 field. These internal faults have no effect on juxtaposition, but could play a role in injection behavior.

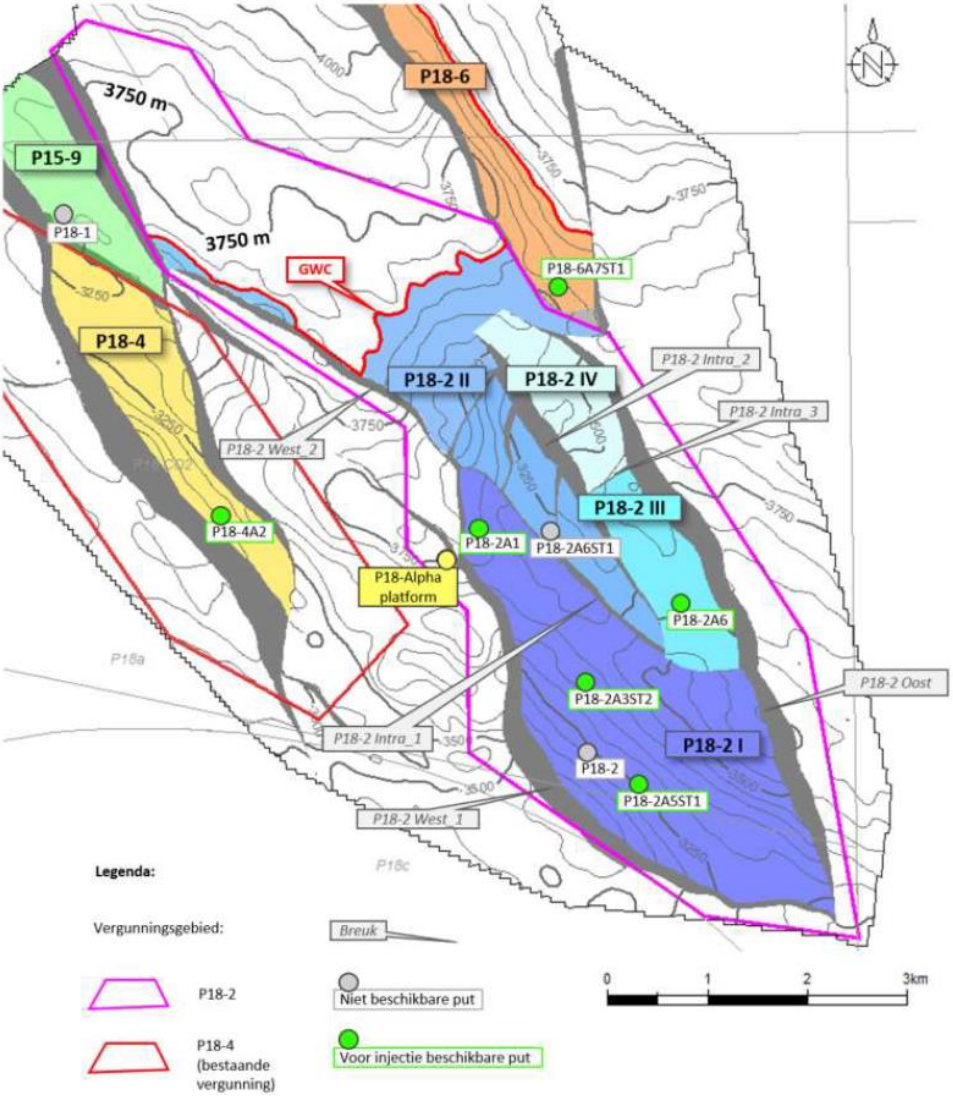

Figure 2.1 Overview of reservoir and block numbers as indicated by the applicant TAQA & EBN, 2021.

2.1.3 Top reservoir interpretation and model

TNO-AGE checked the well-tie of all wells present at the fields with respect to the interpreted and modelled top reservoir and the seismic data. We tested the interpreted and modelled top reservoir that follows the designated seismic wavelet interpreted to be the top Bunter reservoir. Most parts of the modelled area show a reasonable to good match of the seismic data with the interpreted and modelled top reservoir. However, some areas show a significant difference between the modelled top reservoir and the seismic horizon and seismic loop. This has been communicated with the applicant and it seems that numerous stochastic realizations were created of the top reservoir surfaces (pers.comm., 2021). The top reservoir provided by the applicant gave the best fit of the static model GIIIP with the dynamic GIIP, and as the applicated deemed this more important the

differences with the seismic data was taken for granted. TNO-AGE understands the applicants' strive for a good fit of the static and dynamic data.
However, TNO-AGE does not feel that any difference between static and dynamic volumes are adequately resolved by solely altering the top of the reservoir, as reservoir properties such as thickness, porosity and gas saturation also likely play a part. Additionally the chosen methodology ignores the seismic data largely.
The chosen top reservoir model with respect to the seismic data impacts the juxtaposition analysis provided by the applicant in the risk assessment plan.
Below we demonstrate some of the observed differences between the interpreted top reservoir, the modelled top reservoir and the seismic data that could lead to additional juxtaposition of the reservoir.

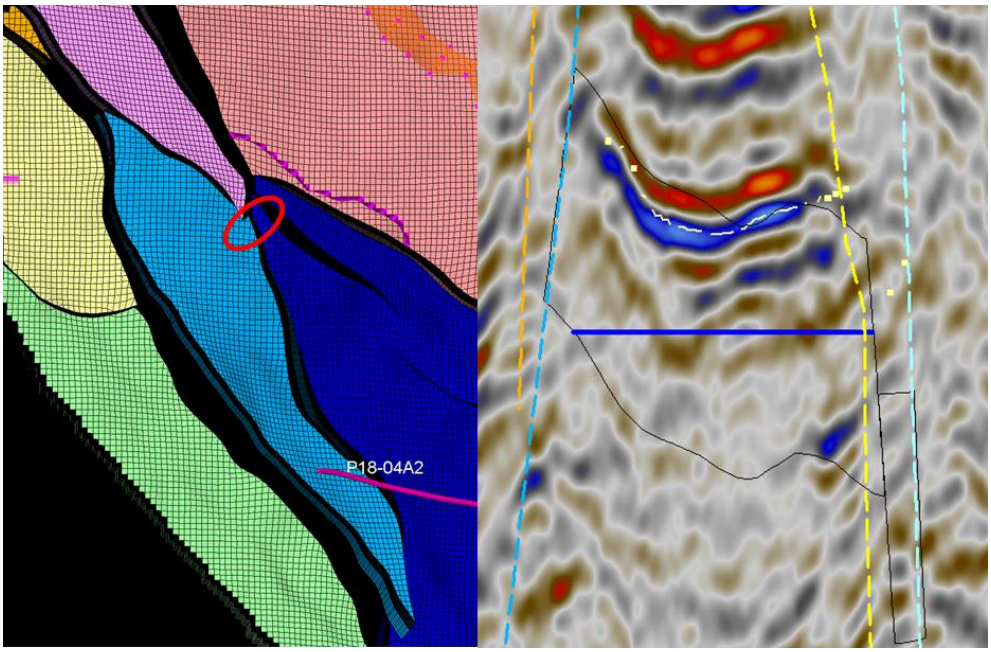

Figure 2.2 Inline 2025. The thin black line indicates the top reservoir surface, the subhorizontal dashed yellow line indicates the seismic interpretation of the top surface. The subvertical dashed lines are fault interpretations.

At the P18-4 field, at the wells P18-01 and P18-04A2 there seems to be a good to decent match between seismic data, interpretation and modeled top reservoir. However, away from the wells, the modeled top reservoir does not always follow the seismic data. Porthos reports a juxtaposition of the P18-4 field with the downthrown block, called P18-2 hanging wall in the Petrel model, at the eastern boundary fault (Figure 2.2). However, the downthrown block does not follow the seismic data as it should. If it would, there would be juxtaposition of the reservoir above the modelled Free Water Level.

At the P18-6 field there is a very poor well-tie between seismic data, interpretation and the welltop. The modeled top Bunter seems to be corrected for this poor match (Figure 2.3). The adjacent downthrown blocks at a specific distance also suffer from this poor match. The question arises whether picking a different modelled top reservoir could lead to a juxtaposition of reservoir between the P18-6 field and the downthrown block of P18-2 Block II (Figure 2.4).

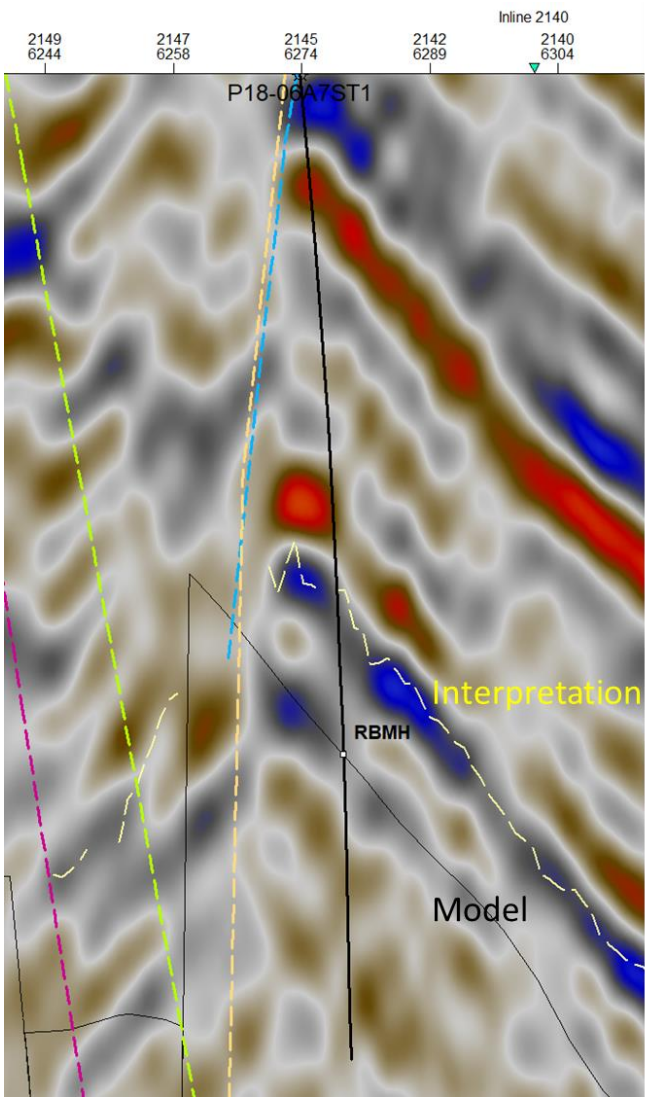

Figure 2.3 Cross-section through the P18-06A7ST1 well. The thin black line indicates the top reservoir surface, the subhorizontal dashed yellow line indicates the seismic interpretation of the top surface. The subvertical dashed lines are fault interpretations.

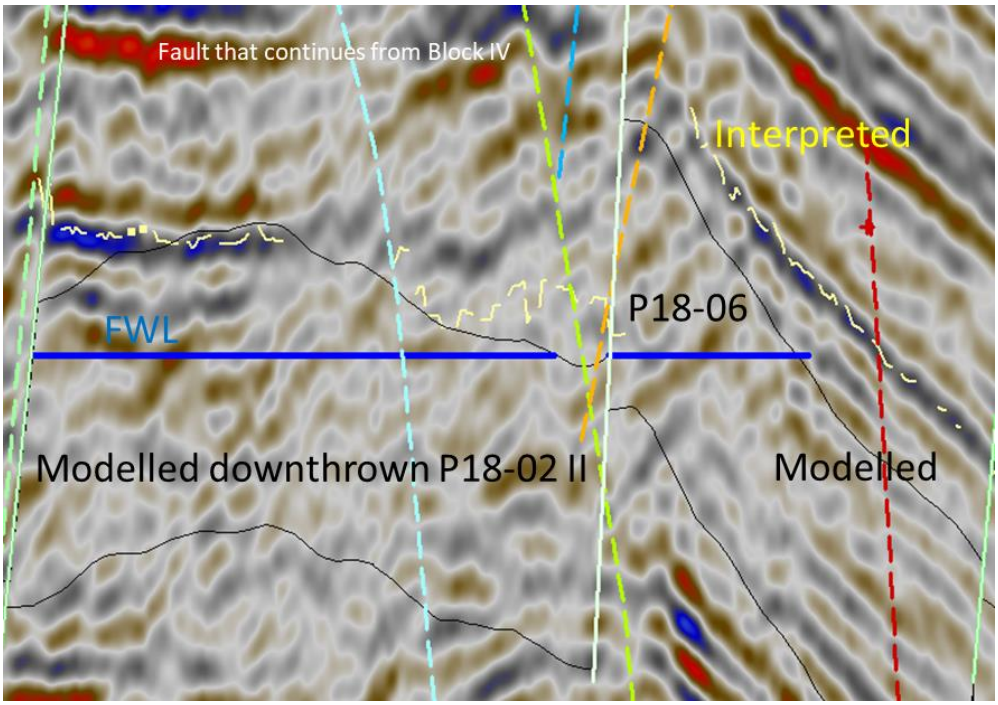

Figure 2.4 Inline 2115. The thin black line indicates the top reservoir surface, the subhorizontal dashed yellow line indicates the seismic interpretation of the top surface. The subvertical dashed lines are fault interpretations.

At block IV, the applicant reports a reservoir juxtaposition with the downthrown block. However, when comparing the modeled top reservoir with the seismic data/interpretation, it appears there is a poor match and the modeled reservoir seems to be shallower than the seismic data suggests (Figure 2.5). The downthrown side however, seems to be more in line with the seismic data. If the seismic data is correct, and the model is aligned, it could be that there is juxtaposition of the reservoir with the downthrown block. It is possible that this juxtaposition continues up to the northeastern tip of block III.

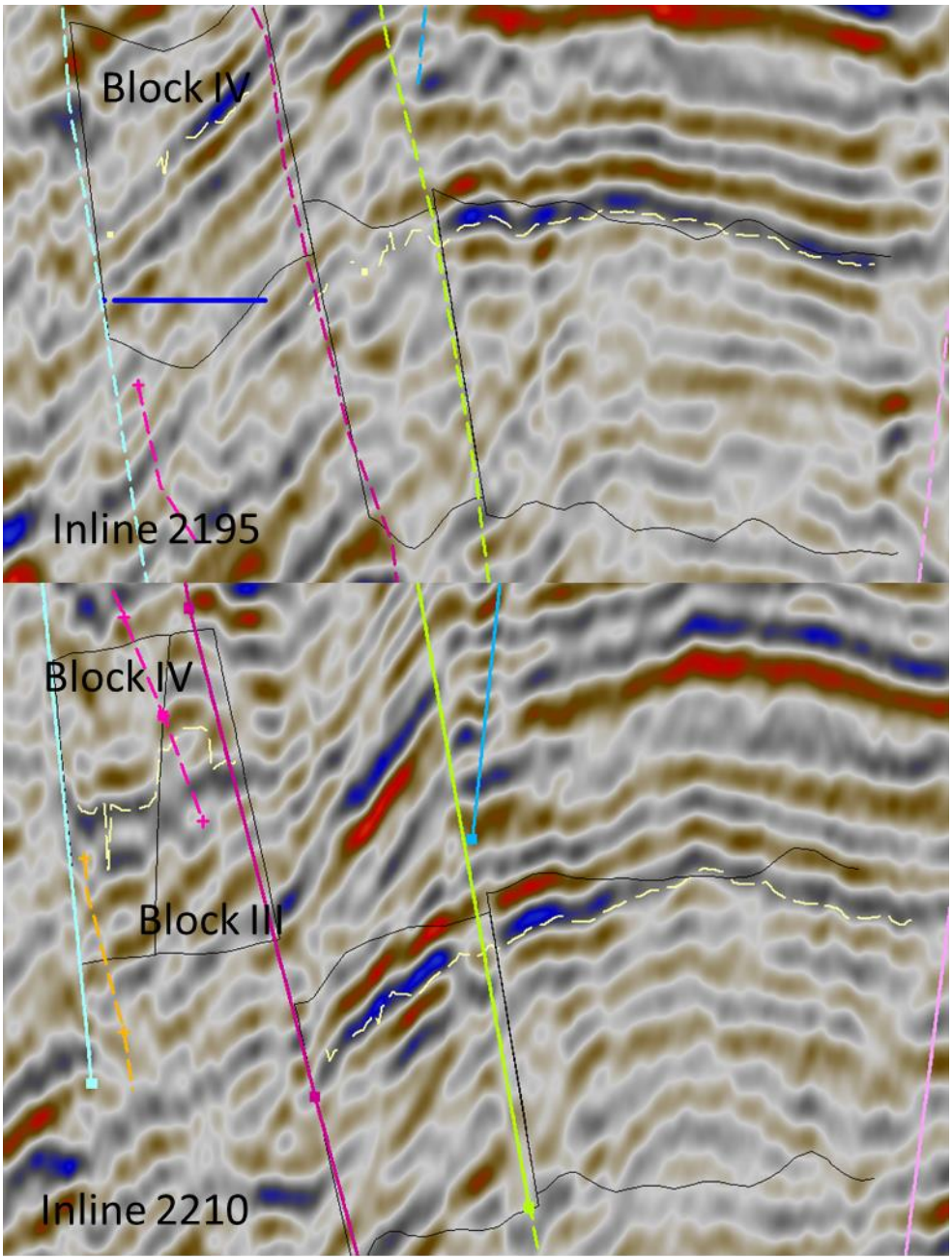

Figure 2.5 Multiple inlines through block IV and block III. The thin black line indicates the top reservoir surface, the subhorizontal dashed yellow line indicates the seismic interpretation of the top surface. The subvertical dashed lines are fault interpretations.

2.1.4 Juxtaposition and uncertainty

The applicant reports several juxtapositions of reservoir across faults at the P18-02 field, P18-4 field and the P18-6 field. The juxtaposition is derived from the model and directly affected by the top reservoir surface. As noted earlier, the applicant decided to use this top reservoir as it gave the best static/dynamic GIIP match, despite deviating from the seismic data significantly by several loops. The provided Petrel model does not contain any uncertainty ranges, at least not in the top reservoir. TNO-AGE considers the use of this single top reservoir surface a significant omission. Although the surface best matches the static/dynamic GIIP

there are multiple equiprobable realizations possible. For instance, when the seismic data is honored, more possible juxtapositions appear to be present and the risk assessment will need to be changed accordingly.

2.1.5 Conclusion and recommendations

A technical review was performed on the interpretation of faults and top reservoir of the P18-2 reservoir and surrounding area. The most important outcomes of this review are listed below.

- TNO-AGE agrees with the majority of modelled faults that were provided in the Petrel model.
- TNO-AGE does have a concern regarding the discrepancy at some (larger) areas of the top reservoir model and interpretation along with the seismic data. Although explained by the applicant that this top reservoir results in the best static/dynamic GIIP match, TNO-AGE considers the lack of uncertainty of different top reservoirs (close to the best static/dynamic GIIP) an omission in relationship to the presence and extension of reservoir juxtaposition across faults through the area. Ultimately affecting potential leak path evaluations

For future updates of the model, TNO-AGE would recommendations:

- Reinterpret the northwestern extension of Block IV of the P18-2 field. It appears to continue further than what the applicant demonstrates. This could have implications on the possible juxtaposition of P18-6 with the northern downthrown block of P18-2 as is reported now.
- Internal faults are observed in the P18-4 field and all blocks of the P18-2 field. While having no effect on the juxtaposition, they could have an effect on the injection.
- Test multiple top reservoir possibilities, while staying close to the best static/dynamic GIIP match, but also considering that e.g. thickness and porosity variation through the field can play a role and preferably while the seismic data is honored. This should give insight on the uncertainty of juxtaposition at the boundary faults at all fields.

2.2 Reservoir property distribution

2.2.1 Reviewed documentation and data

The following overview summarizes the documents and other material that was considered relevant for the reservoir properties distribution:

- Aanvraag CO_2-opslagvergunning reservoir P18-2 (Taqa & EBN, February 2021) TAQA & EBN, 2021.
  - Specifically: Deel II: Beschrijving CO_2-opslag reservoir P18-2 (Taqa & EBN, February 2021).
- Bijlagen behorende bij Aanvraag CO_2-opslagvergunning reservoir P18-2:
  - Attachment 7: CO_2 feasibility study (TNO, 2019)
    - Attachment B: Subsurface model descriptions
  - Attachment 8: Storage capacity technical note (Porthos, 2020).
- P18 Static model

A full petrophysical evaluation was carried out on the application, details are described in the Appendix.

2.2.2 Core description

Core analysis is based on the analogue core retrieved from well P18-07 drilled just northeast from the P18-2 complex. Log correlation indicates that the petrophysical properties can be correlated to the P18-2 storage site.
Cores were available for the Hardegsen and upper part of the Detfurth. While average permeability is quite good in the Hardegsen as stated by the applicant [1] at 254 mD based on arithmetic average. The effective rock properties are highly variable. The top ~15 m of the Hardegsen show the highest transmissivity (see also chapter 6), however the core measurements show that this varies from measurements of ~1mD to values exceeding 1000 mD within this interval. The cores clearly show this as the layers with relatively poorly sorted sandstones are highly cemented with dolomite (Figure 2.6 and Figure 2.7). These facies seem to have slightly poorer sorting and indicate a fluvial/sheetflood depositional setting. The highly porous zones have very good sorting, well rounded grains with fine to middle sand sizes. Compaction effects are limited and remnants of dolomitic cements in these zones indicate leeching of the dolomite cement. This means that the high permeability is likely a secondary feature occurring after burial.

Based on these observations the effect of detrital clay content on effective porosity and permeability is indirect at best.

The high permeability zone in P18-07 consists of 8 zones with an average thickness of 30 cm and a standard deviation of ~10 cm. These are not directly correlatable as the lateral extent of the facies is limited, however the log response in the P18-2 storage complex does indicate a similar permeability distribution. This does mean that the permeability is extremely heterogenic vertically, even within the upper Hardegsen zone. Additionally the limited lateral extent of the eolian facies will result in a tortuous path of injection fluid and a resulting limitation of net effective permeability (see also well correlation panel in Figure 2.8). TNO-AGE therefore recommends using a geometric average for upscaling the permeability (see appendix), thereby attaining a more representative flow pattern in the dynamic modelling.

Figure 2.6 Example of highly dolomite cemented facies with permeabilities of ~1 mD.

Figure 2.7 Example of highly porous and permeable facies in well 18-2. Note some dolomite cement is still present in the finer grainsize layers, most has been dissolved in the larger grainsize bands resulting in local core plug permeabilities in excess of 1000 mD.

2.2.3 Property modelling of porosity and permeability

Given the vertical variability in horizontal permeability of three to four orders of magnitude the current grid cell thickness with a median of ~3 m and arithmetic upscaling of the permeability by the applicant raises doubts on the representativeness of the actual effective flow dynamics.

The applicants have used a simulated gaussian stochastic modelling technique to populate the interwell model grid cells. The variables based on the observations are individually adequate, using e.g., a range of ~300 m. However, each individual layer has been modelled independently while honoring the upscaled well data. The static model therefore shows the expected coarsening upward sequences with the highest permeable layers in the top (Hardegsen Formation). Due to the independent stochastic population of the model this trend is not present in the model further from the wells (e.g. Figure 2.9). This will likely greatly influence the flow direction and rates in the dynamic reservoir modelling.

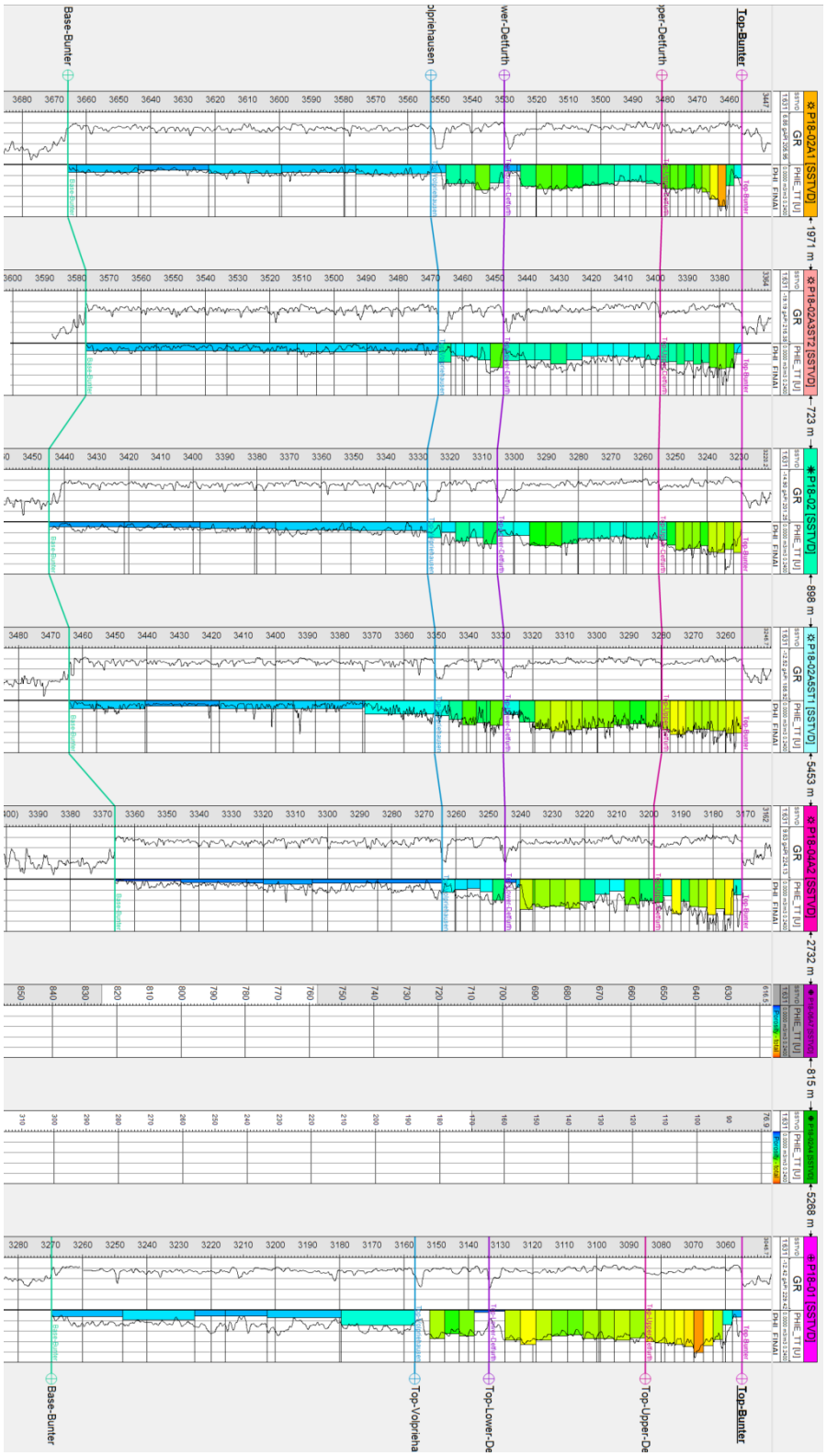

Figure 2.8 Well correlation panel through the P18-2 complex. Note the general trend can be correlated well at formation level. Smaller heterogeneities within the formations vary significantly across the storage complex.

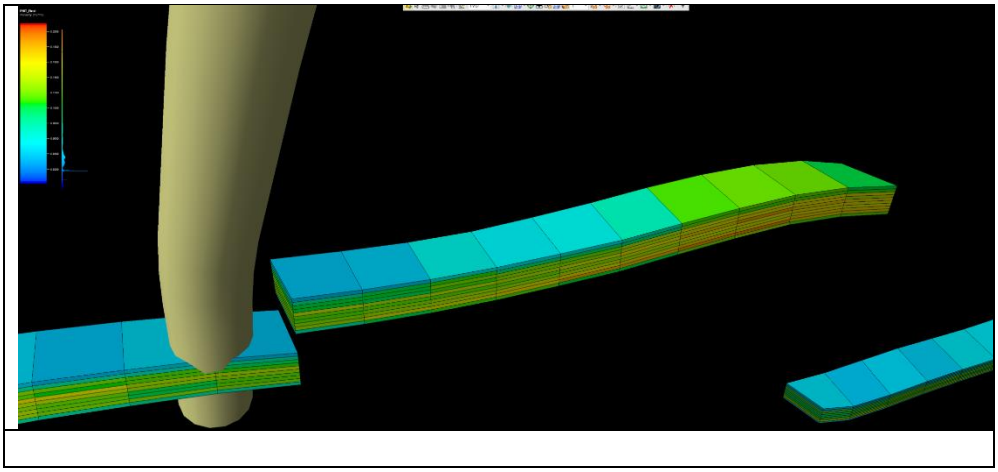

Figure 2.9 Example of lateral change in permeability away from the wellbore in the P18-2 static model.

2.2.4 Discussion and conclusions

(1) Upscaling of the log and core permeabilities should be carefully considered given the 3 orders of magnitude vertical heterogeneity in permeability.

(2) The lateral permeability will likely be lower than a the well as the decimeter scale high perm streaks are not laterally continuous but will not extend further than ~decameter scale. This causes a lateral baffle as fluid flow will have to move through the lower permeable zones (see 3.2)

(3) The average trend of a high perm streak in the upper Hardegsen is likely to be found in the entire reservoir.

(4) The observed upward increase in permeability is observed in all wells, however the applicant does not honor this trend in between the wells in the static model due to the stochastic method of populating the static model.

(5) The reservoir property distribution chosen by the applicant will influence the dynamic modelling projections significantly. TNO-AGE advices to take into account the high permeability contrasts by upscaling the permeability using geometric averaging.

(6) Finally the choices in determining well reservoir property and subsequent population of the static model will have a significant influence on CO_2 flow projections.

3 Dynamic reservoir modelling

3.1 Reports used for evaluation

The following reports supporting section II of the main application documents for P18-2 and P18-4 were used for the TNO-AGE assessment of the dynamic modelling:

- Appendix 7: CO_2 storage feasibility study in the P-18 depleted gas field (TNO, 2019)
- Appendix 8: Storage Capacity Technical note (Porthos, 2020)
- Appendix 9: P18 Porthos well injectivity (Porthos, 2020)
- Appendix 11: Injection plan Porthos (Porthos, 2020)
- Dynamic models:
  - Eclipse 300 isothermal gas production and CO_2 injection forecast models
  - CMG GEM isothermal gas production and CO_2 thermal forecast models

3.2 History matched geological model

Only one geological model realization was generated, and history matched (Appendix 8 in the license application report) using the gas production data, making sure the reservoir porous volume and well data were respected. Even though the P18-2 field is well-know and the model could match the production data, it remains to be seen whether it will be capable of predicting the CO_2 injection process, especially the moving directions of CO_2 cold fronts. A good estimate of CO_2 cold front is essential to the “seismicity management,” specially predicting fault stability. As the report itself mentions (Appendix 11), well injection rates will be controlled in order avoid the cold front to reach nearby faults, especially in the initial phase where there are considerable pressure differences in the reservoir due de depletion in the former producing zone. Once the pressure is stabilized near initial pressure, this become less of an issue, but thermal fracking in the seal and thermal destabilization of faults could still be an issue (See Chapter 5 for more detailed discussion). It is common practice in oil fields developments to do field management with an ensemble of model realizations, which can account for uncertainty in geological properties and their distribution, and also fault number and locations TAQA & EBN, 2021. In the latter, an ensemble of realizations is history matched by assimilating the field historical data, and this ensemble of model realizations used for predictions and optimizations accounting for uncertainty TNO, 2020.[3][4]. Even though the model used match GIIP values and there is a lot of information from the near-wellbore regions, there are still equiprobable realizations (also uncertainty). This is evident in how the geological features as high-perm streaks and faults that did not play a large role in the gas production, but may significantly affect the CO_2 distribution throughout the reservoir.

3.2.1 Model geological fidelity

As explained in Chapter 3, the numerical grid used to represent geological properties is much coarser than the geological variations observed in the well logs (centimeters to meters scale, as you can see in Figure 3.1). The model does seem to represent the high-perm streak observed in the upper Hardegsen on an averaged grid level. But given the thin bedded nature of each high perm streak it is not expected that each individual streak is connected away from the wellbore, consequently, influencing CO_2 distribution.

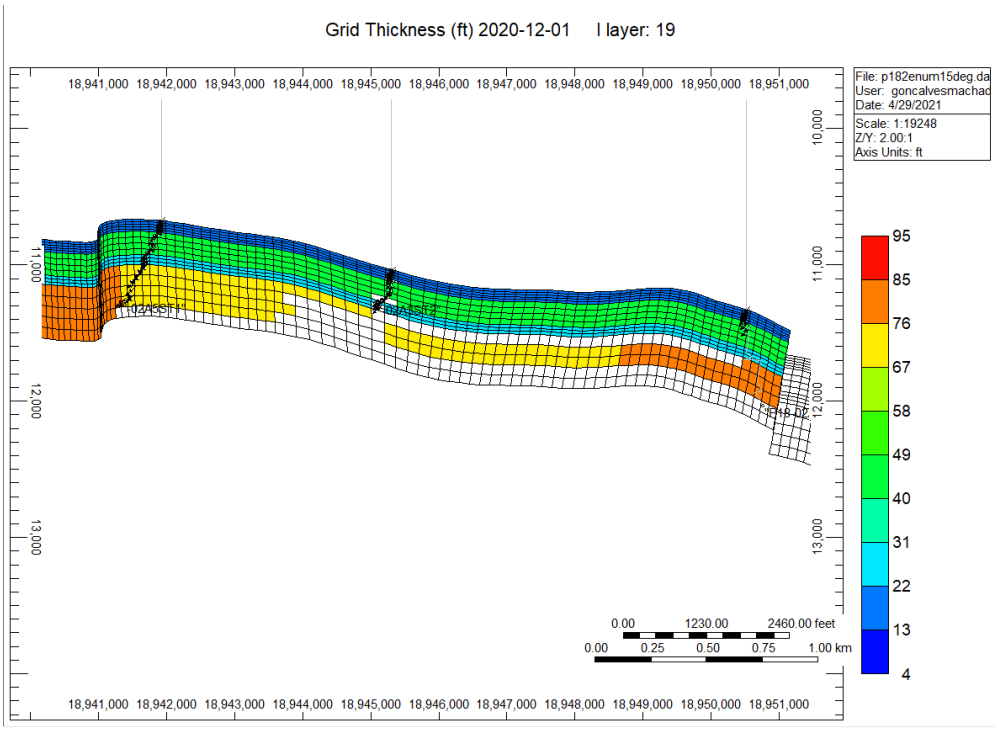

(a)

(b)

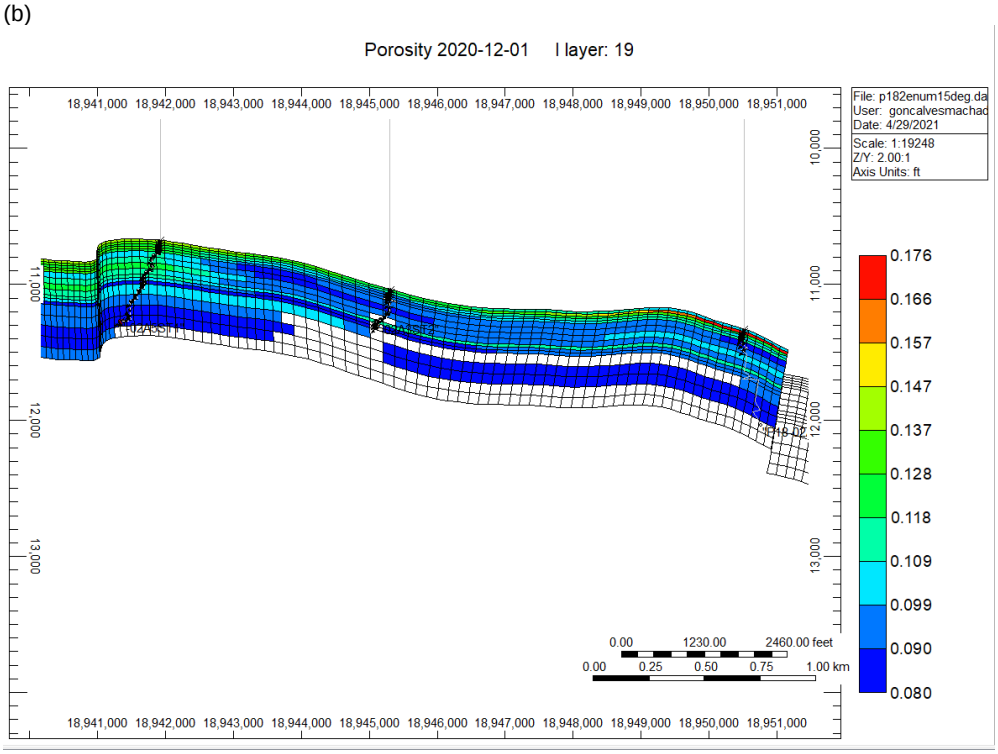

Figure 3.1 Numerical reservoir grid block thickness (a) and porosity (b) for vertical cross section J-K number 19.

3.2.2 Isothermal versus thermal History-match

Porthos has first calibrated the Eclipse 300 model, then generated a GEM model identical to the Eclipse 300 model (Section II, Modelling of CO_2 Storage). Both models were isothermal, there is no mention of verifying that the thermal numerical model would be capable of reproducing the production data. Even though thermal effects should not a play a role during production, temperature/pressure changes due Joule-Thompson and adiabatic expansion effects could still happen. Before actually modeling the thermal injection process, it seems it was not checked if the thermal simulation model would still match the production data.

3.3 Forward modelling CO_2 injection field development phase

For the dynamic modelling of CO_2, several reservoir numerical models were created using the geological model realization cited above. In the technical report (Appendix 7) is mentioned the use of Eclipse and Tough2 reservoir simulation for the initial studies of the behavior of CO_2 injection in the depleted natural field P18-2. Tough2 was used to estimate, in a homogenous model, the position of the CO_2 cold front. Information was incorporated in the initial geomechanical studies with MACRIS. Salt precipitation was also modelled, but considered negligible in P18-2. The Eclipse model use for the initial studies was history matched with the production data. This was an isothermal model (126 degrees ^oC). In order to do more realistic studies, this history matched Eclipse model was translated into an CMG GEM isothermal model, and an extra thermal model was created based on the isothermal model. In this thermal model it is assumed CO_2 is injected at 15^oC into the 126^oC reservoir. No report is made of sensitives studies regarding the variations of injection temperature. Different well injection rate strategies were presented, including the worst case scenario and the base case (the strategy intended to be used in the field development).

3.3.1 P/Z monitoring

P/Z versus Cumulative Gas Production plots were mentioned as a tool for monitoring the triggering of mechanical fractures in the reservoir (Technische werksessie TAQA/EBN/MEAC/adviseurs (P18-2) at April 20, 2021). This is a well-known material balance method to monitor gas production [5], assuming a linear relationship between P/Z and the gas volume produced. If the data deviates from the linear behavior, one might expect e.g. water influx (active aquifer) or fracture initiation. However CO_2 injection is a non-linear process, where the deviation from the expected P/Z curve could have multiple additional causes such as two-phase flow (supercritical fluid and gas fluid), or incorrect input data. Also, TNO-AGE has doubts on how well pressure and temperature may be evaluated from the wells. Monitoring through solely P/Z seems unlikely to allow clear and timely processes to be monitored further in the reservoir (i.e., the p/Z(p,T) plot being able to reflect a fracture propagating into the seal).

In [7] a linear a p/z *versus* (Gp – Ginj) is shown. Here Gp is the accumulated surface volume of produced gas and Ginj represents the accumulated volume of CO_2 injected into the field. However, in this paper the CO_2 does not goes through supercritical phase, and the minimum Z-factor is ~0.6, while the GEM modelling for the Porthos project indicates Z-factors of ~0.2 around the well when CO_2 is in supercritical state during the first few year of injection (Figure 3.3). Given the cold CO_2 injection, it can be shown from the field material balance that including known temperature, the plot of p/(zT) vs. (Gp – Ginj) would give a linear curve. In practice this would lead to the

question, how to compute the temperature to be used? As can be seen in Figure 3.4, after shutting the well, would take 20 years for the temperature to stabilize and 10 years for the pressure. This figure was generated by closing all the wells after 3 years of planned CO_2 injection. And this disregards any uncertainty in the thermal modelling.

To better estimate these curves, TNO-AGE re-run the thermal GEM model outputting the grid Z-factor for both gas and supercritical phases. We observed that the average reservoir Z-factor will decrease from 1.08 to around 0.8 during injection. In the near-wellbore zone, there is large variation in the Z-factor, dropping to around 0.2 when CO_2 around the well is in the supercritical state. This contrast of Z-factor between near-wellbore region and the far region filled with natural gas can persists for several years (Figure 3.2). Concluding; TNO-AGE has serious doubts on the potential of using P/Z plots as an adequate monitoring tool. We recommend a plot of the p/Z curves versus Cumulative Produced Gas minus Injected CO_2 with and without a fracture to be generated to show the potential of P/Z as monitoring tool within cold CO_2 injection into depleted gas fields.

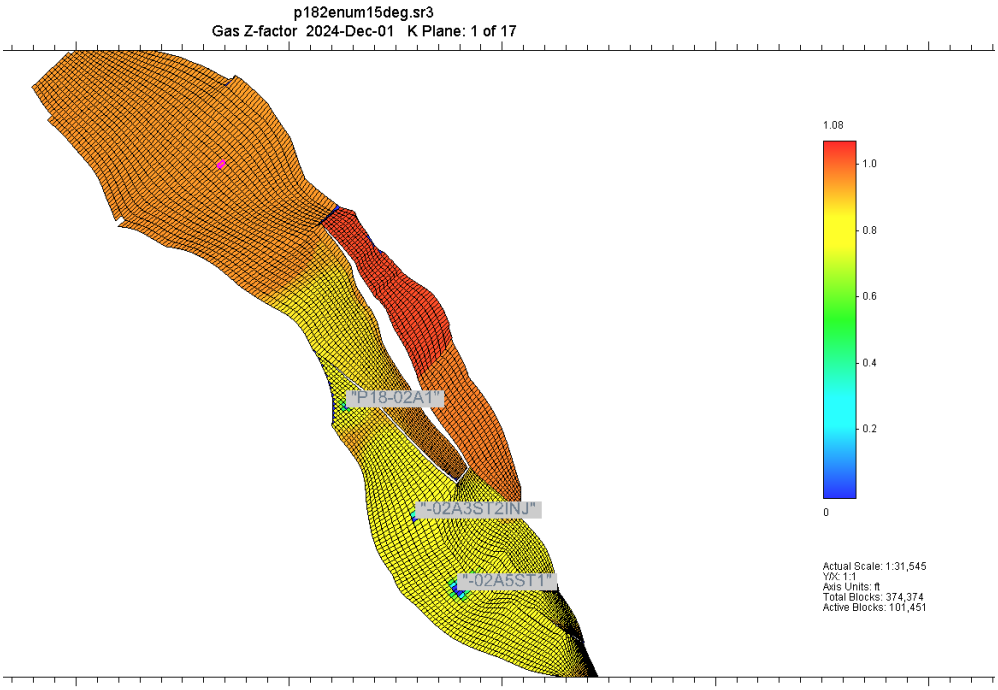

(a)

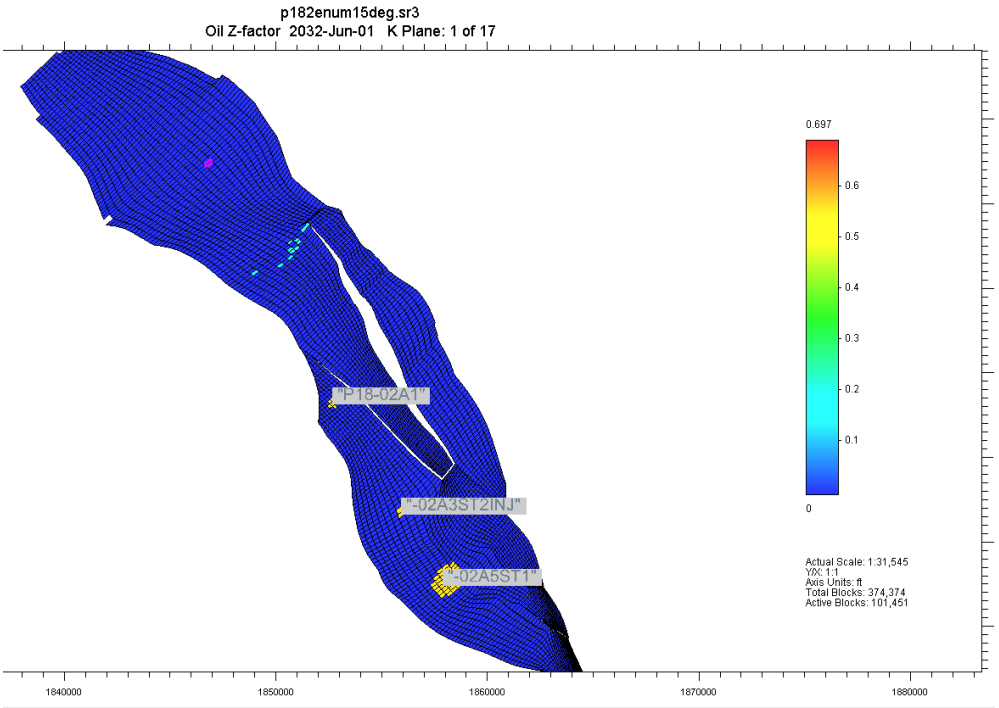

(b)

(c)

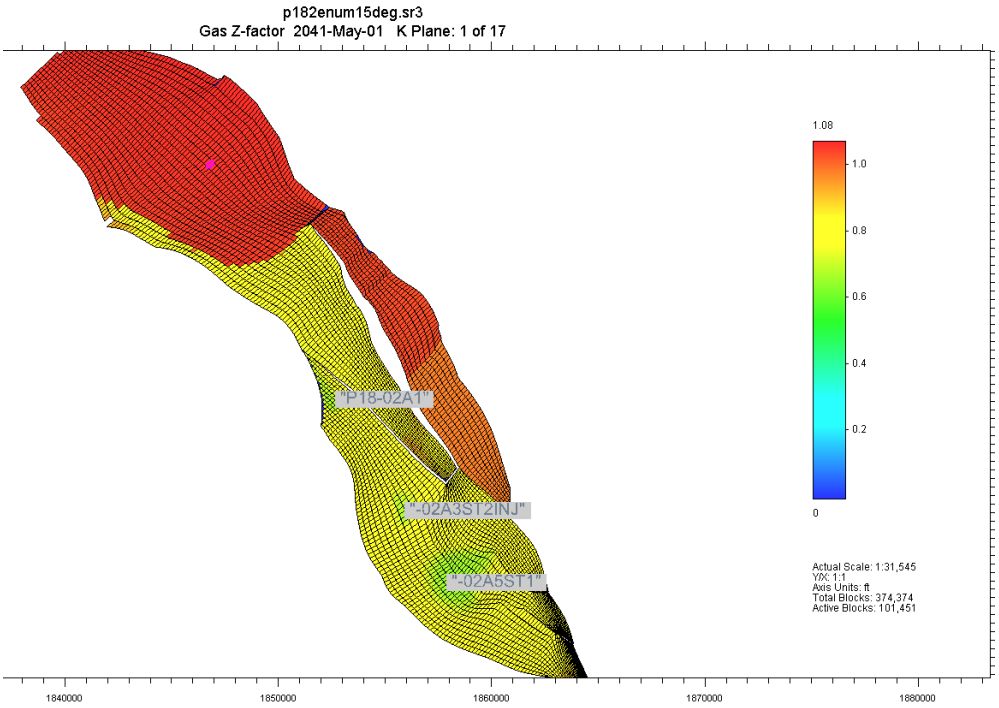

Figure 3.2 Z-factor distribution in the reservoir along CO_2 injection development. Note; here oil phase denotes supercritical phase.

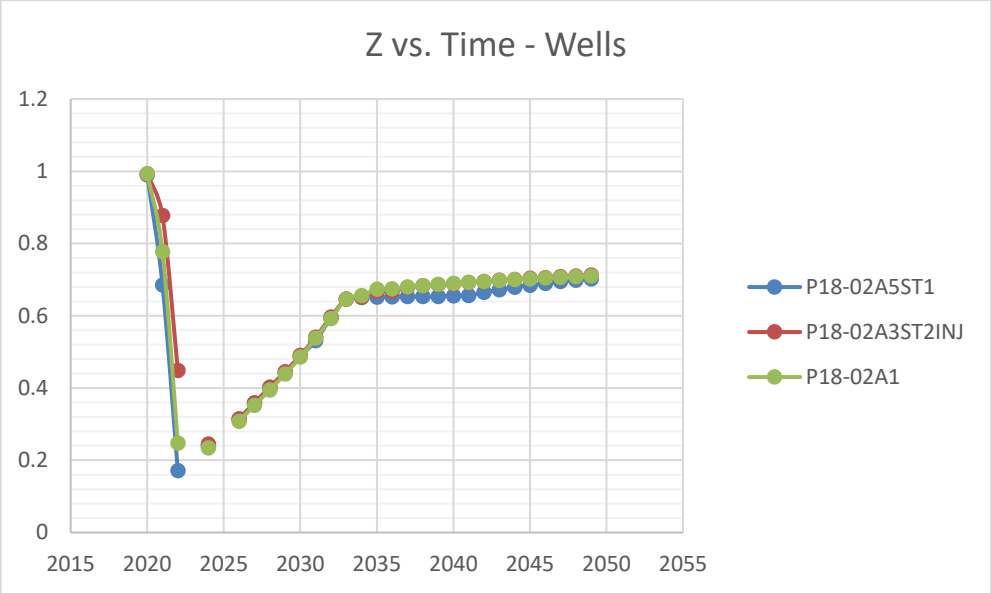

Figure 3.3 Z-factor versus time during CO2 injection development phase nearby the wells extracted from the GEM thermal model.

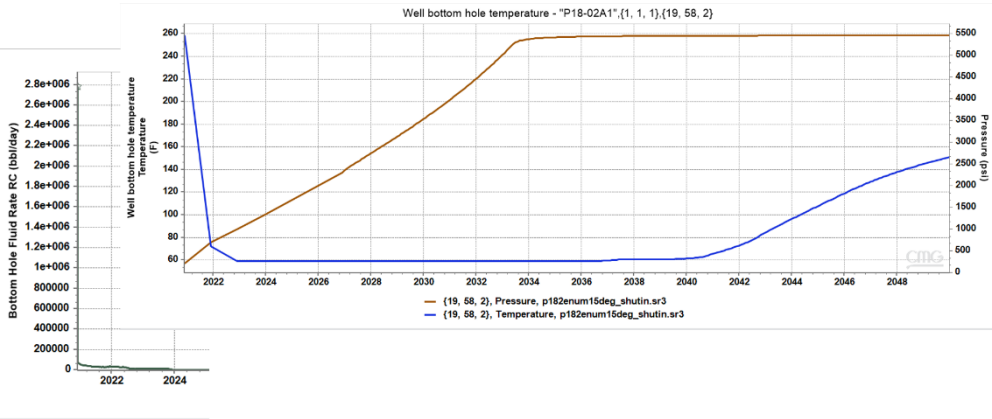

Figure 3.4 Pressure and Temperature at wellbore P18-02A1 grid versus time. If we close all wells after 3 years of injection, it would take around 10 and 20 years for pressure and temperature stabilizing, respectively.

3.3.2 Non-Darcy Effects

In the model, no non-Darcy effects were considered. In order to understand the importance of turbulence in the near-wellbore region.

Porthos has communicated by email that the well skin would vary from 0 during supercritical phase to maximum 10, with a value of 7.5 s/m^3 for the D-factor. It was also communicated that “we think that the D factor will only be applicable in gas phase and not when the CO_2 reaches dense phase.” [6] shows that based on experimental data loss of injectivity occurs when CO_2 reaches supercritical phase resulting from multiphase flow and cooling effect. We suggest the model to be re-run assuming an appropriate Forchheimer factor to estimate of the effects and importance of turbulent flow in the near-wellbore region in all phases of CO_2 injection field development.

3.3.3 *CO_2 Distribution in the Reservoir*

Based on the CMG GEM thermal model provided by EBN with the strategy presented in the application v.1, we plotted the CO_2 distribution in P18-2 after 50 years of start of storage (Figure 3.5). For this case the CO_2 is contained in the storage complex, but if it will be contained or not depends on the injection strategy to be applied.

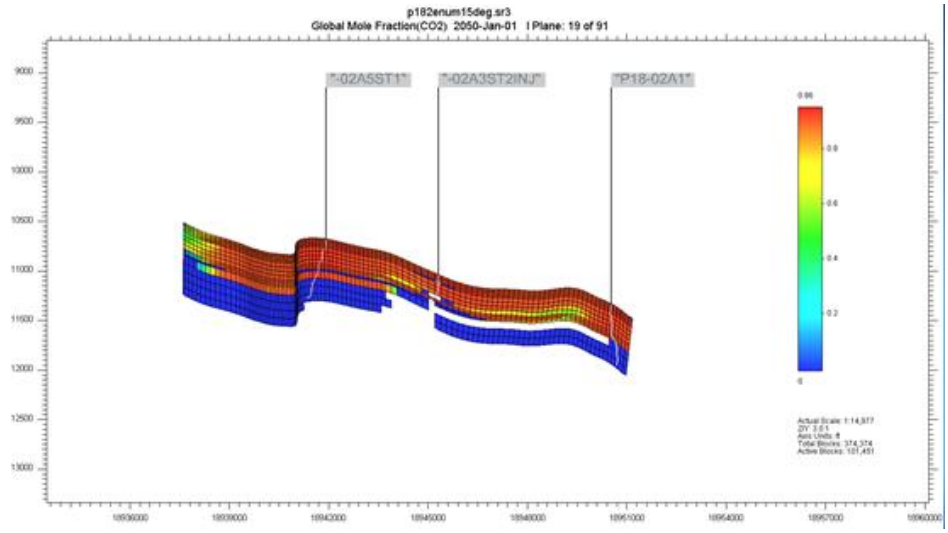

(a)

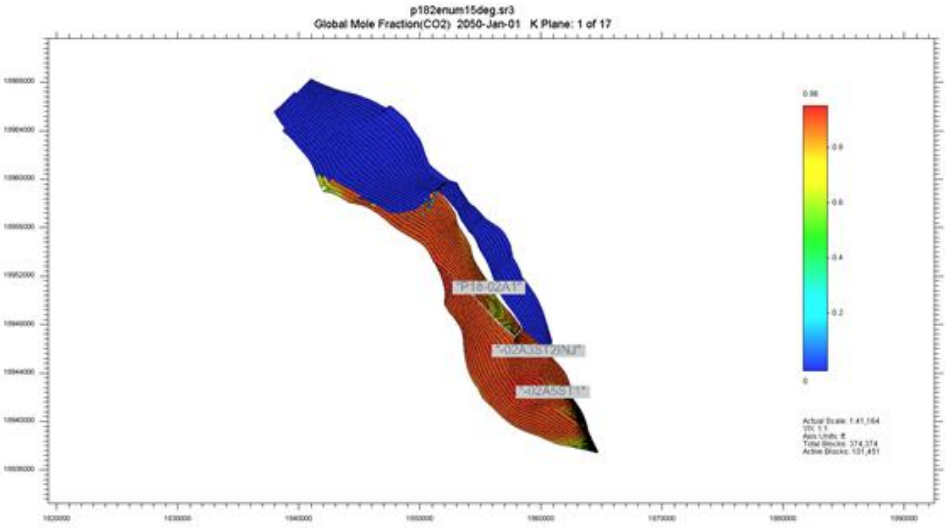

(b)

(c)

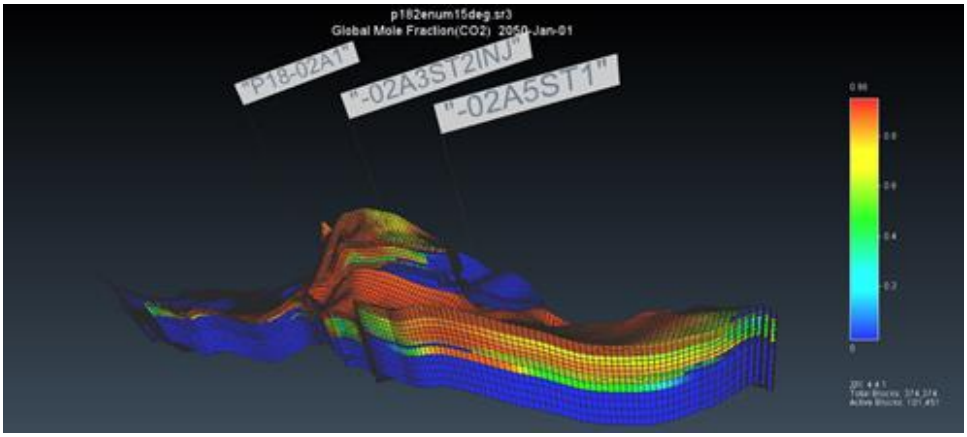

Figure 3.5 Distribution in the reservoir 50 years after injection in j-k section 19 (a), i-j section 1 (b) and 3D view (c).

3.4 Conclusion and recommendations

- We recommend the uncertainty in the geological model (e.g., flow barriers and facies distributions) to be considered in the dynamic modelling studies, allowing for uncertainty quantification of injectivity and CO_2 distribution predictions.

- We suggest the model to be re-run assuming an appropriate Forchheimer factor to estimate of the effects and importance of turbulent flow in the near-wellbore region in all phases of CO_2 injection field development.

- We recommend a plot of the p/Z curves versus Cumulative Produced Gas minus Injected CO_2 with and without a fracture to be generated to show the potential and effectiveness of p/z as monitoring tool within cold CO_2 injection into depleted gas fields.

- We recommend PTA modeling to be used for monitoring and model calibration in the future should not neglect thermal effects.

3.5 References

[1]Emerick, A. A., & Reynolds, A. C. (2013). Ensemble smoother with multiple data assimilation. Computers & Geosciences, 55, 3–15. https://doi.org/10.1016/j.cageo.2012.03.011
[2] Jeong, H., Sun, A. Y., Jeon, J., Min, B., & Jeong, D. (2020). Efficient Ensemble-Based Stochastic Gradient Methods for Optimization Under Geological Uncertainty. Frontiers in Earth Science, 8. https://doi.org/10.3389/feart.2020.00108
[3] Perrone, A.. , and E. Della Rossa. "Optimizing Reservoir Life-Cycle Production Under Uncertainty: a Robust Ensemble-Based Methodology." Paper presented at the SPE Reservoir Characterisation and Simulation Conference and Exhibition, Abu Dhabi, UAE, September 2015. doi: https://doi.org/10.2118/175570-MS
[4] Nguyen, Ngoc T., Chen, Zhangxin , Dang, Cuong T., Nghiem, Long X., Yang, Chaodong , Bourgoult, Gilles , and Heng Li. "Integrated Modeling for Assisted History Matching and Robust Optimisation in Mature Reservoirs." Paper presented

at the SPE/IATMI Asia Pacific Oil & Gas Conference and Exhibition, Nusa Dua, Bali, Indonesia, October 2015. doi: https://doi.org/10.2118/176290-MS
[5] Dake, L.P. 1978. Fundamentals of Reservoir Engineering. Amsterdam: Elsevier Scientific Publishing Co.
[6] Grigg, Reid B., Zeng, Zhengwen, and Laxman V. Bethapudi. "Comparison of Non-Darcy Flow of CO2 and N2 in a Carbonate Rock." Paper presented at the SPE/DOE Symposium on Improved Oil Recovery, Tulsa, Oklahoma, April 2004. doi: https://doi.org/10.2118/89471-MS
[7]Lai, Y. T., Shen, C. H., Tseng, C. C., Fan, C. H., & Hsieh, B. Z. (2015). Estimation of Carbon Dioxide Storage Capacity for Depleted Gas Reservoirs. Energy Procedia, 76, 470–476. https://doi.org/10.1016/j.egypro.2015.07.887
[8] CMG GEM User Manual
[9] ECLIPSE User Manual

4 Geomechanical processes

4.1 Reports used for evaluation

The following reports supporting section II and III of the main application version 2.0 for P18-2 and P18-4 were used for the TNO-AGE assessment of geomechanical processes affecting the integrity of the storage complex:

- Appendix 7: CO_2 feasibility study (TNO, 2019)
- Appendix 12: Seismic Risk Evaluation (Fenix, version June 2021)
- Appendix 12a: Geomechanical Study of Fault Stability and Caprock breach (Fenix, version May 2021)
- Appendix 12b: Thermal Fracture Simulation (Fenix, version December 2020)
- Appendix 12c: P18 Subsidence Evaluation (Fenix, version October 2019)
- Appendix 14: P18 Core Test Evaluation (Fenix, version February 2021)

4.2 Introduction

In this Chapter, the main geomechanical processes that could negatively affect the integrity of the storage complex are treated. It intersects with a number of advisory subjects, including the suitability of the storage complex and operational and geotechnical limits. Well integrity issues are excluded in this assessment, as this is covered by SSM.

This chapter starts by describing the key geomechanical processes and mechanisms that are relevant here. In the following sections, the used data, models and model assumptions of the applicant are assessed, as well as the interpretation of the model results provided by the applicant. Relevant insights for monitoring will also be treated.

4.3 Geomechanical processes affecting the integrity of the storage complex

There are two main geomechanical processes that could potentially compromise the integrity of the P18-storage complex:

- Injection-induced fracturing of reservoir, caprock and underburden
- Depletion- and injection-induced fault reactivation and induced seismicity

Firstly, significant fracturing of reservoir rock could result in connections between wells and permeable faults or isolated pockets in the storage complex. Furthermore, fractures in the reservoir may extend into the caprock or underburden. At worst, both cases of fracturing might lead to CO_2-migration out of the storage complex. Secondly, seismic or aseismic fault reactivation during past and ongoing gas production (depletion-induced) or during the planned CO_2-injection, could change sealing properties of faults which in turn could lead to CO_2-migration out of the storage complex. In the worst case, without preventive barriers or mitigation, fracturing or fault reactivation might lead to leakage into the ocean and atmosphere.

Injection-induced fracturing and fault slip are strongly dependent on the operational injection pressures, temperatures and rates. In addition, the extent to which these processes affect the integrity of the storage complex depends on the location and timing of occurrence of these processes within the storage complex, which is

predominantly controlled by the operational conditions and reservoir (geomechanical) limits. These aspects therefore need to be jointly assessed.

4.3.1 Mechanisms for injection-induced fracturing

Mechanisms for injection-induced fracturing of reservoir, caprock and underburden include (TNO R11739, 2015):

- Fracture initiation or (re)opening and subsequent propagation due to:
  - Cooling of rock inducing thermal stresses that lower the minimum horizontal stresses.
  - Application of injection pressures which lead to reservoir pressures exceeding minimum horizontal stresses.

Tensile fracturing occurs when reservoir pressures exceed fracture initiation or opening pressures of the reservoir, caprock or underburden. Generally, it is assumed that most rock formations lack any tensile strength due to the presence of pre-existing fractures or micro-cracks (Zoback, 2007). A commonly adopted measure to prevent tensile fracturing, is to keep bottom-hole pressures below the minimum horizontal stresses of the formations. In case of cold fluid injection, such as water or supercritical CO_2, cooling-induced reduction of minimum horizontal stresses also needs to be taken into account. In the case of CO_2-injection in P18, the low permeability of the lower reservoir units (Lower Detfurth and Volpriehausen, see Chapter 3) together with the density contrast imposed by the gas-water contact, will likely prevent significant cooling and subsequent fracturing of the underburden (Lower Germanic Triassic Units and Zechstein).

4.3.2 Mechanisms for depletion and injection-induced fault reactivation

Mechanisms for depletion and injection-induced fault reactivation and induced seismicity include (TNO R11259, 2015):

- Differential pressure evolution (compaction) and stress arching (depletion and injection phase);
- Pressure diffusion into faults with higher permeability than reservoir rocks (injection phase);
- Irreversibility of stress paths during production and injection (injection phase);
- Thermal stresses due to injection of CO_2 (injection phase).

The mechanisms above may occur simultaneously or sequentially and may work in conjunction or counteract each other, all depending on location of the faults and timing of operations. For P18, TNO-AGE considers differential pressure evolution during the depletion and injection phase, combined with injection-induced thermal stresses, to be the most relevant mechanisms

Differential pressure evolution

Differential pressure evolution is a relevant mechanism for faults that act as a side-seal between a depleted reservoir or compartment and juxtaposed formations with virgin (hydrostatic) pressure. If the reservoir or compartment on one side of the fault is depleted, there may evolve a difference in pressure and compaction between the reservoir and juxtaposed layers on the other side of the fault. This results in an increase in shear stresses on the fault plane which could destabilize the fault. This mechanism is relevant for the P18-2 and P18-4 bounding faults that are sealing the reservoir fault blocks (horst) from the surrounding non-reservoir blocks (grabens). Pressure differences between depleted block and non-depleted blocks may reach

up to 350 bar at the end of depletion. However, due to the depth of the P18 reservoir, initial porosities were already low (13% for the Hardegsen, 7-8% for the Upper and Lower Detfurth and 4% for the Volpriehausen). Therefore, the amount of depletion-induced compaction is expected to be small. This is confirmed by grain compressibility measurements on core samples (Appendix 14), showing an average relative porosity reduction of just 1%. Such a small amount of additional induced compaction will likely limit the effect of differential compaction on fault stability (see section 5.5.2).

Pressure depletion of the reservoir could also change stresses outside the reservoir. As the reservoir contracts laterally, horizontal stress decreases laterally outside the reservoir, while it increases above the reservoir. These stress changes promote normal faulting at the sides of the reservoir, as well as reverse faulting above and below the reservoir, in case of horizontal stresses exceeding vertical stresses (Segall & Fitzgerald, 1998; TNO R100043, 2019).

Pressure diffusion into faults
Faults that may become critically stressed during depletion should in general become less critically stressed due to the poro-elastic rebound during the injection phase. However, low-permeability formations could show less or no poro-elastic rebound during the injection. Therefore, faults embedded in a low-permeability matrix rock that may or may not have become critically stressed during injection, could remain critically stressed or become critically stressed during the injection phase (TNO R11259, 2015). This mechanism is not expected to contribute significantly to destabilization of the P18 faults during the injection phase, since no majore faults residing in a low-permeability zone close to the injection wells are observed (Chapter 3). However small faults with minimal offset are visible throughout the reservoir in the seismic data.

Irreversibility of stress paths
The evolution of stresses during phases of deformation, e.g. loading or unloading, can be represented visually as a stress path in a Mohr-Coulomb diagram. When a rock deforms purely elastic during loading and subsequent unloading (or vice versa), it would reverse to its original stress state following the same initial stress path. In case of P18, irreversibility of stress paths may be caused by elasto-plastic behaviour of the reservoir during reservoir first-time depletion (Pijnenburg et al., 2019). As plastic deformation does not reverse during re-pressurization, the poro-elastic stress path during re-pressurization differs from the elasto-plastic stress path during depletion. As mentioned earlier, depletion-induced compaction is expected to be small. Therefore, the effect of possible non-elastic deformation on stress path irreversibility is also likely to be small. Other causes of differences in stress paths during depletion and injection could be fault slip during the depletion phase, differences in pore pressure loading during the depletion and injection phase (see Differential pressure evolution), and reservoir temperature changes during injection (see Thermal stresses due to injection of CO_2).

Thermal stresses due to injection of CO_2
CO_2-injection with lower temperatures than ambient reservoir temperatures will induce thermal stresses on reservoir, caprock and nearby faults. Lowering the reservoir temperature will lead to thermo-elastic contraction of the reservoir, increasing the differential stress in a normal faulting regime, which may promote

fault reactivation (TNO R100043, 2019). For P18, the thermo-elastic effect is expected to be significant for faults that are near or within the CO_2-cooling front (near the injection wells).

4.4 State of stress and geomechanical properties

This section assesses the state of stress and geomechanical properties presented by Fenix in Chapter 3 of Appendix 12.

4.4.1 Stress field orientation

Fenix briefly discusses the orientation of the maximum horizontal stress (Smax) in the vicinity of P18 based on regional experience, drilling data and the GFZ World Stress Map (Heidbach et al., 2016). From Chapter 3 of Appendix 12 (e.g. Fig. 9 and 10) it is not possible to determine exactly which wells were used by Fenix to derive the orientation of SHmax for P18. Drilling-induced fractures in P18-2A6 in the Detfurth and Volpriehausen formations yield orientations for SHmax varying between 295 – 328.2 degrees from North, with an average of 310 degrees from North (AMOCO Netherlands B.V., 1997).The 40 degree NW orientation used by Fenix is in general agreement with orientations from P18-2A6 and regional trends presented by EBN in a recent compilation (Mechelse, 2017).

4.4.2 Stress magnitudes

Fenix assumes a normal faulting regime for P18. The magnitudes of the three principal stresses: vertical stress (Sv=S1), maximum horizontal (SHmax=S2) and minimum horizontal stress (Shmin=S3) can be estimated for relevant depths using stress gradients. The stress gradients reported by Fenix are based on density logs, Leak-Off Tests (LOT), and fracture tests. Fenix adopts fixed gradients of 0.205 bar/m and 0.16 bar/m for Sv and SHmax, and a range between 0.14-0.145 bar/m for Shmin. Fenix assigns a ‘low’ uncertainty to Sv as it is relatively well constrained by density logs. For Shmin, Fenix gives an uncertainty range of 0.14-0.16 bar/m, presumably based on a selected range of Shmin values from Formation Integrity Tests (FIT) in Fig. 9 of Appendix 12, but that is not explicitly mentioned. A larger uncertainty range of 0.16-0.19 bar/m is given for the SHmax. In Chapter 3 Appendix 12 it is explained that 0.16 bar/m is based on an assumed ratio of 0.79 between Sv and Shmax. EBN (Mechelse, 2017) shows that the ratio between SHmax and Shmin should be larger than 1 for most wells, as the well data (borehole-breakouts, fractures, etc.) show stress orientations that are in agreement with the main NW-SE orientation. Therefore, choosing an SHmax magnitude range in between Sv and Shmin, is reasonable. However, no explanation is given for this ratio, the origin of the upper bound of the uncertainty range and possible implications of (locally) changing stress regimes (e.g. strike-slip when SHmax approaches Sv). Occurrence of a strike-slip regime instead of normal faulting regime, will decrease fault stability (e.g. Vilarasa 2016).

4.4.3 Geomechanical properties

Fenix uses a combination of core measurements and indirect log measurements to constrain the main geomechanical parameters for the reservoir and overburden, including Young’s Modulus (*E*) and Poisson’s ratio (*v*). The main range of used parameters are summarized in table 5.1 below:

Table 4.1: Table 2, Chapter 3 of Appendix 12. Range of geomechanical parameters and stresses, with associated uncertainty ranges.

Hierarchy by Effects	Unit	Base Case	Simulated range	Uncertainty range	Comments
		[P18-4 P18-2]			
Minimum Stress gradient (Virgin)	(kPa/m)	14.5	14-14.5	14-16	Nearby minifracs
Biot coefficient	(-)	0.8	0.8-1.0	0.6-0.9	Derived from E, pr, Kg
Young's modulus (E)	(GPa)	27	18-36	18-36	Measured
Linear Thermal expansion Coefficient	(1/K)	9.0E-06	9.0E-06	low	Measured
Poisson ratio (Pr)	(-)	0.20	0.15-0.20	0.15-0.25	Measured
Grain modulus (Kg)	(GPa)	75	75	60-90	Measured
Fault Dip angle	(deg)	varies	[-10, +10]	[-10, +10]	Measured
Initial Reservoir Pressure	(bar)	[348, 375]	[348, 375]	low	Measured
Initial Reservoir Temperature	(C)	[117, 126]	[117, 126]	low	Measured
Depleted Reservoir Pressure	(bar)	20	20	low	Measured
Vertical Stress Gradient (Virgin)	(kPa/m)	20.5	20.5	low	Density log
Maximum Horizontal Stress Gradient (Virgin)	(kPa/m)	16	16	15-19	Regional data
Pressure Gradient @GWC (Virgin)	(kPa/m)	10.4	11	low	Measured
Rock Heat Capacity	(J/kg·K)	1000.0	1000.0	low	Measured
Rock Thermal Conductivity	(J/m·s ·K)	2.0	2.0	intermediate	Measured
Calibration/Sensitivity					
Fault pressure	(bar)	avg	res, avg, virgin	unknown/high	Sensitivity
Friction Coefficient	(-)	0.6	0.55, 0.6	unknown/high	Analogues
Fault Cohesion	(bar)	varies	[0-150]	unknown/high	Calibration

Results of the core measurements are reported separately in Appendix 14. Unfortunately, core measurements are only available for the reservoir (Hardegsen and Upper Detfurth). Values for the caprock are implicitly assumed to be similar to the reservoir, as can be seen in the assumed values for the caprock in Table 7, Chapter 4 of Appendix 12. Data from the final CATO-2 report (2011) seem to be discarded, including data from core measurements in the caprock (Röt/Sollingen) of a nearby field (Q16) and reservoir data from Dipole Shear Sonic logs. An *E of* 26 GPa (range of 20 to 30 GPa is reported in the conclusions) and *v* of 0.3 are reported for the caprock in the CATO-2 report (2011).

The Biot coefficient, ranging from 0.8 - 1 is derived from the measured *v*, *E* and Grain Modulus. Linear thermal expansion factor is fixed at $9.0 \cdot 10^{-6}$ and is supposedly based on measurements, but no supporting reference or report is provided by Fenix.

For both the reservoir and caprock in the base-case scenario, *E* and *v* are assumed to be 27 GPa and 0.2, respectively. The *E* of 27 GPa, assumed for the caprock, is in line with the reported range in the CATO-2 report (2011), but *v* is significantly lower at 0.2 instead of 0.3, which is more typical for clay-rich rock. A lower *v* will increase the caprock strength. In the log profiles of *E* in Fig. 7 and 8, Chapter 3 Appendix 12, the layers directly above the main reservoir show a higher *E* than the main reservoir, while the overlying Jurassic overburden has a much lower *E*. No clear interpretation of these results and associated uncertainties are given.

Large contrasts in geomechanical properties and stresses between reservoir and overburden layers are important for fault-slip and fracturing behaviour. Some of these aspects are briefly touched in the chapters on fault stability and caprock integrity, but the impact of these contrasts is not discussed.

In Table 8 of Chapter 4, Fenix presents geomechanical properties for the entire layer stack from the reservoir up to the North Sea Group. From Chapter 3 in Appendix 12a, it becomes clear that the densities and geomechanical parameters above the reservoir and caprock are all derived from log data. Fenix explains that these properties are used together with fixed stress gradients to initialize the virgin state of stress for the two different scenarios in the COMSOL geomechanical model used for the fault stability analysis.

4.4.4 Conclusion TNO-AGE

TNO-AGE considers the assumed stress field orientation in line with available data. Assumed stress magnitudes are based on available measurements for P18 wells and are in agreement with regional stress data. Geomechanical properties of the reservoir are either based on direct core measurements or determined from log data. However, the assumptions on geomechanical properties of the caprock and possible implications of property (and stress) contrasts between caprock and reservoir lack substantiation. Based on the reported range in the CATO-2 report (2011), a value of 0.3 for the Poisson's ratio is more appropriate (which is outside the uncertainty range used by Fenix in Appendix 12 – see Table 5.1). TNO-AGE notes that the information in Appendix 12 on assumed values for parameters in relation to the modelled scenarios is presented in a fragmented way throughout the report. This is partly solved with Chapter 3, Part II: Description of CO_2 Storage. However, a dedicated chapter in Appendix 12 with figure(s) and table(s) providing a complete overview of the scenarios used in each modelling phase, including all assumed parameters for both reservoir and caprock, together with applied operational limits, would be a welcome addition.

4.5 Geomechanical simulations

This section assesses the geomechanical modelling workflow presented by Fenix in Chapter 4 Appendix 12 (Fenix, Jan 2021). A short overview of the workflow is given and the main model interdependencies and assumptions are discussed.

4.5.1 Modelling workflow

Fenix uses a combination of the GEM GMC reservoir simulator with limited integrated stress modelling capabilities and the COMSOL Multiphysics modelling suite, which is used as a dedicated tool for finite element modelling of stress. (Fig. 11, Chapter 3, Part II: Description of CO_2 Storage).

The GEM reservoir simulator is used for the following:

Depletion phase:

- Modelling pressure, temperature and stress;
- Base-case (Shmin = 0.145 bar/m) and low-stress scenario (Shmin = 0.14 bar/m);
- Pressures are transferred to the COMSOL geomechanical model for modelling stresses during depletion.

Injection phase:

- Modelling pressure, temperature, stress, thermal fracturing and cap rock breach;

- Base-case (Shmin = 0.145 bar/m) and low-stress scenario (Shmin = 0.14 bar/m);
- Base-case and worst-case injection scenario;
- Longitudinal and transverse fracturing scenario;
- Pressures and temperatures are transferred to the COMSOL geomechanical model for modelling stresses during injection and for modelling cap rock breach.

The COMSOL geomechanical model is used for the following:

Pre-production phase:
- Modelling virgin stresses;
- Model initialization and calibration with base-case (Shmin = 0.145 bar/m) and low-stress scenario (Shmin = 0.14 bar/m).

Depletion phase:
- Modelling stresses and faults stability from start to end of depletion;
- Input pressures from GEM;
- Base-case and low-stress scenario virgin stresses from pre-production phase;
- Providing input stresses for fault stability analysis and seismic moment estimation at the end of depletion.

Injection phase:
- Modelling stresses;
- Modelling caprock breach;
- Base-case and low-stress scenario state of stress from end of depletion;
- Input pressures and temperatures from GEM (fractures, longitudinal and transverse fracturing scenario);
- Providing input stresses for fault stability analysis and seismic moment estimation during injection.

4.5.2 Main model assumptions and boundary conditions

Input for the dynamic GEM reservoir models is based on a single (static) reservoir model. It is unclear how errors/changes the in static model would propagate or translate into dynamic reservoir models and geomechanical models. This is partly remediated by Fenix by running the models with a worst-case scenario (Section 5.5.3), but it remains unclear if this worst-case scenario sufficiently covers the potential outcomes given the uncertainties of the static model.

Within the modelling workflow, there are several instances where pressure and/or temperatures from the GEM reservoir model are transferred to the COMSOL geomechanical model (one-way coupling). As Fenix indicates in the report, a weak point in the modelling workflow is that the stresses modelled with the COMSOL model are never transferred back to the GEM model (two-way coupling), which could potentially affect the amount and dominant direction of fracturing.

Stress rotation

There are significant differences in stress orientations after the depletion phase between the GEM and COMSOL stress models. Fenix explains this difference in Chapter 10 Appendix 12a . GEM uses a simplified one-dimensional, uniform compaction calculation to estimate the stresses at the end of depletion and the

bounding fault surfaces are used as non-displacement boundary conditions. COMSOL uses a larger bounding box with more distant non-displacement boundary conditions yielding less boundary effects within the reservoir. Clamping effects in GEM are therefore more significant, resulting in larger stress rotations after depletion compared to the COMSOL model.

For P18-2, the GEM model returns a rotation of the horizontal stresses of 24° CCW at the end of depletion, while the COMSOL model shows a maximum rotation of 7.6° CW during the depletion phase with just 1.2° CW at the end of depletion. For P18-4 the difference is even larger. Here, the GEM model returns a rotation of the horizontal stresses of 73.5° CCW at the end of depletion, while the COMSOL model shows a maximum rotation of 13.4° CW during the depletion phase with just 0.5° CW at the end of depletion.

Given the large discrepancy between stress rotations in GEM and COMSOL, Fenix included two scenarios for the direction of fracturing: longitudinal (parallel to SHmax and the main boundary faults) and transverse fractures (perpendicular to SHmax and the main boundary faults). Both scenarios are also included in the fault stability assessment.

Elastic vs. plastic deformation
Fenix assumes full elastic stress recovery after depletion based on experience with gas-storage reservoir such as Bergermeer, Norg and Grijpskerk. Although the Bergermeer gasfield showed relatively strong depletion-induced seismicity, only minor injection-induced seismicity was recorded during the initial cushion gas injection, with seismicity diminishing with time during later injection-production cycles. This appears to be a valid assumption for the three gas storage reservoirs, but it is unclear if these observations alone are sufficient to assume the same for the P18-fields. No local monitoring of (micro)seismicity or subsidence has been conducted for P18 during the depletion phase that could further constrain the geomechanical and seismogenic behaviour. Core measurements (Appendix 14) with loading and unloading experiments indicate that an average relative porosity reduction of 1% has occurred during depletion. The effects of irreversible plastic deformation are therefore deemed small. Due to the relatively low porosities (4-13%) of the P18 reservoir units, the assumption of full elasticity for P18 is justifiable, as the difference with an elasto-plastic model is likely to be (sufficiently) small (e.g. Pijnenburg et al., 2019).

4.5.3 Definition of base-case and worst-case scenario

In order to obtain insight into the operational limits, Fenix defined a base-case and stress-test scenario. In the introduction of Chapter 4 of Appendix 12, it is made clear by Fenix that the stress-test scenario is not intended as a realistic operational scenario, but to find the geomechanical limits of reservoir and caprock. The stress-test scenario combines worst-case scenarios for injection rates and temperatures, state of stress, geomechanical parameters and injectivity (Table 10, Section 3.6.3., Part II: Description of CO_2 Storage). In this stress-test scenario, maximized injection rates and lowest downhole temperatures are imposed to promote fracture initiation and propagation and to maximize cooling of nearby faults. For P18-2, the P18-2A1 well closest to the faults and with the lowest injectivity was selected as main injector. Additionally, upper limits for injection pressure were removed, allowing for

injection pressures higher than virgin reservoir pressures. Finally, geomechanical parameters were adjusted to enhance fracturing and to maximize fault instability.

For the base-case, Fenix applies operational conditions following the flow assurance design phase for injection rates and temperatures, as well as less conservative assumptions for the state of stress, geomechanical parameters, and injectivity. The scenario is designed to prevent or limit fracturing and to minimize fault instability. Fenix stresses that this base-case scenario is not the final operational base-case, which will be obtained by integrating geomechanical limits into the flow assurance modelling (p.17, Chapter 4, Appendix 12).

4.5.4 Conclusion TNO-AGE

TNO-AGE considers the applied modelling workflow appropriate for the P18 field as it covers both injection-induced fracturing and depletion- and injection induced fault reactivation and seismicity. A weaker point in the modelling workflow is that the stresses modelled with the COMSOL model are never transferred back to the GEM model (two-way coupling), which could explain the difference in modelled stress rotation between the two models. Transferring the COMSOL stresses back into the GEM model might also affect the amount and dominant direction of fracturing. The assumption of full elastic stress recovery is justifiable based on the observed low relative compaction reduction from the unloading experiments.

A structural limitation of the modelling workflow is the input for the dynamic GEM reservoir models based on a single (static) reservoir model. It is unclear how errors/changes the in static model would propagate or translate into dynamic reservoir models and geomechanical models.

4.6 Injection-induced fracturing

One of the identified risks by Porthos is injection-induced fracturing of reservoir and/or caprock. Fenix uses the built-in Barton-Bandis smeared-crack fracture simulator in GEM to assess the effect of fracturing on the pressure and temperature evolution in the reservoir. For the caprock integrity assessment, Fenix combined a GEM model for the reservoir with a COMSOL model for the caprock.

4.6.1 Thermal fracturing in the reservoir

Fenix has modelled several scenarios to assess fracturing in P18-2 and P18-4. In Table 6 of Appendix 12, a summary of the results of the thermal fracture simulations is given. For multiple scenarios (including the base-case and stress-test scenario), resulting fracture lengths and maximum differences in BHP between pure matrix injection and thermal fractures are presented.

Fenix concludes that thermal fracture growth in the P18-2 reservoir is possible, but unlikely for the base-case scenario. Fracture growth is unlikely in P18-2A3 and P18-2A5 wells for all scenarios. Due to the high transmissivity in these wells, the cold zone is also expected to infiltrate Detfurth and Volpriehausen horizons, spreading the cooling over more rock volume. Fracture growth is possible in P18-2A1 well, but unlikely with the base-case scenario. For the stress-test scenario, both longitudinal and transverse fractures are modelled with lengths of up to 1 km, both terminating at the North-Western bounding fault (P18-2 West_3 in Fig. 4, Part II: Description of CO_2 Storage) in 2035 (Fig. 35 – 54, Appendix 12). For the P18-4A2 well, fracture

growth is likely in all scenarios. Maximum fracture lengths of 1 km are modelled for the longitudinal fractures. Transverse fractures reach a modelled length of 290 m, propagating in two directions towards the Western and Eastern bounding faults (Fig. 55 – 67, Appendix 12).

Effect of fracturing on bottom hole pressures
In Fig. 41 of Appendix 12, the effect of thermal fracturing in the reservoir on bottomhole pressures (BHP's) in P18-2A1 is compared to pure matrix injection during the injection phase. Both the modelled BHP and excess injection pressure (Fig. 42, Appendix 12) show a significant pressures drop after initiation of fracturing. Alongside the initial BHP and excess pressure drops, associated with fracture initiation/opening, the BHP remains ~260 bar lower during injection while excess injection pressures varies around ~50 bar.

Only P18-2A1 and P18-4A2 show instances of fracturing. The other wells, P18-2A3 and P18-2A5, show no fracturing at all. For P18-2A1, the base-case scenario results in negligible amounts of fracturing with low maximum ΔBHP's (~10bar), while the stress-test scenario yields fracture lengths of up to 1 km with associated maximum ΔBHP's of up to 260 bar. In contrast, P18-4 shows significant fracturing for all cases with fracture lengths between 290-1000 m, while the maximum ΔBHP varies only between 5 and 10 bar.

Monitoring pressure and injectivity to identify fracturing in the reservoir
In the section on Monitoring in Appendix 12 (p.51), it is suggested that monitoring of injectivity could be used to detect thermal fracturing. This requires monitoring of excess injection pressure (over reservoir pressure). In Table 2, Part IV: Monitoring Plan, threshold deviations (±10%, ±20%, ±30%) for reservoir pressure and temperature are provided to determine the need for additional monitoring or corrective measures. Given the pressure drop (ΔBHP of 260 bar) modelled for the case of fracturing in P18-2A1, it should be possible to detect fracturing with pressure monitoring and take actions to mitigate the consequences. However, it is questionable if the modelled pressure drop (ΔBHP of 5-10 bar) in P18-4A2 could be distinguished from other small-scale pressure perturbations that may arise during the injection phase. It is also unclear how the pressure signal caused by fracturing in P18-2A1 well would scale with a scenario in between the base-case and worst-case scenario. Fenix also indicates that the inferring fracture size from interpreting pressure fall-offs is further complicated by the phase behaviour of CO_2.

4.6.2 Thermal fracturing in the cap rock

Models
Fenix unsuccessfully attempted to use GEM to also model fracturing in the caprock with the Barton-Bandis smeared-crack fracture model due to convergence issues. To circumvent this problem for P18-2A1, Fenix used COMSOL to model thermal stresses in the caprock. Pressures and temperatures of the reservoir from the GEM reservoir model where transferred to the COMSOL geomechanical model (one-way coupling). In the COMSOL model, no dynamic fracturing was modelled, only temperature penetration and stress redistribution in the caprock. For P18-4A2, Fenix only used GEM (without the Barton-Bandis smeared-crack fracture model) to model temperature and stresses in the caprock and identify tensile conditions that may lead to fracturing. For both P18-2A1 and P18-4A2, fracture length is inferred

from the maximum vertical length within the caprock where the in-situ fracture pressure (conservatively assumed by Fenix as equal to the bottom hole pressure) exceeds the Shmin of the caprock.

Scenarios
In Table 7, Chapter 4 of Appendix 12, Fenix describes the two geomechanical scenarios that were used for modelling thermal fracturing in the cap rock. It is unclear what operational scenarios were tested. For the base-case scenario, the same *E* (27 GPa), *v* (0.2) and Shmin of the reservoir are assumed for the caprock. For the worst-case scenario, the Shmin from the low-stress scenario is adopted, while both the *E* and Biot coefficient (*α*) are raised to 34 GPa and 1, respectively. For a third, alternative scenario, Fenix uses a higher Shmin in the caprock (High stress Keuper). Fenix explains that such a stress contrast between reservoir and caprock is commonly observed in hydraulic fracturing jobs in Buntsandstein reservoirs, but no reference or source is provided to support this observation. However, it could be a plausible assumption as stress contrasts are often observed in shale gas hydraulic fracturing jobs, where shale-rich layers often act as frac-barriers due to a higher Shmin compared to sand-rich layers (viscoelastic stress relaxation, e.g. Zoback and Kohli 2019). Still, no (stress) data is presented by Fenix for P18 to substantiate this assumption.

Fracture lengths and containment
Fenix shows for P18-2A1 in Fig. 82 of Appendix 12 that thermal fracture growth is possible, ranging from 10 m for the worst-case geomechanical scenario to no fracture growth for the elevated Shmin in the caprock (high-stress Keuper). Thermal fracture growth in the caprock is also possible near P18-4A2 (Fig. 74 and 76, Appendix 12) but limited to 10-15 m for the base-case and worst case geomechanical scenarios. For the scenario with an elevated Shmin in the caprock (high-stress Keuper), no tensile conditions are reached in the caprock.

Fenix argues that at the start of injection there is very strong fracture containment, as diffusive cooling of the caprock is slow, reservoir pressures are still low, and depletion-induced stress arching may have also increased the Shmin above the reservoir (TNO R100043, 2019). In Fig. 84 of Appendix 12 Fenix shows that during injection, the average effective Shmin in the cap rock decreases due to cooling and a reduction of the depletion-induced stress-arching, while the reservoir pressure increases.

First tensile conditions are modelled by Fenix in the caprock at around 2029 for P18-2 and 2028 for P18-4. For both P18-2 and P18-4, the largest fracture lengths are reached at the end of injection, as reservoir pressures are the highest and the cooled rock volume of the caprock is the largest (and thus the largest reduction of Shmin). As explained by Fenix, the higher injection pressures required for low-injectivity wells for a given injection rate combined with lower maximum injection rates that can be sustained, cause the cold front in the reservoir to remain relatively close to the well, inducing more localized cooling in the reservoir and in the caprock above.

Injection pressure head-room and monitoring of fracturing in the caprock
For P18-2, it is shown that at the beginning of injection there is a 350 bar injection pressure head-room that steadily decreases to 120 bar at the end of the injection

phase. As the modelled transition from fracture containment to caprock breach is very abrupt, Fenix recommends a maximum injection pressure of 100 bar at the end of injection. As with fractures in the reservoir, fractures in the caprock are likely to difficult to identify with pressure monitoring.

4.6.3 Conclusion TNO-AGE

TNO-AGE agrees with Fenix on the containment of fractures in the reservoir in the early stages of the injection phase. It is likely that tensile conditions are reached in the reservoir first before the caprock due to the faster (advective) cooling. Additionally, a possible stress contrast between reservoir and (uncooled) caprock will further prevent fracturing in the caprock during the early stages of supercritical CO_2-injection. Fracturing will therefore predominantly occur in the reservoir before possibly extending in the caprock during the late stages of injection. TNO-AGE agrees with Fenix that the highest risk of fracturing the caprock occurs near low-injectivity wells where the CO_2 remains closer to the well and the caprock may experience stronger and more localized cooling.

TNO-AGE has some reservations regarding the proposed monitoring of pressure and injectivity as a tool to identify fracturing. For the P18-2 wells, it is clear that the modelled fractures in the stress-test scenario would be detectable due to the significant modelled drop in pressure. However it is not sufficiently clear if the pressure signal would be as strong in case of fracturing for other, less extreme scenarios or for fracturing in the caprock. The P18-4 field only contains a single well, which will also act as a CO_2-injection well. The insignificant modelled pressure response after inducing thermal fractures of up to 1 km in length, indicates that pressure monitoring might be inadequate to detect fracturing in the reservoir, let alone in the caprock. Nonetheless, the likelihood of caprock fracturing in P18-4 is small due to the high injectivity of P18-4A2, limiting the build-up of high excess pressures in fractures, inhibiting fracture propagation in the seal.

4.7 Fault stability and depletion- and injection-induced seismicity

The stresses modelled on selected fault surfaces in COMSOL are used to assess the fault stability based on the Mohr-Coulomb failure criterion. From the largest continuous aggregation of critically-stressed fault patches, a critical shear area is estimated. It is assumed that this critical shear area on the fault is equal to the fault slip area. Then, a correlation between fault slip area and moment magnitude is used to estimate the maximum magnitude (Mmax). In Fig. 1, Chapter 2 of Appendix 12, Fenix shows two correlation lines inferred for the Groningen gas field and Bergermeer gas field seismicity. For P18, Fenix uses the Bergermeer correlation line (Technische werksessie TAQA/EBN/MEAC/adviseurs on 20-04-2021), but no further explanation is given for this choice. Moment magnitudes are not only dependent on fault slip area but also on the stress drop. From an earlier geomechanical study by Fenix on the Bergermeer gas storage (Fenix, Mar 2018), it becomes clear that for the Bergermeer seismicity, a small stress drop of 3 bar was assumed for the injection phase. Since no seismicity has been recorded for P18 and surroundings, it is not possible to verify the assumed relation between fault slip area and stress drop. The stress drop magnitude depends on fault properties that are not known for P18, and may be strongly heterogeneous. Therefore, estimated magnitudes might also vary between different faults, resulting in a relatively large uncertainty.

4.7.1 Scenarios and assumed causes for lack of seismicity

Fenix applies different scenarios for modelling fault stability and subsequent seismogenic response (Mmax), including scenarios with or without thermal fracturing of the reservoir, for selected boundary faults, and for a generic intra-reservoir fault.

The frictional properties of the faults are assumed to be the main parameters controlling the lack of observed seismicity in the P18 field and surroundings. Fenix tested the cohesion *c* and coefficient of friction *μ* for calibrating the models. First, Fenix adjusted *c* to obtain an Mmax of M1.5 at around a pressure depletion of 30% of the virgin pressures, which according to Fenix is a commonly observed threshold for the onset of seismicity in Dutch gas fields. This resulted in very high magnitudes for Mmax, up to M3.5, at the end of depletion, greatly exceeding the detection limit of ~M2 of the KNMI network. Therefore, Fenix decided instead to calibrate the model by adjusting both *c* and *μ* in such a way that the modelled Mmax at the end of depletion falls around the detection limit of ~M2 of the KNMI network.

Fenix concludes that calibrating seismicity with cohesion worked best, as varying *μ* did not significantly affect the results. However, Fenix only shows models where *μ* was varied between 0.55 and 0.6, while *μ* might reach higher values during long periods of fault inactivity (see section 5.7.2). In the end, Fenix obtains a range for *c* of 0 to 36 bar for different faults. According to Fenix, these values fall within a realistic range for measured cohesion based on triaxial tests on core samples which may reach values of up to 200 bar. Fenix did not provide references to support this claim.

Fenix also briefly mentions the possibility of aseismic fault slip (slow slippage) as an alternative explanation for the absence of seismicity (Chapter 4, Appendix 12). However, the implications of the choice for cohesion over aseismic fault slip are not discussed.

4.7.2 The role of fault gouge properties and juxtaposition on seismogenic behaviour

fault gouge properties may play a significant role in controlling the reactivation and frictional sliding behavior of the fault. Fault gouge properties depend on a combination of the deformation and hydraulic history of the fault, as well as on the mineralogical composition. The latter is largely determined by the juxtaposition history of (different) layers on each side of the fault. All of these aspects could affect both the present-day hydraulic properties (sealing vs. permeable) as well as the seismogenic behaviour (seismic vs. aseismic). Due to the large displacements, it is plausible that the fault gouge of the main boundary faults contains more clay due to juxtaposition of clay-rich caprock against the reservoir (see Allen juxtaposition diagrams in section 2.3.1, Part II: Description of CO2 Storage). This might explain the inferred sealing capabilities of the main bounding fault, as well as the lack of observed (<M2) seismicity. In friction experiments, fault gouges containing abundant clay minerals typically develop little or no cohesion (e.g. Bos & Spiers, 2000; Carpenter et al., 2012; Hunfeld et al., 2020). Although aseismic fault slip was briefly mentioned by Fenix, this conflicts with the cohesions that Fenix derived from calibration for some of the boundary faults.

On the other hand, intra-reservoir faults with low offsets will predominantly have reservoir-reservoir juxtaposition (sandstone). Therefore, the clay content will likely

be lower and faults are expected to be permeable. From literature (e.g. Tenthorey & Cox, 2006; van den Ende & Niemeijer, 2019; Hunfeld et al., 2020), it is also known that quartz- or carbonate-rich faults can build up significant cohesion and an increased (static) coefficient of friction during long periods of inactivity. At the same time, the stress drop of these strong faults will be higher in case of failure (e.g. Shapiro & Dinske, 2021). As no (<M2) seismicity has been observed on these intra-reservoir faults, it is plausible that they have not (yet) been critically stressed. Possible reasons could be the limited pressure differences across these faults due to their permeability or buildup of strength during long periods of inactivity. For the intra-reservoir faults in particular, calibration of Mmax with cohesion during the depletion phase is a justifiable choice. Given the possibility of clay-rich fault gouges for the main bounding faults, calibration of Mmax using cohesion can be considered a conservative choice, as it might lead to larger stress drops and a higher Mmax during the injection phase (although more pressure depletion is required for reactivation compared to cohesionless bounding faults).

4.7.3 Modelling results and interpretation

The modelling results (Fig. 92 – 94, Appendix 12) show that for P18-2 the Western and North-Western boundary faults could have reached criticality during depletion. However, Fenix expects no detectable seismicity during the injection phase, based primarily on the absence of recorded seismicity during the depletion phase.

For the injection phase, Fenix varied several key parameters to analyze the sensitivity of the seismicity to changes for the Western and North-Western boundary faults. Key parameters that are varied include: a higher Mmax at the end of depletion, the aspect ratio of the destabilized fault patches, low or high Shmin, fault dip, longitudinal or transverse fractures, fault pressure, and the *E* of reservoir and overburden. In Fig. 107, Appendix 12 the resulting variation in Mmax is plotted against pressure. Mmax shows a monotonic decline from M2 - M2.5 at maximum depletion to M0 - M0.5 at a reservoir pressure of around 275 bar. This indicates that refilling the reservoir will result in a net-stabilization of the Western boundary fault. Fenix also shows tornado diagrams for the sensitivity at two timesteps during the injection phase with a reservoir pressure of 120 bar and 290 bar, respectively. This shows that the impact of variation also decreases with increasing reservoir pressure.

The results of the North-Western fault go directly against one of the main conclusions of Fenix stating that CO_2-injection will result in net-stabilization of faults by restoring pressure close virgin pressure (Executive Summary, Appendix 12). Mmax only declines up to a reservoir pressure of around 100 bar before it increases to slightly below or above the Mmax at maximum depletion. So here, repressurization does not seem to lead to increased fault stability. Furthermore, more than half of the cases in the sensitivity analysis show an Mmax that actually exceeds the Mmax at maximum depletion, including the base case itself. The highest Mmax of ~M2.3 is reached for cases with a lower fault dip or increased *E* of reservoir or Jurassic overburden. What is notable, is that the fracturing scenario does not seem to affect fault stability, as it follows an identical path as the base-case scenario. Apparently, fault slip area is not significantly affected by fracturing.

The modelling results show that for P18-4 the Western (Fig. 102 – 104, Appendix 12) and Eastern (Fig. 113 – 115, Appendix 12) boundary faults could have reached

criticality during depletion. For the base-case model during the injection phase, the model results show similarities with the P18-2 results. The P18-4 Eastern fault shows the same decline of Mmax with reservoir pressure as the P18-2 Western fault. Like the P18-2 North-Western fault, the P18-4 Western fault only shows a decline during the first period of the injection phase, followed by an increase to slightly below or above the Mmax of maximum depletion, depending on tested parameters. Between ~150 to 250 bar, no seismicity is expected. As with the P18-2 faults, fracturing does not seem to affect the Mmax significantly.

As a last hypothetical scenario for both P18-2 and P18-4, Fenix modelled the stability of a relatively large intra-reservoir fault close to an injection well that would experience significant cooling. A low Shmin is assumed for this scenario, which already yields near-critical conditions at the end of depletion. Next, Fenix adjusts μ to obtain an Mmax that is around the detection limit (~M2). Unfortunately, no extensive sensitivity analysis was conducted. Only the fault dip was varied, revealing a shift from the most critical dip at the end of depletion at 50° - 60° to a dip ~70° during injection. For a dip of 70°, Fenix models an Mmax of up to M2.8 at the end of the injection phase. Fenix stresses that this Mmax is very unlikely as the model assumptions are conservative and the probability of large undetected faults near the injection wells is low. TNO-AGE agrees that major faults are likely not present near injection wells.

4.7.4 Seismic risk assessment

In Chapter 5 of Appendix 12, Fenix applies the SRA (Seismische Risico Analyse) screening method to assess the seismicity risk for P18 (SSM, 2016).This method was designed for screening potential hazards of depletion-induced seismicity for small (onshore) gas fields. Fenix' assessment using the SRA method results in a negligible risk for P18 gas production, but with theoretical Mmax between 3.9 (based on compaction energy release) and 4.1 (based on fault surface area). TNO-AGE has checked the calculations by Fenix of the Mmax based on fault geometries (Table 12, Appendix 12). TNO-AGE did not find any irregularities, apart from an inconsistency between the reservoir heights of 200 m that were used by Fenix, and the reservoir heights of 210 m for P18-2 and 229 m for P18-4 reported by Fenix in Table 11 of Appendix 12. Changing the reservoir height to 210 m or 229 m for P18-2 and P18-4, respectively, would change the Mmax for some faults by M0.1, but does not change the largest Mmax. Assuming that the two western bounding faults (fault 10 + 14, Table 12, Appendix 12) or the two eastern bounding faults (fault 17 + 19, Table 12, Appendix 12) would act as a single fault raises the Mmax to 4.2.

Next, Fenix compares the P18 project with several other CCS projects (e.g. Sleipner, Salah and Weiburn) to argue that risks for P18 are indeed negligible. Given the geological differences and the larger injection volumes planned for P18, the value of this comparison for assessing the risks for P18 seems limited. Fenix also compares P18 with Dutch gas storage reservoirs. Although more appropriate in terms of geology and state of stress, the amount of cooling induced by CO_2-injection in the P18-complex is likely to be significantly larger.

Fenix also refers to one of the main conclusions from KEM-01 WP7 final report on a safe operational bandwidth for underground gas storage. Here, it is stated that it is unlikely for seismicity to occur during the injection phase when no seismicity has been recorded during depletion, with refill pressures at or below virgin pressures.

This conclusion implicitly describes the Kaiser effect, also mentioned by Fenix in their report on the Bergermeer gas storage (Fenix, march 2018). However, the absence of detectable (<M2) seismicity near P18 during depletion is not conclusive evidence for a total absence of seismicity. Based on the negligible risk obtained from the SRA method and the aforementioned Kaiser effect, Fenix concludes that monitoring with the regional KNMI network alone would be sufficient for P18. However, the SRA method is designed for seismic hazard screening for (onshore) gas production. Furthermore, the Kaiser effect may not be an appropriate assumption for P18 due to significant amount of cooling induced during CO_2-injection and the possibility of undetected seismicity during depletion. This is further demonstrated by some of the modelled moment magnitudes for the P18-2 North-Western fault in Chapter 4 of Appendix 12 (e.g. Fig. 104, 105, 109 and 110), where Mmax values at the end of injection are larger than the assumed Mmax of M2 at the end of depletion. Finally, if the Kaiser effect holds true, it might only be relevant for faults in the reservoir that will remain isothermal throughout the injection phase. This excludes both the bounding faults and intra-reservoir faults in the vicinity of injection wells, which might not have been critically stressed during the depletion phase, but may become critically stressed due to injection-induced cooling.

A final (potential) problem with the proposed monitoring is that it relies solely on the pre-existing onshore KNMI network. In case the behaviour modelled by Fenix for the P18-2 North-Western and P18-4 Western faults proves to be accurate, there is no possibility for an early detection of such an increasing seismicity trend during late-stage injection.

4.7.5 Conclusion TNO-AGE

TNO-AGE considers the applied methods for modelling fault stability appropriate and calibration of Mmax with cohesion as a reasonable approach given the limited data on seismicity. Calibration of Mmax to the detection limit of M2 varying cohesion can be considered a conservative approach for the main boundary faults, as the fault gouges of these faults may be clay-rich, possibly preventing build-up of fault strength (cohesion). Build-up of fault strength during inactivity is a more likely scenario for the intra-reservoir faults.

TNO-AGE agrees with Fenix that given the absence of recorded seismicity during depletion, it is difficult to project possible seismicity during the injection phase. However, the absence of detectable (<M2) seismicity near P18 during depletion is not conclusive evidence for a total absence of seismicity. Furthermore, absence of recorded seismicity during depletion is no guarantee for absence of seismicity during injection of CO_2, as stabilization due to repressurization might be cancelled out by significant cooling-induced stresses. The implicitly assumed Kaiser effect does not appear to be a valid assumption for non-isothermal repressurization, as is also supported by Fenix' models, showing a higher Mmax for some of the faults at the end of injection compared to calibrated Mmax at peak depletion.

TNO-AGE has verified the maximum magnitude estimates from Fenix based on fault geometries but disagrees with the use of the SRA method for determining the appropriate seismic monitoring, as it is designed for onshore gas production and not for CO_2-storage. The choice to solely rely on the KNMI network for (micro)seismic monitoring during the injection phase needs further elaboration. Especially in light of the seismogenic behaviour modelled by Fenix for the P18-2 North-Western and

P18-4 Western faults, showing an increasing seismicity trend during late-stage injection.

4.8 Subsidence and rebound

Fenix applies the same methods described in Geertsma (1973) and van Opstal (1974) that are also used by TNO-AGE for assessing subsidence of small field onshore gas production and geothermal operations. It appears that the measured average *E* from the P18 Core Test Evaluation (Appendix 14) of 27 GPa has not yet been used for calculating the compaction coefficient. Instead, Fenix assumed an average *E* of 18 GPa for the reservoir (Appendix 12c). Therefore the applied compaction coefficient should be approximately 33% lower, which will likely lead to 33% less subsidence during depletion, as well as 33% less rebound during injection. Due to the lack of subsidence measurements during production, it is not possible to validate these estimates made by Fenix. Depending on the amount of permanent plastic deformation that has occurred in the reservoir due to compaction, a significant portion of the depletion-induced subsidence will likely be reversed during injection. So far, the (unknown) amount of subsidence during depletion has posed no problems for operations. It is expected that rebound during the injection phase will pose no problems as well, as upheave will likely be less than the subsidence.

4.8.1 Conclusion TNO-AGE

Unfortunately, no surface measurements are available for the field that could validate subsidence estimates. However, TNO-AGE does not foresee problems with upheave during injection as it will likely be less than the depletion-induced subsidence.

4.9 Concluding remarks TNO-AGE

- Fenix conducted an elaborate modelling study on the seismic hazard of P18
- All aspects that could be reasonably assessed and modelled, given the lack of data and seismicity observations, were treated:
  - Injection-induced fracturing of reservoir and caprock
  - Depletion- and injection-induced fault reactivation and induced seismicity.
- Results of the modelling seem reasonable, but are not (yet) verifiable with observations and uncertainty ranges are difficult to constrain:
  - No observations of seismicity
  - No subsidence measurements available
- Input for the dynamic GEM reservoir models is based on a single (static) reservoir model. It is unclear how errors/changes in the static model would propagate/translate into dynamic reservoir models and geomechanical models. This is partly remediated by Fenix by running the models with a worst-case scenario, but it remains unclear if this worst-case scenario sufficiently covers the potential outcomes given the uncertainties of the static model.
- Fenix provides just a base- and worst-case scenario for the injection plan, but not a strictly defined limit on rates, pressures, and temperatures. Fenix explains that operational parameters used for the base case are also not yet final and might be subject to later changes.
- Uncertainty of some parameter choices and possible implications are not always adequately discussed.

- An extensive sensitivity analysis of fault stability is only conducted for the (main)bounding faults and not for the intra-reservoir fault scenario.
- The sensitivity analysis for cap rock breach is limited: only Shmin was varied.
- Monitoring of fracturing will only be conducted using pressure measurements in the well, as indicated in the monitoring plan.
- As Fenix has shown for P18-4A2, the modelled pressure signal for fracturing can be relatively weak (5-10 bar) which may be difficult to detect over other sources that affect well pressures.
- The implicitly mentioned Kaiser effect as argument for absence of future seismicity is questionable, as conditions during injection will be different (non-isothermal) compared to depletion. This is particularly relevant for intra-reservoir faults which may only become critically stressed during the injection phase, but also for boundary faults that will experience significant cooling.
- The SRA for onshore gas production was designed to assess depletion-induced seismicity risks for small onshore gas fields. It was not designed to assess the seismicity risk for non-isothermal injection of CO_2. The derived negligible risk for the gas depletion phase of P18 is not directly transferrable to the injection phase. The choice to solely rely on the KNMI network for (micro)seismic monitoring during the injection phase needs further elaboration. Not only for the purpose of induced seismicity risks but also in light of the need for adequate monitoring of thermal fracturing in reservoir and overburden.
- TNO-AGE considers the proposed seismic monitoring, relying solely on the pre-existing onshore KNMI network, barely sufficient. Finally, this project will be the first large-scale CCS project in the Netherlands (and the world) storing CO_2 in an empty gas field. Information gathered during the different phases of the project might prove invaluable for improving future projects.

5 Discussion and conclusions

5.1 Technical issues (e.g., incorrect/missing details)

Seismic interpretation

- TNO-AGE agrees with the bulk of modelled faults that were provided in the Petrel model.
- TNO-AGE does have a concern regarding the discrepancy at some (larger) areas of the top reservoir model and interpretation along with the seismic data. Although explained by the applicant that this top reservoir results in the best static/dynamic GIIP match, TNO-AGE would advise analysing the uncertainty of different top reservoirs (close to the best static/dynamic GIIP) on the presence and extension of juxtaposition through the area.
- The northwestern extension of Block IV of the P18-2 reservoir could continue further than the applicant indicates. This has potential implications on the juxtaposition of P18-6 with the northern downthrown block of P18-2.
- Internal faults are observed in the P18-4 field and all blocks of the P18-2 field. These should be taken into account in scenarios of static model building and/or dynamic modelling.

Petrophysics and reservoir properties

- TNO-AGE considers the models and parameters used for the interpretations to be adequate.
- There is a sub-optimal match between log based permeability and well test permeability. This requires more study to effectively estimate reservoir wide permeability distribution
- There are multiple inconsistencies in the numbers and description of reservoir properties in the different documents supporting the application. These are in GIIP (static/dynamic), permeability, use of petrophysical re-evaluation.
- Upscaling of the log and core permeabilities should be carefully considered given the 3 orders of magnitude vertical heterogeneity in permeability.
- The lateral permeability will likely be lower than a the well as the decimeter scale high perm streaks are not laterally continuous but will not extend further than ~decameter scale. This causes a lateral baffle as fluid flow will have to move through the lower permeable zones (see 2.2)

Static modelling

- Given the uncertainty in the exact fault and top reservoir interpretation several scenarios of the static modelling should be presented and implications in dynamic behavior demonstrated
- The average trend of a high perm streak in the upper Hardegsen is expected to be found in the entire reservoir.
- The observed upward increase in permeability is observed in all wells, however the applicant does not honor this trend in between the wells in the static model due to the stochastic method of populating.

Dynamic modelling

- We recommend the uncertainty in the geological model (e.g., flow barriers and facies distributions) to be considered in the dynamic modelling studies, allowing for uncertainty quantification of injectivity and CO_2 distribution predictions.

- We suggest re-running the model assuming an appropriate Forchheimer factor to estimate of the effects and importance of turbulent flow in the near-wellbore region in all phases of CO_2 injection field development.

- We recommend a plot of the p/Z curves versus Cumulative Produced Gas minus Injected CO_2 with and without a fracture to be generated to show the potential of p/z as monitoring tool within cold CO_2 injection into depleted gas fields.

- We recommend PTA modeling to be used for monitoring and model calibration in the future should not neglect thermal effects.

Geomechanical evaluation

- Results of the modelling seem reasonable, but are not (yet) verifiable with observations and uncertainty ranges are difficult to constrain:
  - No observations of seismicity
  - No subsidence measurements available
- Input for the dynamic GEM reservoir models is based on a single (static) reservoir model. It is unclear how errors/changes in the static model would propagate/translate into dynamic reservoir models and geomechanical models. This is partly remediated by Fenix by running the models with a worst-case scenario, but it remains unclear if this worst-case scenario sufficiently covers the potential outcomes given the uncertainties of the static model.
- Fenix provides just a base- and worst-case scenario for the injection plan, but not a strictly defined limit on rates, pressures, and temperatures. Fenix explains that operational parameters used for the base case are also not yet final and might be subject to later changes.
- Uncertainty of some parameter choices and possible implications are not always adequately discussed.
- An extensive sensitivity analysis of fault stability is only conducted for the (main)bounding faults and not for the intra-reservoir fault scenario.
- The sensitivity analysis for cap rock breach is limited: only Shmin was varied.
- Monitoring of fracturing will only be conducted using pressure measurements in the well, as indicated in the monitoring plan.
- As Fenix has shown for P18-4A2, the modelled pressure signal for fracturing can be relatively weak (5-10 bar) which may be difficult to detect over other sources that affect well pressures.
- The implicitly mentioned Kaiser effect as argument for absence of future seismicity is questionable, as conditions during injection will be different (non-isothermal) compared to depletion. This is particularly relevant for intra-reservoir faults which may only become critically stressed during the injection phase, but also for boundary faults that will experience significant cooling.
- The SRA for onshore gas production was designed to assess depletion-induced seismicity risks for small onshore gas fields. It was not designed to assess the seismicity risk for non-isothermal injection of CO_2. The derived negligible risk for

the gas depletion phase of P18 is not directly transferrable to the injection phase. The choice to solely rely on the KNMI network for (micro)seismic monitoring during the injection phase needs further elaboration. Not only for the purpose of induced seismicity risks but also in light of the need for adequate monitoring of thermal fracturing in reservoir and overburden.

5.2 General discussion regarding operational plans

Risk plan
The applicants use industry standard methods to evaluate risking. The bow-tie method is used to determine the actual outcome per risk. A risk assessment matrix Is used to assess the outcome of all risks .While the most relevant actual technical risks have been taken into account the lack of sensitivity analysis in the supporting evaluation (see previous chapters) make it impossible to adequately determine the suitability. Additionally the actual remaining risks presented in the risk assessment matrix are not presented quantitatively, which makes interpretation and relative weighting impossible. The definitions used in the matrix are ill defined and require more substantiation.
Vertical leakage is taken into account although some additional static and dynamic modelling situations should be added in order to further assess the end members of vertical fracture propagation. Although the net effect of even a very large fracture will remain minimal if operational limits are adequately defined as the CO_2 will not flow out if pressure is below hydrostatic. Additionally TNO-AGE expects the fracture to close eventually in the ~400 m of clays overlying the storage reservoir.
Lateral leakage is defined for most faults although should be defined further for alternative interpretations and relevant static model variations.

Monitoring plan
The technical evaluation of the proposed monitoring techniques are provided in chapter 5. Given the limitations of these techniques to assess both CO_2 plume distribution, microseismicity and thermal fracking we propose to await a new version of the plans before providing a final technical evaluation.

Mitigating measures plan
Given the updates necessary in the risk assessment and monitoring plans we prefer to defer on commenting on this plan.

Abandonment plan
Porthos proposes to have a short 1 year monitoring period after end of injection before ending their license and abandoning. The requirements for abandonment and the relevant monitoring period will have to be set up based on integration of the models with monitoring result during and after the injection phase. A definite period cannot be set given the current knowledge level.

General TNO-AGE comments regarding operational plans
While all plans contain the main ingredients required to describe them, the premature nature forces us to refrain from giving a final verdict on the plans. Before injection starts the plans will have to be updated including the methodology. Unexpected or undesirable events should be detectable timely in order to allow effective correctional measures (closed loop monitoring). In order to define these

effects forecasts from the models should be updated with adequate uncertainty ranges and based on this limits should be chosen to define a ‘significant deviation in the monitoring range for each potential event.

5.3 General discussion regarding advice questions

5.3.1 Maximum pressure

Hydrostatic pressure

The subsurface has a vertical hydrostatic fluid pressure column measure on a (geological) time scale. But in the event of a strong lowering of the reservoir and compaction (or even by becoming completely closed off) overpressure can occur as compared to the hydrostatic pressure.

Based on the pressure information provided by Porthos (Working Document 2.0, p.47), TNO-AGE expects that the original reservoir pressure in P18-2 is hydrostatic in the sense described above.

Porthos indicates P18-2 was overpressured preceding prediction. The pressure SNS database (TNO, 2015) indicates an overpressure in the range of 10 to 25 bar for the P15/P18 range, however the production data is unconclusive with regard to this; TNO-AGE questions the overpressure assumption. Given the uncertainties TNO-AGE proposes to allow the applicant to resubmit a proposal for the maximum hydrostatic pressure as limit taking into account uncertainties such as water density, RFT measurements etc.

The P18-2 storage reservoirs are near empty gas reservoirs. Much information has been obtained during production, which can now be used to evaluate their suitability for permanent CO_2 storage. The observed p/Z material balance and the fact that no active inflow from aquifers has been observed make these reservoirs an effectively closed tank on the time scale of gas production (about 35 years). However, that does not provide predictions of pressure development in the long term.

Pressure limits

The applicant has investigated a broad spectrum of possible leak paths, either through the overlying seal or along the wells. Migration paths within the storage complex have not been treated explicitly, let alone quantitatively.

In theory, the most conservative scenario would be to keep the pressure inside the storage reservoir always and everywhere below the – assumed - surrounding fluid pressures as this would prevent CO_2 from escaping due to pressure differential even in case of a major seal breaching fracture. However, in practice this poses some problems, such as:

- how can the surrounding fluid pressure be determined sufficiently well?
- to what extent is the proposed pressure monitoring in wells – and associated reservoir modeling - capable of predicting the pressure distribution throughout the reservoir in an sufficiently reliable manner.

This subject is further treated in the Appendix B, including our recommendations for improvement of the fluid pressure distribution analysis, the monitoring aspects and the sensitivity of the storage efficiency to maximum reservoir fluid pressures.

In summary, these recommendations concern taking the uncertainty of the underlying parameters into account, before deciding on any regulatory quantitatively fixed pressure limit.

5.3.2 Reservoir fitness for CO_2 storage

The gas production phase

The P18 storage reservoirs are deeply depleted gas reservoirs. During their production life time, a lot of information has been obtained, that now can be used to evaluate their suitability for permanent CO_2 storage. The p/Z material balance and the fact that no active aquifer influx has been observed, make these reservoirs into an effectively closed tank during gas production.

Natural CO_2 reservoir Werkendam-Deep

The P18 storage reservoirs geologically are analogues of a series of on trend Triassic onshore gas fields [Figure 6.1]. Amongst these is Werkendam-Deep, an unintended discovery of an accumulation containing 75% CO_2 [refs] at a similar depth as the P18 reservoirs. TNO-AGE considers this accumulation a strong indication, that the regional top seal is able to hold CO_2 rich accumulations for geologically long periods

Moreover, microscopic analysis of core taken form the discovery well (WED-3) showed that the very long term exposure of the reservoir rock to CO_2 has not notably degraded the reservoir, confirming the long term integrity of the reservoir itself.

Marked difference from the above geological and gas production considerations is, that now CO_2 will be injected at temperatures significantly below the present reservoir temperature, introducing pressure and temperature induced stress changes in the deeply depleted reservoir rock. We argue that filling up a depleted reservoir is ‘common practice’ in the natural gas storage industry and has not given rise to more seismicity than during depletion (contrary – Kaiser effect).). That leaves temperature effects deserving the most attention as potential sources for fracturing, both at the wells and in the reservoir and seal. In addition to that, the injected CO_2 will go through a phase change from gas to supercritical.

Additionally the current reservoir has been drilled, thereby creating a potential leak path through the seal. Although the risk is probably minor given the large seal thickness and the presence of ~1 km of secondary seal above,

Potential leak paths

Discussed under 5.3.1

Defining Effective versus legal leakage

In the legal definition leakage of stored CO_2 is defined as CO_2 leaving the predefined storage complex. Taking a step back to look at the goal of CO_2 storage, i.e. removing CO_2 emission within relevant time scales (~1000 years) leakage may be defined differently in a technical way.

Additionally; based on the current proposed monitoring system anything but the most extreme and unlikely cases of leakage are not sufficiently distinguishable from migration within the P18-2 storage complex or greater integral P18 storage complex.

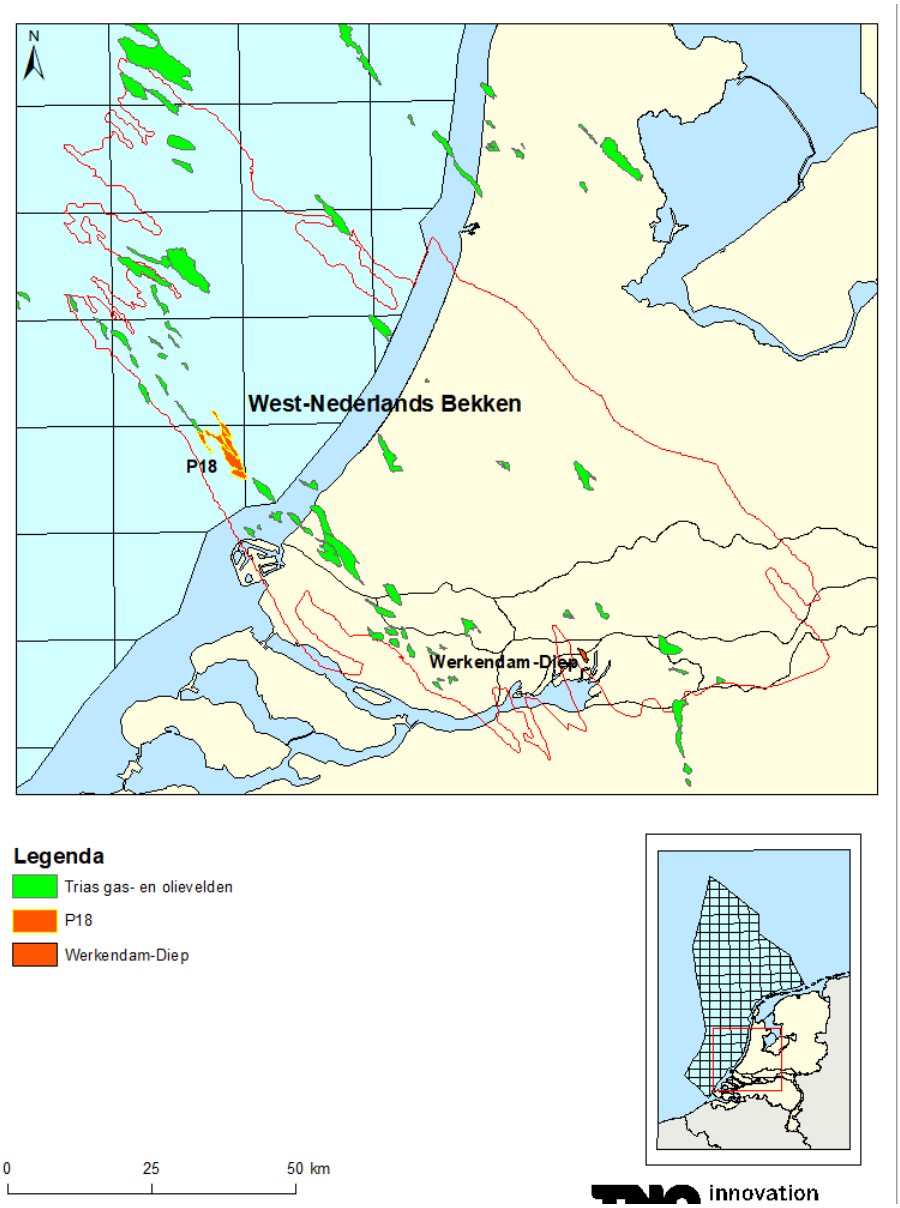

Figure 5.1 The West Netherlands Basin showing all gas fields with proven gas in the Bunter reservoir. The Werkendam-Deep analogue (non-producing) gas field is indicated as is the P18 Complex in red.

Operational Pressure maxima

Porthos proposes to set a maximum on the reservoir pressure at hydrostatic pressure. That is lower than the original gas pressure, depending on the definition of hydrostatic pressure. This at first glance would guarantee that any connection of the storage to the outside world would lead to influx of fluids into the storage, rather than efflux of fluids from the storage. Yet, in the application Porthos leaves room to go to higher pressures based on the lateral change in pressures and the focus on average reservoir pressure.

TNO-AGE advises to take hydrostatic pressure (i.e. virgin pressure) as a condition at the start of the project, and require that Porthos submits a technically

sufficiently underpinned proposal to change the storage plan in case they aim at a higher than hydrostatic pressure. Amongst others actual hydrostatic pressure at the reservoir levels needs to be assessed before defining this.

5.3.3 Injection rate and capacity

The applicants provide a total capacity at ~34-38 MT. For reference TNO, 2020. showed in a portfolio study that the expected capacity of the entire complex to be 36.3 MT theoretical and 32,7 MT practical. Given the inherent uncertainties and dependencies on actual operational strategy on the effective capacity, TNO-AGE does not see the need to further expand on capacities but is sufficiently satisfied with the capacity estimation by the applicant.

5.3.4 Significance for further CO_2 storage

The P18 storage complex is a nearshore option for CO_2 storage in depleted gas fields and lies relatively near a large hub of CO_2 emitters. Likely the success of this project is paramount to further expand CO_2 storage in depleted gas fields further offshore. TNO-AGE strongly feels uncertainties in this project should therefore be closely monitored and studied in order to calibrate relevant models and assess any unforeseen or unwanted effects.

TNO-AGE advises to see this project not only as a viable economic initiative which will store a significant amount of CO_2. This means insisting on a major effort in monitoring the entire chain from the emitter to the storage site. Any learnings may prove vital for the expansion of CO_2 storage on large scale.

6 References

AMOCO Netherlands B.V., 1997. Well: P18-2A6. Report on Processing and Interpretation of Ultrasonic Borehole Imager (UBI) Data.

Bos, B., Spiers, C.J., 2000. Effect of phyllosilicates on fluid-assisted healing of gouge-bearing faults, Earth and Planetary Science Letters, 184(1), https://doi.org/10.1016/S0012-821X(00)00304-6.

Carpenter, B.M., Saffer, D.M., and Marone, C., 2012. Frictional properties and sliding stability of the San Andreas fault from deep drill core. Geology, 40 (8) https://doi.org/10.1130/G33007.1

CATO2-WP3.01-D06, 2011. Feasibility study P18 (final report).

Fenix, March 2018. 3D Geomechanical Model for Gas Storage Bergermeer.

Geertsma, J., 1973. Land subsidence above compacting oil and gas reservoirs, J. Petr. Tech. p. 734-744.

Heidbach, O., Rajabi, M., Reiter, K., Ziegler, M., WSM Team, 2016. World Stress Map Database Release 2016. GFZ Data Services, doi:10.5880/WSM.2016.001

Hunfeld, L. B., Chen, J., Hol, S., Niemeijer, A. R., and Spiers, C. J., 2020. Healing behavior of simulated fault gouges from the Groningen gas field and implications for induced fault reactivation. Journal of Geophysical Research: Solid Earth, 125, e2019JB018790. https://doi.org/10.1029/2019JB018790.

KEM01 WP7, 2019. Safe operational bandwidth of gas storage reservoirs WP7 Report Phase 1 & Phase 2 Final Report.

Mechelse, E., 2017. The in-situ stress field in the Netherlands: Regional trends, local deviations and an analysis of the stress regimes in the northeast of the Netherlands.

Pijnenburg, R.P.J., Verberne, B.A., Hangx, S.J.T., and Spiers, C.J., 2019. Inelastic Deformation of the Slochteren Sandstone: Stress-Strain Relations and Implications for Induced Seismicity in the Groningen Gas Field. Journal of Geophysical Research: Solid Earth, 124, 5254– 5282. https://doi.org/10.1029/2019JB017366.

Segall, P., and Fitzgerald, S.D., 1998. A note on induced stress changes in hydrocarbon and geothermal reservoirs. Tectonophysics, 289, 1–3, https://doi.org/10.1016/S0040-1951(97)00311-9.

Shapiro, S.A, and Dinske, C., 2021. Stress Drop, Seismogenic Index and Fault Cohesion of Fluid-Induced Earthquakes. Rock Mech Rock Eng, https://doi.org/10.1007/s00603-021-02420-3.

SSM (Staatstoezicht op de Mijnen), 2016. Methodiek voor risicoanalyse omtrent geïnduceerde bevingen door gaswinning. Tijdelijke leidraad voor adressering MBB, 24.1.p, versie 1.2.

TAQA offfshore B.V. & EBN CCS B.V., 2021. Application for a CO_2 storage permit reservoir P18-2.

Tenthorey, E., and Cox, S. F., 2006. Cohesive strengthening of fault zones during the interseismic period: An experimental study, J. Geophys. Res., 111, B09202, doi:10.1029/2005JB004122.

TNO, 2020. TNO rapport R10284. CO_2 opslaglocaties offshore – Een portfoliostudie. TNO, 2020.

TNO R100043, 2019. Review of worldwide geothermal projects: mechanisms and occurrence of induced seismicity.

TNO R11259, 2015. Injection Related Induced Seismicity and its relevance to Nitrogen Injection: Modelling of geomechanical effects of injection on fault stability.

TNO R11739, 2015. Thermal fracturing due to low injection temperatures in geothermal doublets.

TNO R10056, 2015. Integrated pressure information system for the onshore and offshore Netherlands, Final Report.

Van den Ende, M.P.A., and Niemeijer, A.R., 2019. An investigation into the role of time-dependent cohesion in interseismic fault restrengthening. Sci Rep 9, 9894, https://doi.org/10.1038/s41598-019-46241-5.

Van Opstal, G., 1974. The effect of base rock rigidity on subsidence due to compaction, Proceedings of the Third Congress of the International Society of Rock Mechanics, Denver, Colorado, September 1-7, 1974. Volume II, part B, National Academy of Sciences, Washington, D.C..

Vilarasa, V., 2016. The role of the stress regime on microseismicity induced by overpressure and cooling in geologic carbon storage. Geofluids 16, doi: 10.1111/gfl.12197.

Zoback, M.D., 2007. Reservoir Geomechanics. Cambridge University Press, ISBN: 978-0-521-14619-7.

Zoback, M.D., and Kohli, A.H., 2019. Unconventional Reservoir Geomechanics. Cambridge University Press, ISBN: 978-1-107-08707-1.

7 Appendix A - Petrophysical evaluation

7.1 Introduction

As part of the overall geotechnical evaluation and advice of TNO-AGE on the P18-2 carbon capture storage (CCS) license application and extension of the P18-4 storage license, a review on the petrophysics was carried out. The goal of the review of the petrophysics was to assess if the reservoir property calculations were conducted adequately and if the implementation of these properties in the static and dynamic models needs to be revised (see section 3.3) .Therefore, the outcomes and conclusions of this review are mainly used in the evaluation of the static and dynamic models.

7.2 Reviewed documentation and data

The following overview summarizes the documents and other material that was considered relevant for the review of the petrophysics:

- Aanvraag CO_2-opslagvergunning reservoir P18-2 (Taqa & EBN, Feb2021).
  - Specifically: Deel II: Beschrijving CO_2-opslag reservoir P18-2 (Taqa & EBN, February 2021).
- Bijlagen behorende bij Aanvraag CO_2-opslagvergunning reservoir P18-2:
  - Attachment 7: CO_2 feasibility study (TNO, 2019) [2].
    - Attachment B: Subsurface model descriptions
  - Attachment 8: Storage capacity technical note (Porthos, 2020) [3].
- Final presentation 2020 PP Evaluation (Across Petrophysics, 2020) [4].
  - Data tables 2020 PP Evaluation.xlsx
  - RFT update 2020 PP Evaluation.xlsx
  - Sedimentology P15-P18.xlsx
- P15-10 Special Core Analysis report (Core Laboratories, 1989).
- P/18 Field Petrophysical Study (BP Field Studies Petrophysics, 2007) [5].
- P18 Static model

An initial petrophysical study was carried out by BP in 2007 [5] on twelve wells. Recently, a petrophysical re-evaluation [4] of 18 wells was conducted by Across Petrophysics (AP), as commissioned by EBN.
There is some inconsistency between the documents regarding the origin of the reservoir properties that were used in the static and dynamic models. Attachment 8 [3] states that the reservoir parameters are based on the study of BP (2007) [5], while part II of the application document [1] states that the models are populated with the reservoir parameters resulting from the petrophysical (re)evaluation. The latter could as well be the recent study by AP [4]. There is also inconsistency in the average permeability per zone (Table 2 in application document [1] vs paragraph 4.2.2.2 in attachment 8 [3]), and the description of the type of porosity-permeability relation that was used (linear vs logarithmic).
Based on the review of the different documents and data TNO-AGE concludes that the models are populated by the reservoir parameters resulting from the study by BP (2007) [5] and that no changes have been made to the models based on the results of the recent study by AP (2020) [4].

7.3 Technical review

This paragraph describes the results of the technical review of the derived reservoir properties, like the clay volume, porosity, permeability, saturation and net-to-gross, and compares the applied methodology and results of the studies of BP [5] and AP [4].

The study of AP [4] was conducted on a larger well selection with respect to the study of BP [5] and includes more P15 wells and the recent well P18-07. An overview of the evaluated wells in the two different studies is provided in Table 7.1.

Table 7.1 Overview of evaluated wells.

Well	Across Petrophysics [4]	BP [5]
P15-01	X	X
P15-02	X	
P15-E-01-S1	X	
P15-10	X	
P15-12	X	X
P15-14	X	X
P15-F-01	X	
P15-G-01-S1	X	
P18-01	X	X
P18-02	X	X
P18-A-01	X	X
P18-A-03-S2	X	X
P18-A-05-S1	X	X
P18-A-06	X	X
P18-A-06-S1	X	X
P18-A-02	X	X
P18-A-07-S1	X	X
P18-07	X	

Table 7.2 GR parameters per well from AP [4].

Well	GR_{clean}	GR_{clay}
P15-01	20	109
P15-02	25	134
P15-E-01-S1	20	125
P15-10	20	120
P15-12	19	118
P15-14	39	142
P15-F-01	20	113
P15-G-01-S1	18	117
P18-01	21	134
P18-02	16	119
P18-A-01	40	137
P18-A-03-S2	29	144
P18-A-05-S1	15	117
P18-A-06	24	137
P18-A-06-S1	38	129
P18-A-02	40	146
P18-A-07-S1	33	134
P18-07	15	115
Average	25	127

7.3.1 Clay volume

Both BP and AP used a linear correlation between the Gamma Ray (GR) measurements and clay volume, which is regarded as common practice.
BP has applied a uniform GR_{clean} and GR_{clay} value of respectively 25 and 140 GAPI for all evaluated wells and formations. AP interpreted the GR_{clean} and GR_{clay} for each individual well, without any variations between the different formations. Table 7.2 shows the interpreted values for each well and the overall average, which is 25 and 127 GAPI for respectively the GR_{clean} and GR_{clay}. For some wells the difference in the resulting clay volume is larger than for others, but on average the GR_{clean} and GR_{clay} of BP and AP are in close agreement. Only the GR_{clay} deviates to some extent, which on average results in a slightly higher clay volume calculated by AP. However, the GR_{clean} usually has a smaller influence on the average clay volume than the GR_{clean} value, as the bulk of the reservoir interval consists of sandstone layers. TNO-AGE considers the clay volume method adequate.

7.3.2 Porosity

7.3.2.1 In-situ correction

Core plug porosity measurements are used by AP (9 wells) as well as by BP (5 wells), to calibrate the porosity curves calculated from log measurements. BP has applied an in-situ correction to the porosity measurements of ca. 0.92 to the median value of 13% porosity. AP on the other hand argues that an in-situ correction is not required for the core porosity measurements. The isostatic stress calculated by AP was 942 psi [4]:

$$\sigma_{iso} = \frac{\sigma_v + \sigma_H + \sigma_h}{3} - P_{fluid} = \frac{710 + 306 + 306}{3} - 375 = 65\ bar = 942\ psi$$

In this formula the pore pressure is subtracted from the lithostatic pressure because it prevents the pores to compact. This calculated isostatic stress corresponds closely to the first pressure step of 800 psi applied on the porosity measurements under confining pressure. At this first step the porosity reduction is still very minimal and therefore AP concludes that no in-situ correction is required.
TNO-AGE considers the approximation by AP to be correct and agrees that an in-situ correction to the core data is not necessary in this case. Also under depleted conditions, with a very low pore pressure, the isostatic stress still does not approach the second pressure step of 2500 psi. Therefore, the amount of porosity reduction due to gas depletion is also considered to be negligible.
The porosity calculated by AP might be slightly higher than the porosity of BP due to the in-situ correction. The porosity calculated by BP is applied in the static model, but considering the good match between the static and dynamic volumes there is no reason to revise the porosity in the models. This difference in porosity possibly (partly) explains the multiplier of 1.1 that was applied to the volume calculation of Block 1, but off course there are many more uncertainties.

7.3.2.2 Porosity logs

BP has based the porosity calculation on the neutron-density log combination, where available, while AP only uses the density log. BP states that the result of the neutron-density porosity gives a better match with the core porosity, and AP states that the density porosity gives a better match. Both provide cross plots to show the results (Figure 7.1 and Figure 7.2) [4 & 5].
Based on the provided documents and information TNO-AGE cannot explain why the density-neutron porosity is a better match in the study of BP, while the density porosity matches better in the study of AP. Usually, in case of a gas filled reservoir

with shaly intervals the neutron-density log combination is considered to give the most accurate result because of the correction for gas and clay volume.
AP applied a constant relatively low fluid density to correct for the gas effect, which is considered to be less optimal by TNO-AGE. Furthermore, AP has applied a constant matrix density for all evaluated formations. However, the Main Buntsandstein Subgroup in this region is characterized by an increasing amount of dolomite cement towards its base. This explains the low porosity of the Lower Detfurth and Volpriehausen formations. An increasing amount of dolomite cement results in an increasing matrix density of the lower formations. This was not taken into account by AP, possibly resulting in a slight underestimation of porosity in these intervals.

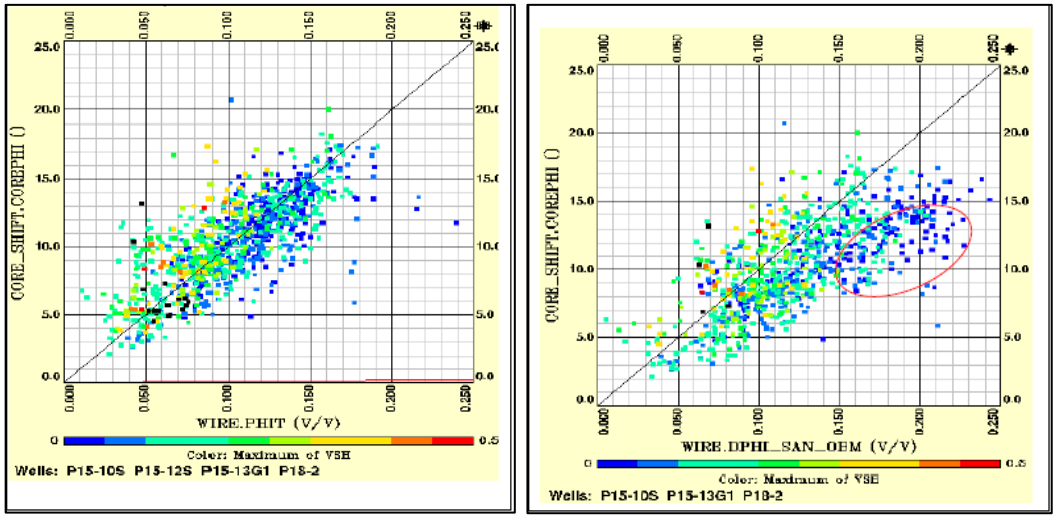

Figure 7.1 Cross plots of core porosity vs log porosity from BP [5]. Left: core porosity vs neutron-density log porosity, right: core porosity vs density log porosity.

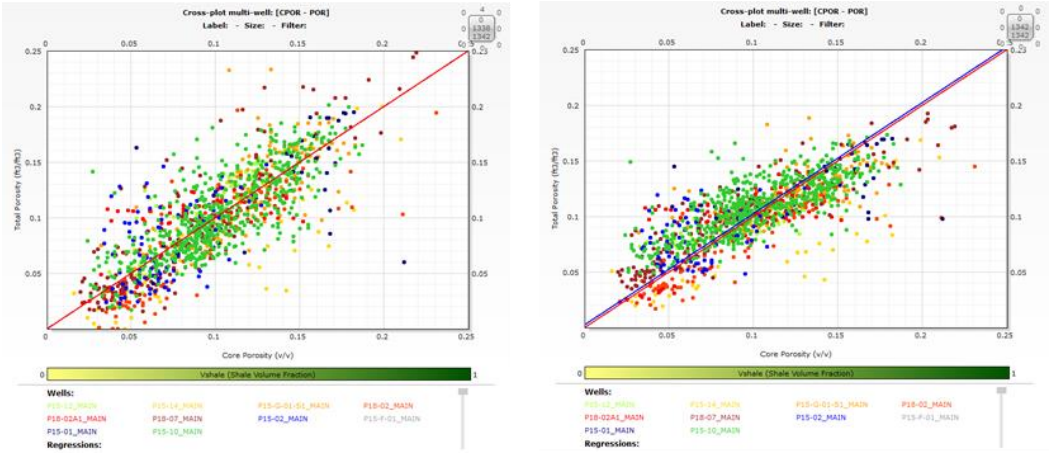

Figure 7.2 Cross plots of core porosity vs log porosity from AP [4]. Left: core porosity vs density log porosity, right: core porosity vs neutron-density log porosity.

The porosity calculated by BP has been used to populate the static model. Considering the arguments above and the good match between the log and core porosity of BP, TNO-AGE supports this choice.

7.3.3 Saturation

Both BP and AP use the Archie equation to calculate water saturation from log measurements. TNO-AGE agrees with the use of the Archie equation, as it is a total water saturation model that fits the total porosity calculation. Both studies used similar Archie parameters (m and n), which are based on the SCAL measurements on core plugs of the P15-10 well. BP determined the water resistivity from a water sample of the P15-09E2 well because at that time no wells were drilled into the water leg. The recent study by AP made use of a Pickett plot evaluation of the P18-07 well, that encountered water bearing formations. A Pickett plot evaluation is regarded by TNO-AGE as more robust, but the resulting water resistivity is similar to the value determined by BP. The determined salinity of 88000 ppm also closely matches the formation water salinity of the Vierpolders geothermal project, which is also targeting the Triassic Main Buntsandstein Subgroup at a similar depth and is located close.

AP recognizes a low resistivity zone in the Upper Detfurth. This effect varies from well to well, but has the clearest expression in wells P18-02 and P18-07. In former studies TNO-AGE also recognized this low resistivity zone in well P18-07. In this zone a relatively high water saturation with respect to the reservoir quality and height above the free water level is calculated from the logs, which results in a mismatch between the log based saturation and the saturation-height model. AP applied a thin bed analysis, as this possibly explains such a low resistivity zone, but the result was not significantly better. Probably because of the low clay content. During investigation of the core of P18-07 TNO-AGE did not observe any thin bed lamination, which supports the choice of AP not to incorporate this analysis.
TNO-AGE thinks that a possible explanation for the unexpected low saturation is the choice of Archie parameters. The SCAL measurements used for the evaluation are from well P15-10, in which this effect is not so clearly observed, and are conducted on samples of the Lower Detfurth and Volpriehausen only. Therefore, the applied m and n values might not be representative for this zone in the Upper Detfurth. While gas saturation may not be represented perfectly this will have little effect on CO_2 modelling.

7.3.4 Permeability

7.3.4.1 Porosity-permeability transforms

To calculate permeability from porosity a core-based porosity-permeability relationship needs to be defined. The study of BP uses an electrofacies analysis to distinguish four different litho-classes: 1) eolian dune, 2) interdune, 3) eolian dolomitic, 4) shales. For each lithology class a different porosity-permeability relationship was defined (Figure 7.3).
Although TNO-AGE considers defining lithology classes based on electrofacies a very uncertain approach, the power relations defined by BP are realistic and as expected for these type of lithology classes.
AP defined various porosity-permeability relationships, using linear and logarithmic relations and incorporating shale volume or not. Based on the highest R^2 of a plot of core permeability vs calculated permeability, AP prefers a logarithmic relation with the shale volume incorporated. TNO-AGE agrees with this choice, as it prefers curved relations in the log-linear plot above linear relations. Incorporating shale volume improves the result, but only slightly. Possibly because the shale content of the reservoir is quite low.

For comparison , TNO-AGE incorporated the poro-perm relationships of BP and AP into a single graph (Figure 7.3). Figure 7.4 shows that the logarithmic relation of AP closely matches the power relation for rock type 1 of BP. The incorporation of the shale content variable in the relation of AP moves the blue line up and down, more

or less between the rock type 1 and 2 lines of BP. This indicates that the porosity-permeability relationships as defined by AP and BP are in very close agreement, especially because the major part of the (net) reservoir interval consists of rock type 1 and 2.

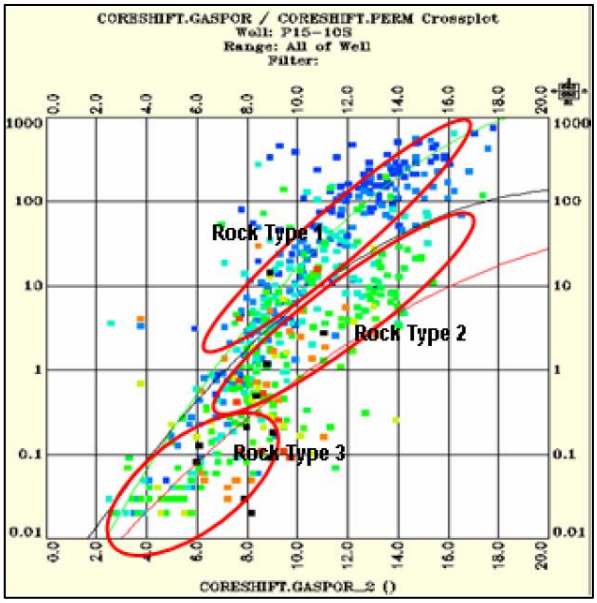

Figure 7.3 Porosity-permeability transforms defined by BP.

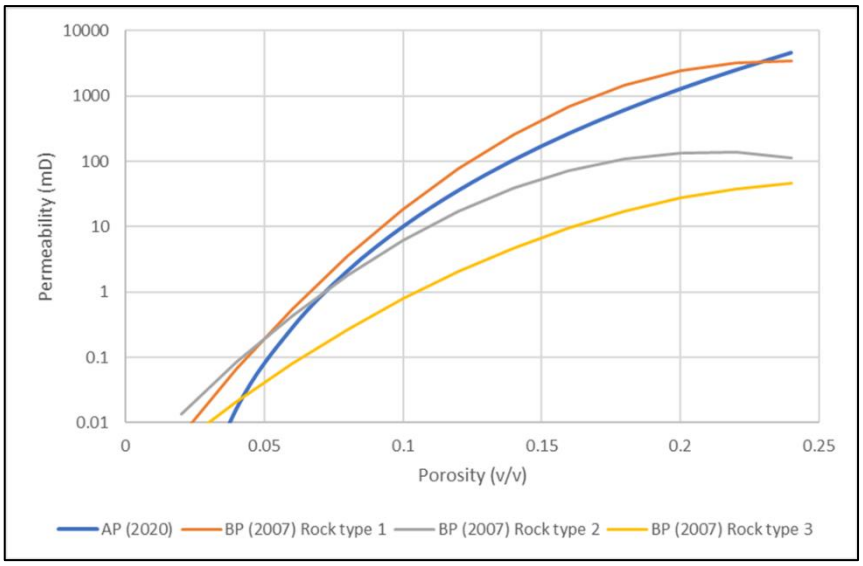

Figure 7.4 Overview plot with porosity-permeability transforms from studies of AP [4] and BP [5].

7.3.4.2 *Allocating core data to reservoir zones*

In the study of AP several methods are applied to allocate the core measurements to groups based on reservoir zonation, lithology, depositional environment, electrofacies, RQI/FZI binning. The overall conclusion of AP this results into very

little or no improvement of the permeability prediction. TNO-AGE agrees with this conclusion as splitting the data would probably lead to a higher average log permeability, while the log permeability is already overestimating the permeability based on well test interpretations. The average log permeability increases because by splitting the data the permeability of the Hardegsen, which forms the largest part of the reservoir interval, will be increased.
TNO-AGE has some additional remarks with respect to the conclusions of AP regarding the splitting of data. AP states that, in case of splitting per zone or lithology class, the separation between the different porosity-permeability lines is small and that there is no consistency with lithology class. TNO-AGE does not fully agree with this conclusion. The plot with separate lines per reservoir zone shows a porosity-permeability relation for the Volpriehausen that is a factor 2 lower than those of the Detfurth and Hardegsen formations, which is as expected. In case of the plot with lithology classes, the separation between the lowest and highest line is almost a factor 5, which is not insignificant.

7.3.4.3 *Permeability uncertainty*

The permeability uncertainty range as applied to the model was 0.3 – 5 times the average permeability. This range is based on the uncertainty from the core plug porosity-permeability plot and the log-based vs well test permeability plot (Figure 7.5).
Because of the scale difference TNO-AGE considers an uncertainty estimation based on a core plug data plot an inadequate approach. However, the uncertainty based on the variation in well test permeability is more adequate and a the proposed range also seems appropriate based on the presented data and information.

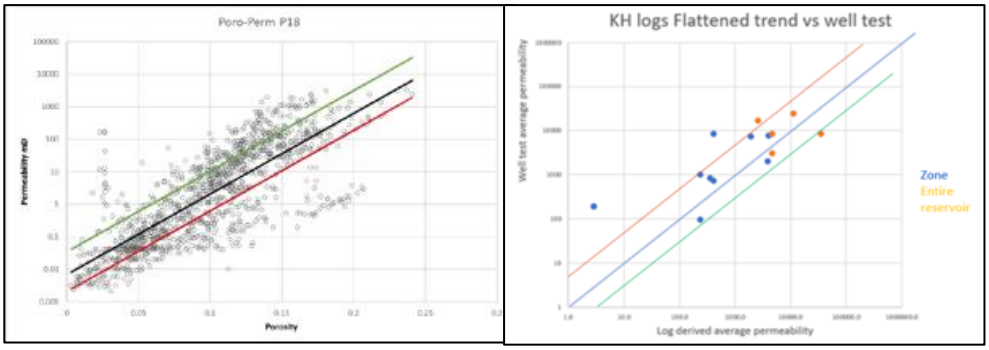

Figure 7.5 Left; core plug porosity-permeability plot with envelope lines defining the uncertainty range [4]. Right; plot of log based permeability vs well test permeability, including envelope lines defining the uncertainty range [4].

7.3.4.4 *Upscaling permeability*

The upscaling of permeability in a static model is a complex problem and often results in a mismatch between the log based permeability and the well test permeability. The arithmetic average is a commonly applied averaging method, but this can result in an average permeability that is 3 to 5 times higher than the well test permeability. The results of the petrophysical analysis by AP also shows a mismatch between the log based permeability and the well test permeability (Figure 7.6).
AP describes three possible solutions for this problem: 1) binning, 2) mathematical (multiplication), 3) adding random noise. Of these three solutions AP considers random noise to be the best option. AP tested this method, but concludes that it does not show a clearly better approximation of the well test permeability (Figure

7.6). However, the relatively large spread in data points in Figure 7.6 makes a comparison difficult. It might be better to do the evaluation per well.
TNO-AGE wonders why the option to use geometrical averaging of the log based permeability was not considered and proposes to test this in the model. Especially in eolian reservoirs with limited layering/lamination and relatively random flow through the reservoir, applying the geometrical average can give a better approximation that is closer to the lower well test permeability.

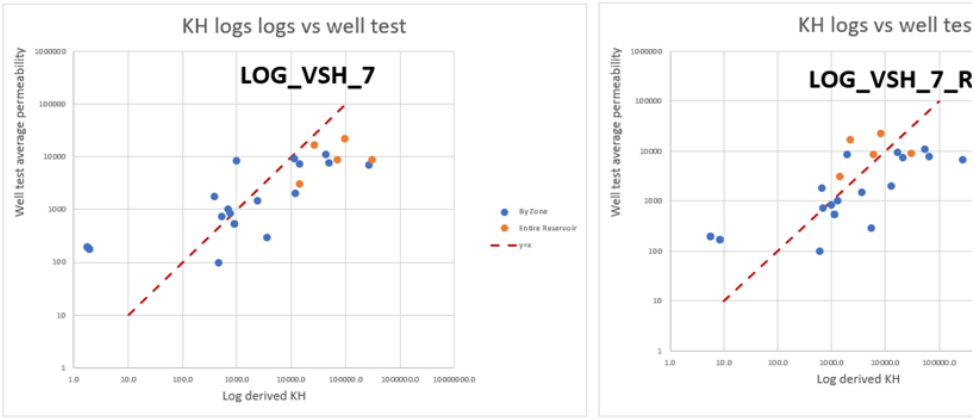

Figure 7.6 Log based permeability vs well test permeability. Left: without random noise, right: with random noise.

7.3.5 *Net-to-gross*

From the documentation that was reviewed four sets of cut-offs were proposed to define the net-to-gross. An overview is presented in Table 7.3.

Table 7.3 Overview of cut-offs reported in different reports and documents.

BP [5]	TNO [2]	AP [4]	Static model (att. 8)
Vsh: 25%	Vsh: 35%	Vsh: 60%	Vsh: -
PHIT: 4%	PHIE: 6% & 8%	PHIT: -	PHIT: 3%

There is some inconsistency in the information and numbers provided in the different documents supporting the license application. For example in attachment 8 (page 10) of the application document is stated that the net-to-gross logs are based on a shale volume cut-off, while in Table 1 in the same attachment (page 12) an effective porosity cut-off of 3% is given. In the study of AP not a lot of effort is spend on the net-to-gross ratio, only a shale volume cut-off of 60% is used.
Assuming that CO_2 more or less behaves as a fluid in the reservoir, and the lower permeability limit for fluid to flow through rock is about 1 mD, the cut-offs as proposed by TNO (2019) might be most adequate. The proposed porosity cut-off of 6-8% corresponds to a lower limit of the permeability of about 1 mD. However, in the end a lot of variation can be applied on the net-to-gross ratio, but the calculated volume has to become close to the 14,5 Bcm P/Z GIIP. Therefore N/G is highly uncertain and should be taken into account as such in dynamic modelling of CO_2 behaviour as sections of the reservoir may be .

7.3.6 Saturation-height modelling

Based on the review of the available documents TNO-AGE concludes that four saturation-height models are proposed by different authors. In Table 7.4 an overview of the models, with some characteristics, is presented.

Table 7.4 Overview of different saturation-height models described in reviewed reports and documents.

BP [5]	TNO [2]	TNO [2]	AP [4]
J-function	Lambda model	J-function	Brooks-Corey
3 functions (based on rock type)	1 function	1 function	2 functions (based on zones)

First, TNO [2] defined a lambda model to model the water saturation. The reason to propose a new model instead of using the saturation-height model of BP [5] is not described in the TNO report [2]. It turned out that the lambda model did not result in a satisfactory history match. Therefore, TNO defined a new model based on a J-function, which is eventually applied to the static model. The match of this J-function with the log saturation is less with respect to the lambda model (Figure 7.7), however the calculated static volume matches very well with the dynamic volume. TNO states that the reason for the mismatch with the log saturation is because the logs represent total water saturation. However, TNO-AGE considers the difference as shown in Figure 7.7 to be too large to be solely explained by the total water saturation log.

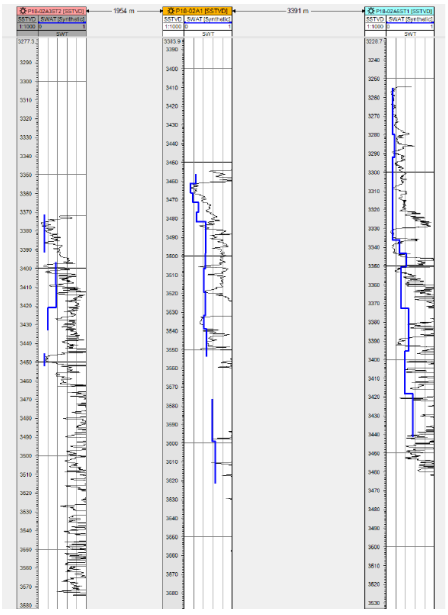

Figure 7.7 (mis)Match between saturation-height model (blue lines) and log based saturation from TNO [2].

In the study of AP [4] two separate relations are defined to get a proper fit in the Upper Detfurth, one for the Hardegsen & Upper Detfurth and one for the Lower Detfurth & Volpriehausen. TNO-AGE shares the opinion of AP that it is remarkable that the model of the Lower Detfurth and Volpriehausen shows a better reservoir quality. This makes the model somewhat questionable. TNO-AGE thinks this can be

explained by the lack of SCAL measurements in the Hardegsen and Upper Detfurth, so no calibration with capillary curves was possible.

TNO-AGE thinks the saturation in this field can be modelled with a single function, but the match of the Upper Detfurth will always be sub-optimal because of the divergent low resistivity zone.

7.3.7 Free Water Level

TNO-AGE has confidence in the determination of the Free Water Level (FWL) that is based on the available RFT data. The regional water line is based on pressure measurements in the water leg of some wells and there is no reason to believe that there are local pressure differences in the aquifer. Also the match between the FWL based on the RFT measurements gives a good fit with the saturation from the saturation-height models. And it also provides a proper match between the static GIIP and the P/Z GIIP. Therefore, TNO-AGE agrees with the FWL determination.

7.3.8 Conclusions

TNO-AGE has carried out a technical review on the petrophysics of the P18-2 carbon capture storage (CCS) license. The most important outcomes of this review are listed below.

- Both studies of BP and AP are carried out in an adequate way.
  - TNO-AGE considers the models and parameters that are used for the interpretations to be adequate.

- The recent re-evaluation of the petrophysics by AP largely confirms the results of the original interpretation by BP.
  - TNO-AGE agrees with AP that an immediate revision of the reservoir parameters and uncertainties is not required.

- Good match between static and dynamic GIIP.
  - Small multipliers are applied to improve the history match.

- Sub-optimal match between log based permeability and well test permeability.
  - Attempts are made to calibrate log based permeability to well test permeability.
  - AP proposes addition of shale volume to the porosity-permeability transform and random noise in the upscaling process, but there is hardly any improvement.
  - Uncertainty in permeability is well defined, based on well test data, and implemented in the models.

- Separate saturation-height models per zone lead to a better match than one single function.
  - Water saturation can also be modeled with a single function, but the in the Upper Detfurth the match will always be poor.

- A uniform FWL at a depth of 3680 mTVDss is determined, based on RFT data.
  - This FWL matches with the results of the saturation-height models of AP.
  - Proper definition of the water line.
  - Good match between static and dynamic volume by using this FWL.

- There are multiple inconsistencies in the numbers and description of reservoir properties in the different documents supporting the application.
  - Inconsistencies in GIIP (static/dynamic), permeability, use of petrophysical re-evaluation.

7.4 References

[1] Taqa & EBN, February 2021, Aanvraag CO_2-opslagvergunning reservoir P18-2.
[2] TNO, 2019, CO_2 feasibility study.
[3] Porthos, 2020, Storage capacity technical note.
[4] Across Petrophysics, 2020, Final presentation 2020 PP Evaluation.
[5] BP, 2007, P/18 Field Petrophysical Study.

8 Appendix B – Fluid pressure distribution effects

In this section the initial, present and future pressure fluid pressure distributions in and around the storage reservoir are evaluated. This evaluation is input to the specification of maximum allowed pressures, which as such is out of scope here. Porthos presents this item in section 3.8 in part II of the V2.0 application document, stating:

1. The reservoir pressure will be maximized at the hydrostatic pressure (351 bar), which is much lower than the initial reservoir pressure.
2. The reservoir pressure will not exceed the initial reservoir pressure (375 bar), not even long term.

8.1 Hydrostatic pressure: definition & determination

From the Werkdocument 2.0 we conclude, that the ‘hydrostatic pressure’ as well as the ‘initial gas pressure’ are defined by Porthos at datum level of 3400 mTVD (hereby assuming this is counting from MSL, and expressed in bar, but that has not been specified). This datum level has no bearing to physical depths like the (original) GWC or top reservoir.

For initial gas pressures it is common practice to specify a certain datum level somewhere within the gas column. But for ‘hydrostatic pressure’ it is not. Moreover, we note that ‘hydrostatic pressure’ may have a geological meaning, that differs from an engineering one:

- In the geological sense, the hydrostatic pressure gradient follows from the density profile in the formation water column stretching all the way from surface to the reservoir at stake, provided that there is an uninterrupted (and quasi instantaneous) hydraulic connection between surface and reservoir. Since salinity of formation water changes with depth, this gradient is depth dependent and generally deviates from a constant pressure gradient.
- In (well) engineering terms, the density of the borehole fluid is the basis for the hydrostatic gradient, mostly taken as a constant value. The same may hold for the pressure profile developing under a supposed leak path from the storage reservoir to outside storage complex. In that case there may be a pressure sink formed by a large aquifer in the overburden of the storage complex.

Recommendation: In describing leakage potential and the impact thereof on the maximum allowed reservoir pressure, Porthos has not sufficiently taken the above mentioned distinctions on the meaning of ‘hydrostatic pressure’ into account. This should be improved.

8.2 Aquifer pressure

Porthos has derived the aquifer pressure depth profile in the P18 reservoirs from just one data point in the well P15-12: 331 bar @ 3200mTV, with a gradient of 0,1 bar/10 m (ref. Werkdocument 2.0). This leads to the following comments:

1. We note that it cannot be ruled out that the pressure measured in P15-12 was lower than original due to gas production in adjacent blocks. At least it is questionable, whether this single pressure data point is representative for the whole P18 aquifer system.
2. The water pressure profile specified by Porthos does not take into account any variations with depth, e.g. the probably higher formation water density in these deep seated reservoirs as compared to the shallow aquifers above the storage complex.
3. Although Porthos states that the P18 reservoirs were initially slightly overpressured (https://www.nlog.nl/pressure-southern-north-sea-psns-database), the pressure point measured in P15-12 is very close to hydrostatic, with a total gradient of 331 bar/ 3200 m = 0,1034 bar/m, i.e. close to a sea water gradient. The low total pressure gradient in the P18 Triassic reservoirs may be explained by 1) the regional absence of salt evaporates and/or 2) the expulsion of relatively sweat water from the basement underneath [Gyllenhammer et al, 2021].

Recommendation: More supporting pressure data and further geological evidence should be provided to support the hydrostatic pressure in and around the P18-2 storage reservoir and the uncertainty therein.

8.3 Depth GWC

First of all, since the pressure values stated by Porthos have been derived from RFT-type data, Free Water Level (FWL) is a more appropriate term than Gas Water contact (GWC).

As a consequence of the above discussion on ‘hydrostatic pressure’, the depth of the GWC / FWL in P18-2 as well as the initial pressure at that depth level, could be different from what Porthos has specified in a deterministic manner.

Recommendation: Porthos should specify the uncertainty in the depth and pressure of the (original) FWL. Constraints by the static GIIP (including spill point) and dynamic GIIP, and the uncertainties therein are to be taken into account.

8.4 Present fluid pressure distribution in the P18-2 storage reservoir

Time lapse RFT data have not been presented in the license application documents. Static pressure data and the p/Z plot indicate, that the P18-2 gas reservoir in a good approximation has behaved as a closed tank. However, that doesn’t give detailed information on the present spatial fluid pressure distribution in the storage reservoir. The fact that the p/Z plot is quite straight and no water influx has been detected in the wells, does not prove that there has been no influx from the aquifer and/or rise of the original water table, associated with a drop of fluid pressure at the original water table.

Recommendation: We advise further analysis of the present pressure distribution in more detail.

8.5 Future fluid pressure distribution in the P18-2 storage reservoir

The applicants state that the reservoir will be filled with CO_2 along a constant pressure gradient ranging from the FWL up to the top of the reservoir. Porthos here (tacitly) assumes:

- the FWL depth and fluid pressure at the start of CO_2 injection are the same as at the start of gas production;
- present FWL depth is known without uncertainty;
- the top of the reservoir is known without uncertainty;
- fluid composition is exactly known (mix of CO_2, impurities and remaining natural gas);
- fluid pressures inside the storage reservoir will build up according to constant gradients (i.e. no pressure differentials between reservoir layers);
- No buildup of fluid pressure assumed after the cessation of CO_2 injection.
-

Recommendation: The applicant should take the validity and uncertainty of these assumptions into account in a revised analysis of the future fluid pressure distribution.

8.6 Sensitivity of storage mass to regulatory pressure limits

In the above, we have refrained from proposing alternative quantitative pressure limits to the injection process. However, we feel it is useful to show the dependency of the stored volume (or rather storage efficiency) on the maximum allowed reservoir pressure.

The figure below (Figure 8.1) shows, that the CO_2 mass stored per incremental bar of reservoir pressure strongly declines from 340 bar upwards. In a good approximation this increment is in the order of 1% per 10 bar. The implication of this observation is, that any discussion on a safe maximum fluid pressure limit will have a modest impact on the overall storage efficiency.

TNO-AGE estimates, that the uncertainty on the (future) fluid pressure distribution inside and outside the storage reservoir is likely to be of the same order of magnitude.

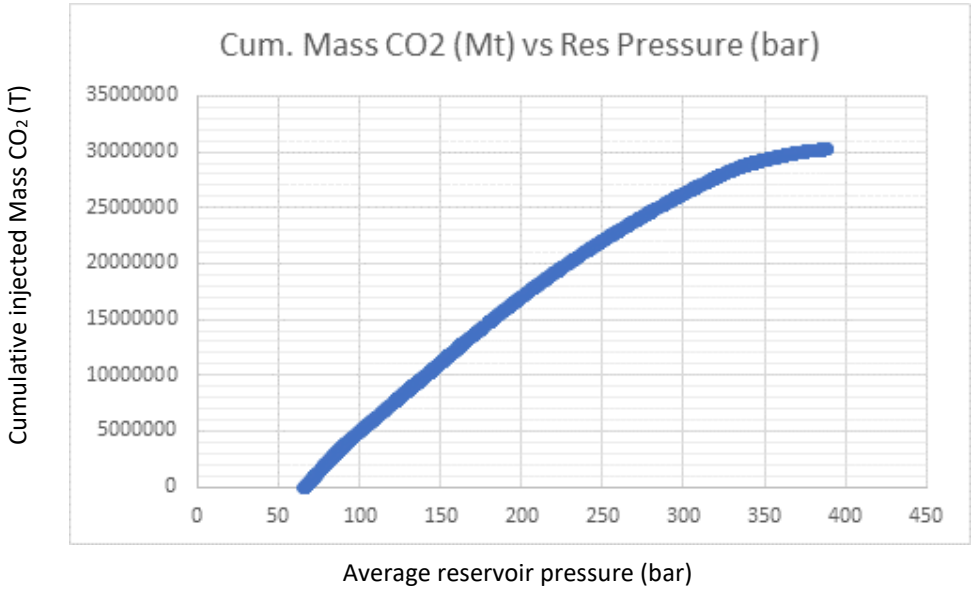

Figure 8.1 Cumulative Mass of CO_2 plotted against average reservoir pressure. Derived from CLG dynamic modelling results.

8.7 References

Gyllenhammer, C.F., Formation water salinity does not vary linearly with depth, proving its mobility and connectivity with salt bodies or fresh water. Does this influence enhanced recovery and nuclear waste repository location? *First Break sept 2021, p. 61 – 71.*